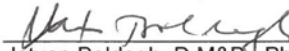The Dissertation Committee for Ling Fang Certifies that this is the

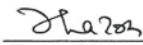approved version of the following dissertation:

ATM REGULATESTHE NF-κB PATHWAY VIA RELA SER 276

PHOSPHORYLATION

Committee:

Allan R. Brasier, M.D., Supervisor

Sanjeev Choudhary, Ph. D., Chair

Istvan Boldogh, D.M&B., Ph.D.

Tapas Hazra, Ph.D.

Zhaohui Wu, M.D., Ph.D.

Dean, Graduate School

ATM REGULATES THE NF-κB PATHWAY VIA RELA SER 276

PHOSPHORYLATION

by

Ling Fang, B.S.

Dissertation

Presented to the Faculty of the Graduate School of

The University of Texas Medical Branch

in Partial Fulfillment

of the Requirements

for the Degree of

Doctor of Philosophy

The University of Texas Medical Branch

July, 2014

Acknowledgements

This dissertation won't be possible without the support and guidance of my mentor Dr. Allan R. Brasier. His guidance and training made me grow from a fresh B.S. to a scientist. I also would like to thank Dr. Sanjeev Choudhary, as my supervisory committee chair, he is deeply involved in developing my project, designing experiment and teaches a bunch of technologies.

I would like to thank other committee members: Dr. Istvan (Steve) Boldogh, Dr. Tapas Hazra, and Dr. Zhaohui Wu. They provide numerous suggestions and ideas on my projects. Also, their valuable corrections and comments made this dissertation much stronger.

I also would like to thank the current and former lab members: Dr. Bing Tian, Dr. Jun Yang, Dr. Mohammad Jamaluddin, Ruwen Cui, Muping Lu. They helped me a lot in the past few years.

Finally, I would like to thank my parents. As the only child of them, I was unable to stay with them in the past several years. I am very grateful for their support, understanding and sacrifice.

ATM REGULATES NF-κB AND ANTIVIRAL RESPONSE PATHWAY VIA RELA SER 276 PHOSPHORYLATION

Publication No._____

Ling Fang, Ph. D

The University of Texas Medical Branch, 2014

Supervisor: Allan R. Brasier

ABSTRACT

Ataxia-Telangiectasia Mutated (ATM), a member of the phosphatidylinositol 3 kinase-like kinase family, is a master regulator of the double strand DNA break-repair pathway after genotoxic stress. Here we found ATM serves as an essential regulator of TNF-and RSV- induced NF-κB pathway. We observed that TNF exposure of cells rapidly induced DNA double strand breaks and activates ATM. TNF-induced ROS promote nuclear IKKγ-ubiquitin association and complex formation with ATM for nuclear export. Activated cytoplasmic ATM is involved in the selective recruitment of the E3-ubiquitin ligase β-TrCP to phospho-IκBα proteosomal degradation. Importantly, ATM binds and activates the catalytic subunit of protein kinase A (PKAc), a ribosmal S6 kinase that controls RelA Ser 276 phosphorylation. In ATM knockdown cells, TNF-induced RelA Ser 276 phosphorylation is significantly decreased. We further observed decreased binding and recruitment of the transcriptional elongation complex containing cyclin dependent kinase-9 (CDK9; a kinase necessary for triggering transcriptional elongation) to promoters of NF-κB-dependent immediate early cytokine genes, in ATM knockdown cells. We conclude that ATM is a nuclear damage-response signal modulator of TNF-induced NF-κB activation that plays a key scaffolding role in IκBα degradation and RelA Ser 276 phosphorylation. In the antiviral response pathway, we observed RSV infection activates ATM and ATM is also required for RSV induced RelA Ser 276 phosphorylation. We further demonstrated that IRF7 gene expression is pRelA Ser 276 dependent and IRF7 is a essential regulator of RIG-I gene expression. Depletion of ATM results in an increased RSV proliferation and reduced IFN and ISG gene expression, indicating the significance of resynthesized RIG-I regulated by IRF7. These results demonstrate a RSV- phospho-Ser 276 RelA-IRF7-RIG-I pathway

mediated by ATM. Taken together, our study provides a mechanistic explanation of decreased innate immune response associated with A-T mutation.

TABLE OF CONTENTS

LIST OF ILLUSTRATIONS

CHAPTER 6

List of Abbreviations

ARD   Ankyrin repeat domain

ATM   Ataxia telangiectasia mutated

CDK9   Cyclin-dependent kinase 9

CE   Cytoplasmic extract

ChIP   Chromatin immunoprecipitation

cIAP   Cellular inhibitor of apoptosis

DAMP   Danger-associated molecular pattern

DMSO   Dimethyl sulfoxide

DSBs   DNA double strand breaks

dsRNA   Double-strand RNA

Gro-β Growth-regulated protein beta

IFN   Interferon

IKK   IκB kinase

IL-8   Interleukin 8

IRF   IFN regulatory factor

ISG   Interferon-stimulated genes

IκBα☐   Nuclear factor of kappa light polypeptide gene enhancer

                in B-cells inhibitor, alpha

LPS   Lipopolysaccharide

LRTI   Lower respiratory tract infection

MAVS   Mitochondrial antiviral-signaling protein

MDA5	Melanoma Differentiation-Associated protein 5
MEF	Mouse embryonic fibroblast
MRN	Mre11-RAD50-NBS1
MSK1	Mitogen stress-related kinase 1
NAC	N-acetyl cysteine
NE	Nuclear extract
NF-κB	Nuclear factor kappa-light-chain-enhancer of activated B cells
NIK	NF-κB inducing kinase
NLR	Nod-like receptor
NLS	Nuclear localization signal
OGG1	8-oxoguanine glycosylase 1
PAMP	Pathogen associated molecular pattern
PI3K	Phosphotidylinositol 3 kinase
PI-3K	Phosphoinositide 3-kinase
PKAc	Catalytic subunit of protein kinase A
PKAc	Catalytic subunit of protein kinase A
Poly(I·C)	Polyinosinic: polycytidylic acid
PRR	Pattern recognition receptor
RHD	Rel homology domain
RIG-I	Retinoic acid-inducible gene 1
RLR	RIG-I-like receptors
RNA pol II	RNA polymerase II

ROS	Reactive oxygen species
RSV	Respiratory syncytial virus
SCF	SKP1-CUL-1-FOX box protein
Ser	Serine
SeV	Sendai virus
shRNA	short hairpin RNA
SID-SRM-MS	Stable isotope dilution-selected Reaction Monitoring-mass spectrometry assays
ssRNA	Single-strand RNA
TAD	Transactivation domain
TLR	Toll-like receptor
TNF	Tumor necrosis factor
TRAF	TNF receptor-associated factor
Ub	Ubiquitination
WCE	Whole cell extract
β-TrCP	β-transducin repeat-containing protein

CHAPTER 1 INTRODUCTION

1.1 The innate immune response

The immune system is a multicellular effector that protects body against disease from pathogens (1). To work properly, it detects various pathogenic patterns on the surface of cells, including viruses, bacteria, fungi and parasitic worms, as well as chemicals, drugs, toxins and foreign particles, triggering protective signaling pathways. In vertebrates, the immune system is composed of 2 different subsystems: the innate immune system and the adaptive immune system (2).

The innate immune system, encoded by germline pattern recognition receptors, is the first line of defense and activated in an antigen-independent fashions (3). It is found in all plants and animals and therefore is an evolutionally conserved defense system (4). The innate immune response is a signaling mechanism designed to limit the spread of infecting pathogen at mucosal surfaces before the adaptive immune response is activated (5).

The first line of innate defense is formed by epithelial surfaces which form tough, intact physical barriers (6). They are impermeable to most infectious agents and prevent the entry and colonization of microbes. The skin and mucous membranes are common examples of the epithelial surfaces (7). Besides these physical barriers, flushing action of tears and saliva, vomiting and diarrhea are

also considered as defensive mechanisms which remove pathogens from the body.

When the body is infected by pathogens like a virus or bacteria, cells of the innate immune system utilize pattern recognition receptors (PRRs) to recognize components of the foreign pathogens. These signatures are referred to as pathogen-associated molecular patterns (PAMPs) (8,9). The PPRs, including Toll-like receptors (TLRs), RIG-I-like receptors (RLRs), Nod-like receptors (NLRs), and cytosolic DNA sensors, are the sensors that cells employ to recognize the signs of infection (10). Sensing PAMPs rapidly trigger the host innate immune response by activating interrelated signaling pathways which mediate expression and activation of various cytokines and chemokines and finally induce protective inflammatory responses (11). The typical signs of inflammatory responses include redness, heat, swelling, pain, and loss of function (12). The primary effect of inflammation is increased blood flow to the infected area, which is caused by the dilation of blood vessels around the site of inflammation (13). Gaps also appear in the cell walls surrounding the infected area, allowing immune cells in the blood to infiltrate the tissue. As a result, more immune cells along with increased blood flow congregate at the site of inflammation and strengthen the immune response (14,15). These responses also initiate the adaptive immune response, which are pathogen-specific, long-term and controlled by the development of B and T lymphocytes (16).

The adaptive immune system, which is also named the acquired immune system, is a vertebrate-specific defense system (17). It reacts against pathogens which are able to evade or overcome innate immune defenses. Adaptive immune responses are mediated by lymphocytes. It is composed of two broad type responses: antibody-mediated responses and cell-mediated immune responses, which are mediated by different classes of lymphocytes, called B cells and T cells, respectively (18). In antibody responses, B cells play a key role. B cells arise from stem cells in the bone marrow. During the developing and maturing, each B cell synthesizes a single type of antibody which inserts into the plasma membrane as a receptor with a unique antigen-binding site. In peripheral lymphoid organs, when antigen binds to the receptor, B cells get activated after getting a signaling from a helper T cell. After that, the activated B cells proliferate and differentiate to antibody-secreting effector cells or memory B cells. The effector cells then secrete antibodies with the same unique antigen-binding site (1). The antibodies circulate in the blood plasma and lymph and specifically bind to pathogens. The binding of antibodies not only prevents the recognition of pathogens by host cells, but also makes them easier targets for phagocytes to destroy (19). In cell-mediated immune responses, activated T cells specifically bind to the pathogens and mediate apoptosis for the infected host cells or activate macrophages and natural killer cells to destroy pathogens (18).

1.2 The NF-κB and immune response

In 1986, the group of Noble Prize laureate David Baltimore discovered the first member of nuclear factor-κB (NF-κB) transcription factor family, which selectively binds to nuclear factor kappa-light-chain-enhancer of activated B cells (20). The NF-κB family regulates various gene expression involved in the immune response, inflammation, cell differentiation, apoptosis, and tumorigenesis (21,22). A number of signals, such as different cytokines and chemokines, or various pathogens, and other stressful conditions like DNA-breaks or reactive oxygen species (ROS) activate the NF-κB signaling pathway (23-25). Incorrect regulation of NF-κB transcription factor has been linked to cancer development, autoimmune diseases, chronic inflammation, and improper immune development (22,26,27).

The NF-κB pathway plays a significant role in the innate immune response. It begins prior to pathogen recognition. The development and maintenance of epithelial tissues, which serve as the first barriers, are mediated by NF-κB (28). Previous studies have shown that NF-κB is required for skin development, repairing damaged lung epithelium, wound reconstitution using intestinal epithelial cells (29-31). NF-κB also plays an essential role in the lifespan of hematopoietic cells and the development of innate immune cells including monocytes, macrophages, dendritic cells, NK cells, granulocytes, and mast cells (32,33).

The members of NF-κB family are heter- or homo- dimers consisting of RelA (p65), RelB, c-Rel, p50 (precursor p105) and p52 (precursor p100) (22,34). These 5 NF-κB monomers share a highly conserved 300-amino-acid Rel homology domain (RHD) in N-terminal that controls DNA binding, dimerization, nuclear localization (35). RelA (p65), RelB, c-Rel have a transactivation domain (TAD) in the C-terminal region to allow these proteins to activate the expression of target genes. p100 and p105, which belong to IκB family, contain an ankyrin repeat domain (ARD) in C-terminals (36). By interacting with the RHD in NF-κB, the ARD masks their nuclear localization signal (NLS) and prevents the nuclear translocation (37). Signals which induce NF-κB activity cause the phosphorylation and subsequent ubiquitination of IκBs, leading to their proteolysis or cleavage of ARD through proteasome, dissociating and releasing NF-κB (38). The free NF-κB then translocates to the nucleus and induces target gene expression.

Currently, NF-κB activation is considered to be controlled by 2 distinct pathways, known as the canonical and noncanonical pathways, respectively (36,39). The canonical pathway largely controls the prototypical NF-κB complex, the RelA•p50 heterodimer, which is activated by IκBα proteasomal proteolysis. Under normal conditions, the RelA•p50 heterodimer binds to the ARD of IκBα and therefore is sequestered in the cytoplasm (40). In response to extracellular ligands or PAMPs, activated death domain-containing receptors assemble submembranous signaling complexes to initiate signaling events for NF-κB activation (3,21). The

central mechanism of NF-κB regulation is the signal dependent post-translational modification of the IκB kinase (IKK) complex leading to phosphorylation of IκBα on 32 and 36 and subsequent ubiquitination by a Skp1-Cul1-F-box protein (SCFs) ubiquitin ligase complex containing the beta-transducin repeat containing protein (β-TrCP). β-TrCP, an F-box protein in the SCF complex, is the substrate binding subunit, which recognizes and binds to pIκBα (41). In vivo study showed that ablation of β-TrCP results in accumulation of IκBα as well as NF-κB pathway inhibition (42). After the association between β-TrCP in the cytoplasm, pIκBα get K-48 linked ubiquitination by the SCFs ubiquitin ligase complex. The ubiquitinated pIκBα then goes ubiquitin-dependent proteolysis (43,44). This process releases the sequestered, inactive RelA•p50 heterodimer.

Current work has shown that RelA release from IκB complex is necessary, but not sufficient for activation of the innate response. An overlapping ROS signaling pathway converging on members of the Ribosomal S6 Kinase family is involved in activating phosphorylation of RelA at serine (Ser) residue 276. Ser276 RelA phosphorylation is a posttranslational modification which is required for the binding and recruitment the positive transcription elongation factor b (P-TEFb), a complex containing cyclin T1 subunits and the cyclin-dependent kinase 9 (CDK-9) (45). The fully activated RelA complex mediates phosphorylation of RNA polymerase II leading to transcriptional elongation and induction of gene expression of a subset of immediate-early cytokine genes (46). In this manner, a

cell transduces external environmental signaling into regulated patterns of gene expression.

By contrast, the noncanonical pathway mainly controls formation of the RelB•p52 heterodimer, which is activated by cleavage of p100 to p52 through the proteasome (47). The NF-κB inducing kinase (NIK) plays a central role in this pathway. Under normal conditions, p100, the precursor of p52, binds to RelB and the RelB•p100 dimer is restrained in the cytoplasm (48). Meanwhile, NIK is maintained in a quite low level mediated by TNF receptor-associated factors (TRAFs). TRAF3 binds to NIK and recruits a complex of TRAF2 and cellular inhibitor of apoptosis 1 and 2 (cIAP1 and cIAP2) ubiquitin ligases (49). In this complex, NIK undergoes ubiquitination by cIAP1/2 ligase resulting in rapid and continuous proteosomal degradation (50,51). In response to noncanonical pathway stimuli, such as lymphotoxin β (LT-β) and B-cell activating factor (BAFF) (52,53), the cIAP1/2, promotes the ubiquitination and proteosomal degradation of TRAF3, instead of NIK. NIK is then released from TRAF/cIAP complex, the protein is then stabilized and accumulates in the activated form (54). The accumulated NIK plays multiple roles in activating this pathway: 1. to activate IκB kinase α (IKKα) by phosphorylating Ser 176 and 180 sites (55); and 2. to serve as a docking site to recruit both IKKα and RelB•p100 dimer into a complex (56). The activated IKKα phosphorylates p100 in its C-terminal domain, leading to proteosome-mediated partial degradation to p52 by cleaving the ARD (43). The free RelB•p52 heterodimer translocates to the nucleus and induces target gene

expression (57,58). The genetic networks under the control of noncanonical NF-κB pathway have not been elucidated. Based on the existing results, it appears that the noncanonical pathway controls a distinct genomic response than that activated by the canonical pathway (59). It is also thought that the noncanonical dependent genes are under cell type-specific control. For example, it mainly controls Naf-1 gene expression in epithelial cells rather than other cells (43,60).

1.3 TNF induced NF-κB activation pathway

Eukaryotic tissues respond to signals in their extracellular environment through the induction of long term phenotypic plasticity. An important mechanism for this plasticity is through the activation of cell surface receptors coupled to intracellular signal transduction networks, the activation of which, in turn, induces a reactive gene expression. One specific example occurs in airway mucosal surfaces that normally promote gas exchange, facilitate particulate matter clearance through the muco-ciliary escalator, and protect against oxidative damage (61). Within this surface, sentinel epithelial cells are responsible for activating the innate inflammatory response upon stimulation with macrophage-derived cytokines via the plasma membrane anchored TNF/Death receptor (TNFR) superfamily (62,63). Liganded TNFRs signal intracellularly through NF-κB. As a result, the mucosal surface assumes a pathogen-resistant and pro-inflammatory phenotype. Because of its central role in airway inflammatory disease, the NF-κB signaling pathway has been extensively investigated.

The TNF induced NF-κB activation through TNFR1 is a well-studied example of cell signaling transduction (64). Upon the stimulation of TNF, TNFR1 recruits the TNF receptor-associated protein with a death domain (TRADD) and the serine–threonine kinase called receptor-interacting protein 1 (RIP1) (65). After its association with TNFR1, TRADD recruits TNF receptor-associated factor 2 (TRAF2) (66). The TRAF2 then binds and recruits cIAP1 and cIAP2, forming a TRADD/RIP1/TRAF2/cIAP1/2 complex (67). TRAF2, together with cIAP1/2, in conjunction with the E2 conjugating enzymes UbcH5, catalyze RIP1 ubiquitination through liner and K63 linkages as well as well as TRAF2 K63-linked ubiquitination (68). The K63 polyubiquitin chain recruits the cytoplasmic TGF-β-activated kinase 1 (TAK1) and IKK complexes and finally leads to the activation of IKK complex and subsequent NF-κB pathway (69,70).

1.4 RSV and the innate immune response

Respiratory syncytial virus (RSV), a negative-sense, single-strand RNA (ssRNA) virus of the paramyxoviridae family, is one of the most important respiratory pathogens for young children all over the world (71). RSV infection induces lower respiratory tract infection (LRTI) in infants and young children, accounting for over 3 million hospitalizations and about 200,000 deaths (72,73). Although almost all the children in United States are infected by RSV before the age of 3, there are no effective vaccines or treatment methods (74). Most patients with

RSV-induced LRTI present at times when RSV titers are falling (75), indicating the significant role of host signaling response to RSV infections in disease pathogenesis.

Once infected, RSV replicates in the nasal mucosa and spreads from cell to cell through intra-epithelial bridges into the lower respiratory tract, or by free virus in respiratory secretions binding to epithelial cilia (76,77). RSV replicates primarily in all mucosal epithelial cells, where it generates bronchial epithelial inflammation, epithelial necrosis, peribronchial infiltration of mononuclear cells, and submucosal edema (78,79). RSV infection and following replication activate innate immune response in airway epithelial cells and therefore these cells constitute the first line of host defense (80-83).

Besides the bacterial lipopolysaccharide (LPS) (84), nucleic acid also serves as one of the major PAMPs. Many pathogens, including RNA virus, are detected through the recognition of their genomes or nucleic acids accumulating during their replication. Cytoplasmic viral genomic RNA is primarily recognized by a family of PRRs which subsequently trigger signal transduction cascade. These cascades include NF-κB and Interferon response factor (IRF) pathway (10,85). Two classes of PRRS that primarily serve as a sensor for viral infection are: 1. RIG-I-like receptor (RLR), including retinoic acid-inducible gene I (RIG-I) and melanoma differentiation-associated gene 5 (MDA5); and 2.Toll-like receptor 3 (TLR3) (86,87). Each are discussed in detail below.

RIG-I is responsible for the signal transduction of antiviral responses after binding double-stranded RNA (dsRNA), a pathway that has been implicated in antiviral responses to a variety of virus types, including Sendai virus, Dengue virus, Junin Virus as well as RSV (88-90). The RLRs, RIG-I and MDA5, are principally responsible for activating IRF3 (85). RIG-I undergoes a conformational switch via inducible K63-linked polyubiquitylation after binding to cytoplasmic dsRNA or 5' triphosphorylated RNA (91,92). This process promotes conformational change of two caspase activation and recruitment domain (CARD)-like domains, which then mediate downstream signaling by binding to CARD-like domains of Mitochondrial antiviral-signaling protein (MAVS) (89,93). This signaling event activates the downstream of TBK1/IKKε complex, which leads IRF3 phosphorylation and translocation to the nucleus.

The TLRs family serves as sensors for exogenous nucleic acids (5). For the antiviral response to RSV, TLRs- 3 and -4 are thought to be major mediators for the downstream signaling (94). In airway epithelial cells, TLR3 is one of the most abundant TLRs (95). During the infection, TLR3 recognizes dsRNA, the replication intermediate of RSV and other RNA viruses (5). Following binding with dsNRA at endosomal compartments, TLR3 recruits TIR-domain-containing adapter-inducing interferon-β (TRIF) and TRAF3, activating IRF3, IRF7 and NF-κB to trigger IFN and cytokine expression (96).

After RSV or other virus infection, the PPRs transduce signaling pathways which lead to the expression of cytokines, chemokines, and interferons (IFNs), including IFN1, 3 and 7. Interferons are central mediators for the mucosal antiviral response by inducing transcription of hundreds of interferon-stimulated genes (ISGs) through the JAK-STAT pathway, whose products reduce viral propagation (97,98). It is considered that Type I (IFNα/β) and type III (IL28A, IL28B, IL29) IFNs are among the most potent antiviral classes. A unique and partially overlapping subset of ISGs is induced by each of these IFNs (99). Although most single ISGs functions are still under investigation, it is widely accepted that the ISGs play a central role in antiviral defense and coordinate the innate immune response to the RNA virus (100,101). Although many aspects of antiviral function are not fully understood, it is widely accepted that induction of a subset ISGs reinforce the IFN signaling pathways for enhanced pathogen detection and immune signaling. Also, recent research has shown that several ISGs directly inhibit virus infection by inhibiting virus entry as well as virus translation and replication (102).

We have found that RSV induces expression of at least 16 cytokine and chemokine genes, among which many are NF-κB-dependent (83,103,104). Upon RSV infection, NF-κB can be activated in airway epithelial cells (105). Previous studies have shown that RSV can induce NF-κB activation through both canonical and noncanonical pathways in pulmonary epithelial cells. In the canonical pathway, RSV induces NF-κB activation through RIG-1•MAVS

complex in the early response as well as TLR3 pathway which is responsible for the post-translation modification of RelA (86). On the other hand, RSV induces the NF-κB noncanonical pathway by activating NIK•IKKα complex, which is also associated with the RIG-1•MAVS complex (106,107).

There are 2 main differences between RSV induced NF-κB activation and other traditional stimuli, like TNF-α: 1. ROS formation induced by RSV is mediated by cytoplasmic oxidases and NOX2 (108,109), while TNF-induced mitochondrial ROS is TRAF-dependent (110). 2. RSV induced RelA Ser 276 phosphorylation is mediated by mitogen stress-related kinase 1(MSK1) (111), while TNF-induced RelA Ser 276 phosphorylation is mediated by the catalytic subunit of protein kinase A (PKAc) (112).

1.5 ATM and activation pathway

In 1988, Ataxia-Telangiectasia Mutated (ATM), which is responsible for the ataxia telangiectasia (A-T) disease was localized to 11q22.3-23.1 (113). A-T, a rare, neurodegenerative, and inherited, autosomal recessive disease results from the mutation of ATM (114). The neurodegenerative events are defined as ataxic movements which are associated with telangiectasia (dilated blood vessels) in the eyes. Although A-T is considered as neurodegenerative disease, it is characterized by a broad spectrum of defects including immune dysfunction, radiosensitivity, sterility, and a pronounced predisposition to cancer (115-117).

The immunodeficiency of A-T patients is variable, but usually implicated by absent or decreased production of IgA, IgE, IgG2 and IgG4 (118). A-T patients have about 25% higher risk of increased cancers development during lifetime, particularly for lymphomas and leukemia (119). One important causes of death in A-T patients is respiratory system diseases, such as chronic lung disease, or other acute respiratory illnesses (120,121).

ATM is a high-molecular-weight (about 350-kD) protein and a member of the phosphotidylinositol 3 kinase-like kinase family (PI3K-like) of Ser/Thr-protein kinases (PIKKs) (122). Canonical ATM activation is induced by DNA double strand breaks (DSBs). Under normal conditions, ATM kinase exists in an inactive dimer in the nucleus (123). In response to DSBs, a DNA damage-sensing complex, the Mre11-Rad50-NBS1 (MRN) complex, recruits ATM to DSBs site through the C-terminal domain of NBS1(124-126). Once recruited, the ATM dimer undergoes autophosphorylation at serine 1981, forming an active monomer that plays an essential role in DNA repair (127). The activated ATM phosphorylats and activates a vast number of substrates, including the key cell cycle checkpoint kinase, chk2, p53 and SMC1 (128-130). These kinases control the cell cycle checkpoints which ensure the accuracy of cell division in eukaryotic cells (122,131,132).

Recently, it has been appreciated that ATM regulates cellular functions unrelated to the DNA repair pathway, encompassing a vast array of cellular functions such as regulation of redox and energy status (133). Several studies have linked ATM deficiency to increased oxidative stress in cells resulting in various metabolic diseases, oncogenesis and neurodegeneration (134-136). Conversely, oxidative stress itself can induce ATM activation via oxidation of its Cys 2991 resulting into a disulfide-crosslinked ATM dimer (137). A-T patients expressing mutated ATM develop insulin resistance and type-2 diabetes (138). In this context, ATM is not only required for optimal activation of the Ser/Thr kinase AKT after insulin treatment but also for the expression of insulin growth factor-1 receptor. These reports clearly suggest a much versatile role of ATM in cellular metabolic processes independently of DSB repair.

1.6 ATM and NF-κB activation

In a mechanism separating from PAMP signaling, endogenous danger-associated molecular patterns (DAMPs) trigger innate pathways via intracellular signaling independent of plasma membrane associated receptors (139). One example is the DNA damage response, where DSBs induce a coordinated set of signaling events that activates a nuclear kinase ATM (140). In addition to coordinating DNA damage-repair by activating the homologous recombination pathway, active ATM undergoes cytosolic translocation to directly activate IKK and the NF-κB pathway. In this process, activated ATM binds to and

phosphorylates Ser 85 of IKKγ in the nucleus, stimulating its ubiquitin-dependent nuclear export (141). The cytosolic ATM•IKKγ complex then activates the IKK complex and subsequent NF-κB dependent gene expression, via a nuclear-cytoplasmic ("inside-out") signaling pathway.

However, the role of ATM in contributing to receptor-initiated ("outside-in") signaling has not yet been described. The canonical pathway inducer, TNF-α, has been reported to induce ROS or DNA damage (112,142-144). Since ATM is activated by ROS or DNA damage, It is worthwhile to investigate whether the role of ATM is achieved through an "outside-in" signaling such as TNF induced NF-κB canonical pathway.

Despite the intensive investigation of the NF-κB pathway, the kinases controlling this pathway are still largely unknown. High-throughput, tandem affinity purification studies have elucidated novel protein interactions in the NF-κB network and demonstrated novel roles of TRAF isoforms (61). However, few regulatory kinases were discovered, perhaps because kinase-substrate interactions are transient and low affinity binding interactions may not have been captured. The recent development of high-throughput siRNA screening assays offers an opportunity for new insights into this and other signaling pathways.

CHAPTER 2. EXPERIMENTAL PROCEDURE

2.1 Cell cultures and reagents

Human A549 pulmonary type II epithelial cells (American Type Culture Collection) were cultured in F-12K medium (Gibco, Invitrogen) with 10% fetal bovine serum, 1.0 mM sodium pyruvate, penicillin (100 U/ml) and streptomycin (100 g/ml) at 37°C in a 5% CO_2 incubator. $ATM^{+/+}$ and $ATM^{-/-}$ MEFs are gifts from Dr. Zhao-hui Wu and were cultured in Dulbecco's Modified Eagle's Medium (Gibco, Invitrogen) with 10% fetal bovine serum 0.1 mM nonessential amino acids, 1.0 mM sodium pyruvate, penicillin (100 U/ml) and streptomycin (100 g/ml) at 37°C in a 5% CO_2 incubator.

ATM, pATM and pRelA (Ser 276) antibodies were purchased from Cell Signaling Technology (Beverly, MA). Lamin B antibody was purchased from EMD Millipore (Darmstadt, Germany). β-tubulin, IKKγ, IκBα, pIκBα, β-TrCP, RelA, PKAc and CDK9 antibodies were purchased from Santa Cruz Biotechnology (Santa Cruz, CA). NF-κB2/p100, pIKKβ and pPolII antibody was purchased from Abcam (Cambridge, UK).

The Stealth RNAi human kinase library, in a 96-well microtiterplate format (8 master plates), which targets 636 human kinase genes, was purchased from Invitrogen.

2.2 High Throughput siRNA screening

Prior to the high-throughput screen, RNAi and transfection reagent concentrations, and transfection efficiency in A549 cells, were optimized. The stealth RNAi master plate collection consisted of three non-overlapping RNAi duplex siRNAs to each target; aliquots from the three sets were pooled into one master plate and diluted to 250 nM of individual RNAi in deep well 96 well plates (Axygen, Union City, CA). Each plate contained low, medium and high GC content Negative Universal siRNA Controls (Invitrogen, Carlsbad, CA). NF-κB - inducing Kinase (NIK) and IKKγ siRNAs were included as positive controls.

For siRNA screening, 25 µl of combined, diluted RNAis were robotically (Biomek FXp, Beckman, Brea, CA) aliquoted into a 96 well plate (Nunc, Rochester, NY), mixed with 25 µl of diluted transfection reagent (0.3 µl/ well of Siquest reagent, Mirus, Madison, WI) and reverse transfected by dispensing A549 –Luc stable cells (10,000 cells in 100 µl) into each well using the Titertek, multidrop 384 cell dispenser (effective concentration of 40 nM for each RNAi from the three duplexes for each target). Each plate was transfected in duplicate to deduce reproducible inhibition. 48 hrs later, cells were incubated in DMEM/BSA and serum starved overnight, followed by TNF treatment (20 ng/ml) for 6 hrs. Cells were washed twice with 1X PBS using the Bio-Plus Pro II wash station (Bio-Rad,

Hercules, CA) before adding 50μl of luciferase lysis buffer and freezing the lysates at -80 ºC.

2.3 Luciferase assay

20 μl of cell lysate from each well in the transfection plates was transferred and mixed with 80 μl of luciferin reagent for measurement of relative luminescence (96 well plate, Nunc). Luciferase activity was measured by microplate reader (SpectraMax M5, Molecular Devices, Sunnyvale, CA).

2.4 Statistical analysis

Z' score calculations were performed in 96 well plates as described (145). The absorbance of CBB binding was fitted to a regression curve and exact protein concentrations determined using least squares regression analysis (Sigma Plot, v11, Sys). The luciferase activity RLU was normalized to absolute the protein concentration for each well where indicated. Normalized luciferase activity was further normalized using the standard Z-score method relative to each plate's mean value (146). The Z score is calculated by subtracting each luciferase value from the plate sample mean and dividing by the plate standard deviation. The criteria for identification of potential hits used a Z-score cutoff of less than -1.65, which corresponded to a p-value of 0.05, for both replicates.

2.5 Virus preparation and infection

The human RSV A2 strain was grown in Hep-2 cells and prepared as described previously (147). The viral titer of sucrose cushion purified RSV pools varied from 8 to 9 log PFU/ml, as determined by a methylcellulose plaque assay. Viral pools were aliquoted, quick-frozen on dry ice-ethanol, and stored at -80°C until they were used. Sendai virus was purchased from Charles River Laboratory. Cells were infected with 100 hemagglutinin units/ml (148).

2.6 Poly(I·C) electroporation

Poly(I·C) was obtained from Sigma (St. Louis, MO). Cells were trypsinized, washed in phosphate-buffered saline (PBS) for 3 times, and pelleted by centrifugation (1000 rpm, 5 minutes). The cell pellet was then resuspended in 100 μl Nucleofector solution (Amaxa; Lonza) with Poly(I·C) (10 μg) into an electroporation cuvette. After that, the cell suspension was electroporated using a Nucleofector I device (Amaxa; Lonza) with Program X-001.

For determinations of cell viability, Cells were trypsinized and the total cell numbers were counted. Cell viability was determined by using a 0.4% solution of trypan blue in PBS (Cellgro) in an automatic cell counter (Invitrogen) (149).

2.7 Nuclear and cytoplasmic extraction

Cytoplasmic and nuclear extracts were prepared as described earlier (150). Briefly, cells were harvested in PBS and centrifuged to collect pellets. Pellets were resuspended in double cell volume of solution A (50 mM HEPES (pH 7.4), 10 mM KCl, 1 mM EDTA, 1 mM EGTA, 1 mM dithiothreitol (DTT), 0.1 μg/ml phenylmethylsulfonyl fluoride, 1 μg/ml pepstatin A, 1 μg/ml leupeptin, 10 μg/ml soybean trypsin inhibitor, 10 μg/ml aprotinin, and 0.5% IGEPAL-630) and centrifuged to obtain the supernatants as cytoplasmic fraction. The nuclear pellets were purified on sucrose cushions (buffer A with 1 M sucrose). After high salt extraction in buffer C (10% glycerol, 50 mM HEPES (pH 7.4), 400 mM KCl, 1 mM EDTA, 1 mM EGTA, 1 mM DTT, 0.1 μg/ml phenylmethylsulfonyl fluoride, 1 μg/ml pepstatin A, 1 μg/ml leupeptin, 10 μg/ml soybean trypsin inhibitor, and 10 g/ml aprotinin), the nuclei were centrifuged at 12,000g at 4 °C for 20 min. The supernatants were saved as NE. The protein concentrations were measured by Bradford protein assay (Protein Reagent, Bio-Rad).

2.8 Western immunoblots

After SDS-PAGE electrophoresis, proteins were transferred to PVDF membrane and blocked in 5% milk/TBST buffer for 1 hr. The membranes were incubated with specific primary antibody for overnight at 4 °C followed by washing with TBST and incubation with secondary antibody for 1 hr. Membranes were

exposed by ECL western blotting solution (Amersham) and the films were developed by Kodak machine.

2.9 Protein-protein interaction by co-immunoprecipitation

Cellular extracts (nuclear, cytoplasmic or whole cell extracts prepared in RIPA buffer) were precleared by incubating with protein A sepharose CL-4B (Sigma) beads for 45 min at 4°C. 1 mg proteins from precleared samples were incubated with 5 µg of specific antibody for overnight at 4 °C. Immune complexes were captured by addition of protein A sepharose CL-4B (Sigma) for 2 h at 4 °C. Following incubation, the beads were washed 4 times with TBS-T (50 mM Tris–HCl, pH 7.4, 150 mM NaCl, 5 mM EDTA and 0.05% Triton-x100) followed by the extraction of the bound protein boiling the beads in SDS PAGE buffer containing β-mercaptoethanol for 5 min. The bound proteins were identified by performing Western blot using specific antibodies.

2.10 PKAc activity assay

Cells were lysed in a buffer containing 20 mM Tris–HCl, pH 7.5, 150 mM NaCl, 5 mM EDTA, pH 8.0, 1 mM PMSF, 10 μM leupeptin, and 10 μM aprotinin. The cell suspension was sonicated for 30 s ×3, centrifuged and supernatant was collected. PKAc activity was measured in the supernatant using PKA-specific

22

peptide (LRRASLG) according to the supplier's recommendations (PepTag assay, Promega, Madison, WI). Phosphorylated and nonphosphorylated peptides were separated by electrophoresis on a 0.8% agarose gel, and quantitated by measuring absorbance at 570 nm. Data were presented as percentage of absorbance relative to 0 h.

2.11 Q-RT-PCR

Total cellular RNA was extracted by Tri Reagent (Sigma-Aldrich). cDNA was synthesized from 1 μg of RNA using iScript cDNA Synthesis Kit (Bio-Rad). 3 μl of cDNA products was amplified in 20 μl reaction volume containing 10 μl iQ SYBR Green Super Mix (Bio-Rad) and 400 nM primer mix. All reactions were processed in MyiQ Single-Color Real-Time PCR Detection System (Bio-Rad) and results were analyzed by IQ5 program (Bio-Rad).

2.12 Chromatin immunoprecipitation (ChIP)

Two-step cross-link chromatin immunoprecipitation was performed as described previously (151). Briefly, A549 cells were washed twice with PBS and incubated with disuccinimidyl glutarate (2 mM for 45 min) for protein-protein cross-linking. Subsequently, protein-chromatin cross-linking was performed by incubating the cells with 1% formaldehyde for 30 min. Equal amounts of sheared chromatin

were immunoprecipitated overnight with 4 ug of the indicated antibody in ChIP dilution buffer at 4°C. Immunoprecipitates were collected with 40 μl protein A magnetic beads (Invitrogen), washed, and eluted in 250 μl elution buffer for 15 min at room temperature. Samples were de-cross-linked in 0.2M NaCl at 65 °C for 2 - 4h. The precipitated DNA was phenol-chloroform extracted, precipitated with 100% ethanol, and dried.

The promoter-specific primers used for quantitative PCR of each gene are as followings. Gro-β: forward: 5'- TCGCCTTCCTTCCGAACTC-3', reverse: 5'-CGAACCCCTTTTATGCATGGT-3'; IκBα: forward: 5'-GACGACCCCAATTCAAATCG-3', reverse: 5'- TCAGGCTCGGGGAATTTCC-3'; IL-8: forward: 5'- AGGTTTGCCCTGAGGGGATG-3', reverse: 5'-GGAGTGCTCCGGTGGCTTTT-3'.

2.13 Stable isotope dilution (SID)-selected Reaction Monitoring (SRM)-mass spectrometry (MS) assays

The SRM assays for total RelA, IKKγ and phosphor-Ser 536 RelA were described previously (152). The SRM assay for Phospho-Ser 276 RelA was developed using a workflow described previously (152). The signature peptides and MS parameters of each SRM assay are listed in **Table 1**. Stable isotope standard (SIS) peptides were chemically synthesized incorporating isotopically labeled

[13C615N4] Arginine or [13C615N4] Lysine to a 99% isotopic enrichment (Thermo Scientific).

Ubiquitin-conjugated IKKγ or RelA were immunoprecipitated using anti-Ubiquitin or RelA Ab, and immune complexes captured by protein A magnetic beads (Dynal Inc). For the measurement of the level of ubiquitin-conjugated IKKγ and phospho-Ser 276 RelA, the proteins on the beads were digested with trypsin as described previously (153). Briefly, the beads were washed with PBS for three times and then resuspended in 30 μL of 50 mM ammonium hydrogen carbonate (pH 7.8) and 20 μL of 0.1 μg/ μL of trypsin were added. The samples were mixed and trypsinized by gentle vortexing overnight at 37 °C. After digestion, the supernatant was collected. The beads were washed with 50 μL of 50% acetonitrile (ACN) three times and the supernatant was pooled, and dried. The tryptic digests were then reconstituted in 30 μL of 5% formic acid-0.01% TFA for MS analysis. For the measurement of the level of phosphor-Ser 536 RelA, the protein on the beads were digested with Glu-C (Indianapolis, IN) as described previously (152). The peptides were extracted from the beads as described above and then reconstituted in 30 μL of 5% formic acid-0.01% TFA for MS analysis. An aliquot of 10 μL of diluted SIS peptides were added to each digest before LC-SRM-MS analysis.

LC-SRM-MS analysis was performed with a TSQ Vantage triple quadrupole mass spectrometer (Thermo Scientific, San Jose, CA) equipped with nanospray

source (Thermo Scientific, San Jose, CA) as described before. The online desalting and chromatography were performed using an Eksigent NanoLC-2D HPLC system (AB SCIEX, Dublin, CA). An aliquot of 10 μL of each of tryptic digests were injected on a C18 peptide trap (Agilent, Santa Clara, CA), desalted with 0.1 % formic acid at a flow rate of 2 μL/min for 45 min. Peptides were eluted from the trap and separated on a reversed phase nano-HPLC column (PicoFrit™, 75 μm x 10 cm; tip ID 15 μm) packed in house using Zorbax SB-C18 (5-μm diameter particles, Agilent, Santa Clara, CA). Separations were performed using a flow rate of 500 nL/min with a 20-min linear gradient from 2-40% mobile phase B (0.1 % formic acid-90 % ACN) in mobile phase A (0.1 % formic acid), followed by 0.1-min gradient from 40-90% mobile phase B and 5-min 90% mobile phase B. The TSQ Vantage was operated in high-resolution SRM mode with Q1 and Q3 set to 0.2 and 0.7-Da Full Width Half Maximum. All acquisition methods used the following parameters: 1800 V ion spray voltage, a 275 °C ion transferring tube temperature, a collision-activated dissociation pressure at 1.5 mTorr, and the S-lens voltage used the values in S-lens table generated during MS calibration. All SRM data were manually inspected to ensure peak detection and accurate integration. The chromatographic retention time and the relative product ion intensities of the analyte peptides were compared to those of the SIS peptides. The variation of the retention time between the analyte peptides and their SIS counterparts were within 0.05 min, and no significant difference in the relative product ion intensities of the analyte peptides and SIS peptides were observed. The peak area in the extract ion chromatography of the native and SIS

26

version of each signature peptide were integrated using Xcalibur® 2.1. The

default values for noise percentage and base-line subtraction window were used.

The ratio between the peak area of native and SIS version of each peptide were

calculated.

Table 1. **SRM parameters of SRM assays of targeted proteins and posttranslational modifications. Masses listed are for the native forms of the peptides.** Abbreviations: CE, collision energy; Q, quadropole

Gene Name	Swissprot No	Sequence	Q1 m/z	Q3 m/z	Ion type	CE (V)
RelA	Q04206	TPPYADPSLQAPVR	756.396	867.504	y8	27
			756.396	982.531	y9	27
			756.396	1053.568	y10	27
			756.396	1313.684	y12	30
IKKγ	Q9Y6K9	AQVTSLLGELQESQSR	873.455	976.469	y8	27
			873.455	1033.490	y9	27
			873.455	1146.574	y10	27
			873.455	1259.658	y11	27
			873.455	1346.690	y12	27
Phospho-Ser 536 RelA	Q04206	DFSS[Phosphoryl]IADMDFSALLSQISS	1057.455	521.256	y5	35
			1057.455	634.34	y6	35
			1057.455	747.424	y7	35
			1057.455	818.461	y8	35
			1057.455	905.493	y9	35
			1057.455	1008.467	Reporter	35
			1057.455	1052.562	y10	35
			1057.455	1167.589	y11	35
			1057.455	1298.629	y12	35
Phospho-Ser 536 RelA	Q04206	DFSS[Phosphoryl]IADM[Oxid]DFSALLSQISS	1065.453	521.256	y5	35
			1065.453	634.34	y6	35
			1065.453	747.424	y7	35
			1065.453	818.461	y8	35
			1065.453	905.493	y9	35
			1065.453	1016.464	Reporter	35
			1065.453	1052.562	y10	35
			1065.453	1167.589	y11	35
			1065.453	1314.624	y12	35
Phospho-Ser 276 RelA	Q04206	RPS[Phosphoryl]DR	355.653	306.664	Reporter	15
			355.653	457.144	y3	15
			355.653	554.197	y4	15
			355.653	710.298	y5	15

2.14 Comet assays

DNA double-strand breaks were quantitated by a Comet assay (Trevigen, Inc, Gaithersburg, MD) as we described previously (154). Briefly, cells were suspended in 0.6% low melting-point agarose. The cell/agarose suspension (80 μl) was applied onto pre-coated microscope slides (Trevigen Inc). Slides with solidified agarose were placed in lysis buffer (2.5 M NaCl, 100 mM EDTA, 10 mM Trish-HCl (pH 10), 1% sodium sarcosinate and 1% Triton X-100) for 24 h. Slides were placed in pre-cooled (4 °C) electrophoresis tanks, and electrophoresis was carried out at pH 7.8 in a buffer provided by the manufacturer (Trevigen Inc). After electrophoresis at 1.25 V per cm) at 4 °C, preparations were air-dried and DNA stained by SYBER green. Comets were analyzed by using the Comet Assay IV v4.2 system (Perceptive Instruments, Suffolk, UK) image analysis software (4). The fold change in tail comet moments are expressed as the mean (± SD) from three paralel experiments.

2.15 ShRNA mediated ATM knockdown in A549 and HeLa cells

ATM and control shRNA are gift from Dr. Sankar Mitra (Methodist hospital, Houston, TX). Plasmids were transfected to A549 and HeLa cells using FuGENE HD kit (Promega, Madison, WI). 5 μg plasmid was mixed with 15 μl of FuGENE HD Transfection Reagent for 5 min. Afterwards, the mixture was added to 10 cm

cell plate and mixed gently. 48 h later, cells were selected in puromycin (6 μg/ml)

for 2 weeks.

CHAPTER 3 HIGH THROUGHPUT SiRNA SCREENING IDENTIFIES ATM CONTROLLING THE CANONICAL NF-κB PATHWAY

3.1 High Throughput siRNA (HT-siRNA) mediated screening

To identify kinases important in mediating the canonical NF-κB pathway, we performed loss-of-function analyses using HT-siRNA screening for 636 human kinases. In preliminary assay development, we optimized culture conditions, cell number/well, siRNA and stimulation doses and timing of TNF exposure; the Z' Factor served as a measure of the effect size relative to the assay variation. A Z' score of 0.65 was achieved (data not shown), indicating that the assay was sufficiently robust for HT-siRNA screening (145). The strategy for HT-siRNA screening is shown in Figure 1. 10,000 A549 NF-κB/Luc stable cells were plated into the transfection reagent/siRNA mixture, containing the combination of the three separate siRNA duplexes to each kinase, in each well. Cells were stimulated with TNF and luciferase activity subsequently measured. The data was analyzed for relative differences in TNF inducible luciferase activity. In initial pairwise plots to survey the plate-to-plate reproducibility, we found that there was significant signal variation (Figure 2 upper panel). This variation was likely the result of differences in cell number in each well as a result of plate manipulations (plating, washing and serum starvation); subsequent normalization of the luciferase signals to protein signals in each well significantly reduced the plate-to-plate variability, with Pearson correlation coefficients exceeding 0.9 (Figure 2 lower panel).

To identify kinases involved in the TNF activated canonical NF-κB pathway, wells corresponding to positions where the normalized luciferase activity was significantly different using the standard Z-score method relative to each plate's median value were chosen (146). Briefly, this method assumes that the majority of kinases do not have an effect on the signaling pathway and that the plate serves as its own control. This approach reduces edge effects produced as a result of controls on the outside wells (155). Plate signals are rescaled relative to within-plate variation by subtracting the average of the plate values and dividing the difference by the standard deviation estimated from all measurements of the plate (146).
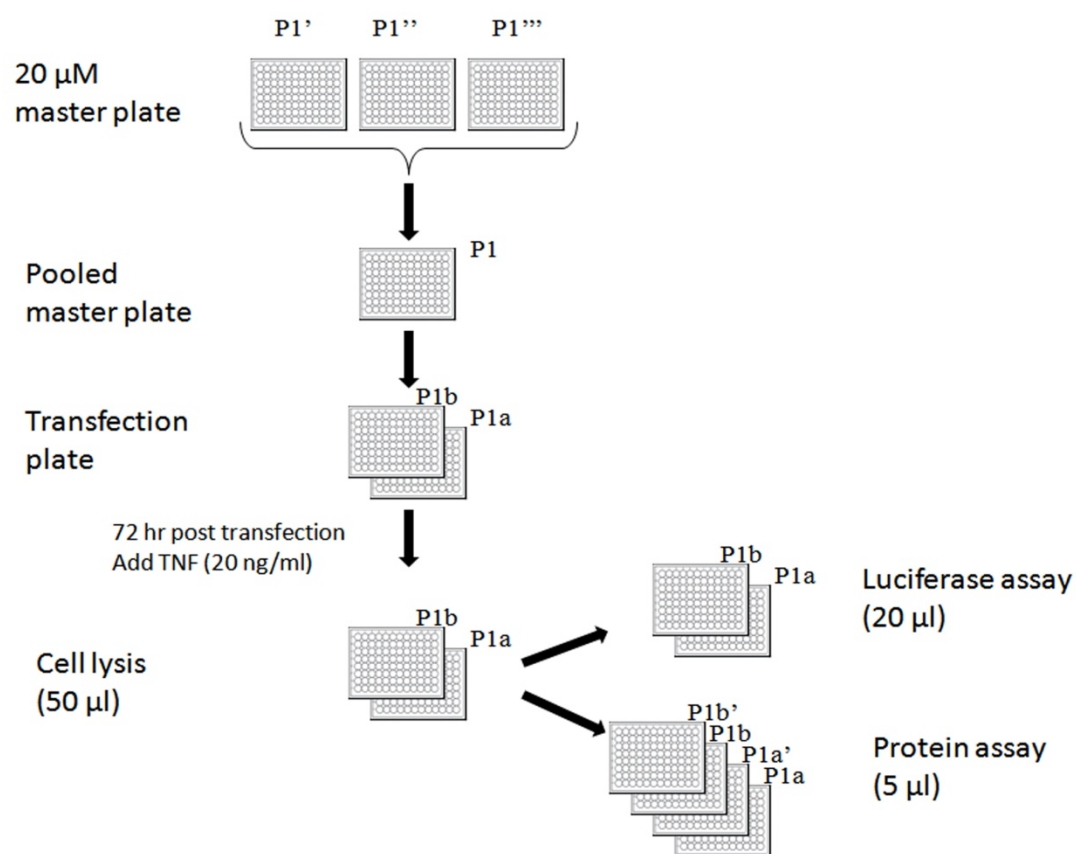
Figure 1. High-throughput SiRNA screening strategy. Shown is a schematic diagram of the siRNA strategy for kinome siRNA screening. From master plates, three target-specific siRNAs were pooled into working transfection plates. siRNA pools from each transfection plate was reverse transfected into NF-κB/Luc cells. After 72 h of transfection, the plates were stimulated with TNF and lysed. The lysates from each plate were measured for raw luciferase activity (in duplicate) and protein measurements were performed in duplicate.
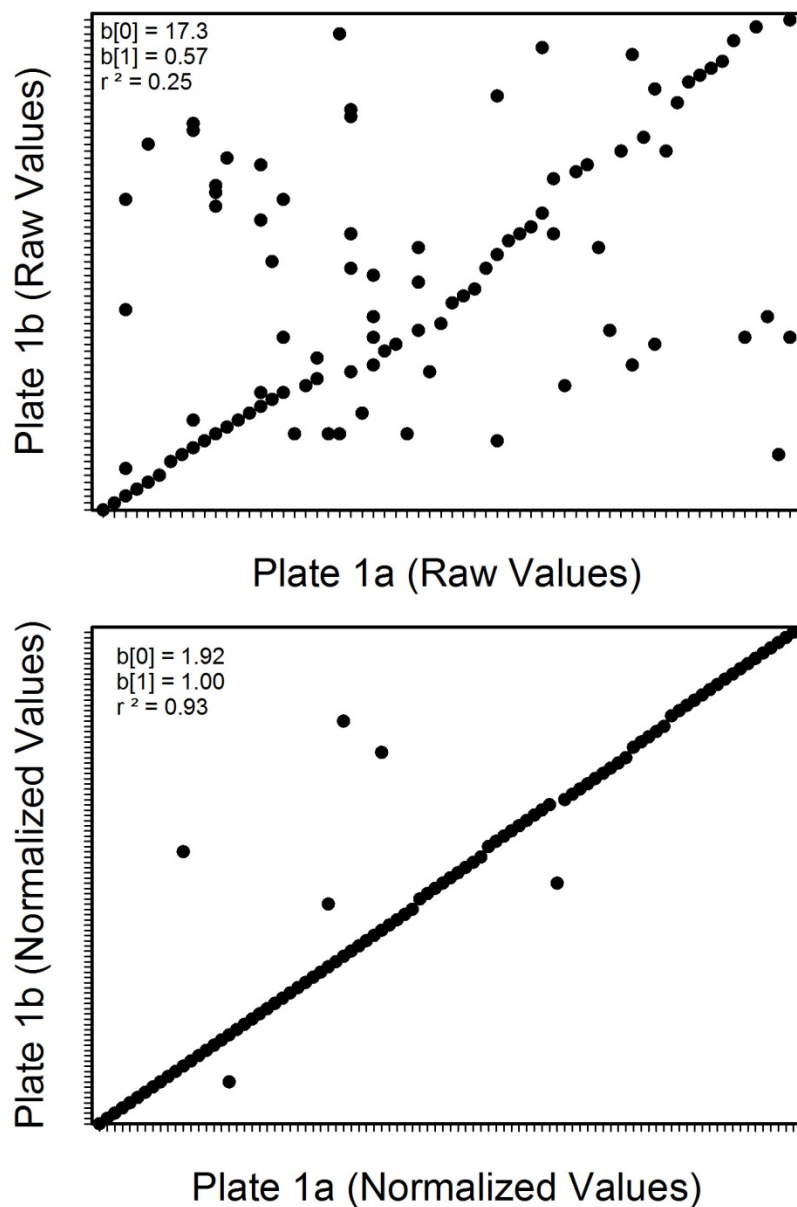
Figure 2. Plate-to-plate reproducibility. Shown is a pairwise plot of uncorrected ("raw") luciferase values from plate 1a to its replicate (1b). Top row, uncorrected luciferase values are plotted. Bottom row, luciferase activity normalized to total protein in each well. Insets, linear regression calculation of the pairwise comparison. B[0], y intercept; b[1], slope. Note that the reproducibility of measurements within replicates is significantly improved by the normalization to protein concentration.

3.2 Analysis of the positive controls

The luciferase activity for siRNA targeting IKKγ demonstrated a Z-score deviation of -1.3 and -0.75, in separate replicates (data not shown). The data was rank order-filtered by the mean Z score, and candidates identified as those with Z-score deviations of < -1.3, a stringent cut-off that we intentionally selected to reduce the number of false positives (Figure 3). Using this cut-off, we identified those hits corresponded to siRNAs that produced a mean Z-score inhibition of >-1.3. IKKβ, another well established kinase involved in TNF-induced canonical NF-κB activation pathway, had an inhibition score similar to that of IKKγ; however, it also missed the stringent filter cut-off. We then identified 36 candidate genes, which produced a greater inhibition than that produced by the positive control IKKγ siRNA (Table 2). In addition, a number of siRNAs produced enhanced reporter activity (Figure 3); the analysis and validation of this group of kinases is beyond the scope of the present study. Focusing on the kinases required for TNF-inducible reporter activity, we observed an enrichment of Cyclin Dependent Kinases (CDKs) -2, 5, 7 and 11B, CDC2-like kinases, and mitogen activated protein kinases (MAPK). Although some of these kinases have already been shown to be involved in canonical NF-κB signaling, including protein kinase C zeta [PRKC (156)], MAP3K3 (157), and MAPK-activated protein kinase 5 (MAPKAPK5) (158,159), the remainder of the kinases in (Table 2) have not been previously implicated in canonical NF-κB pathway signaling.
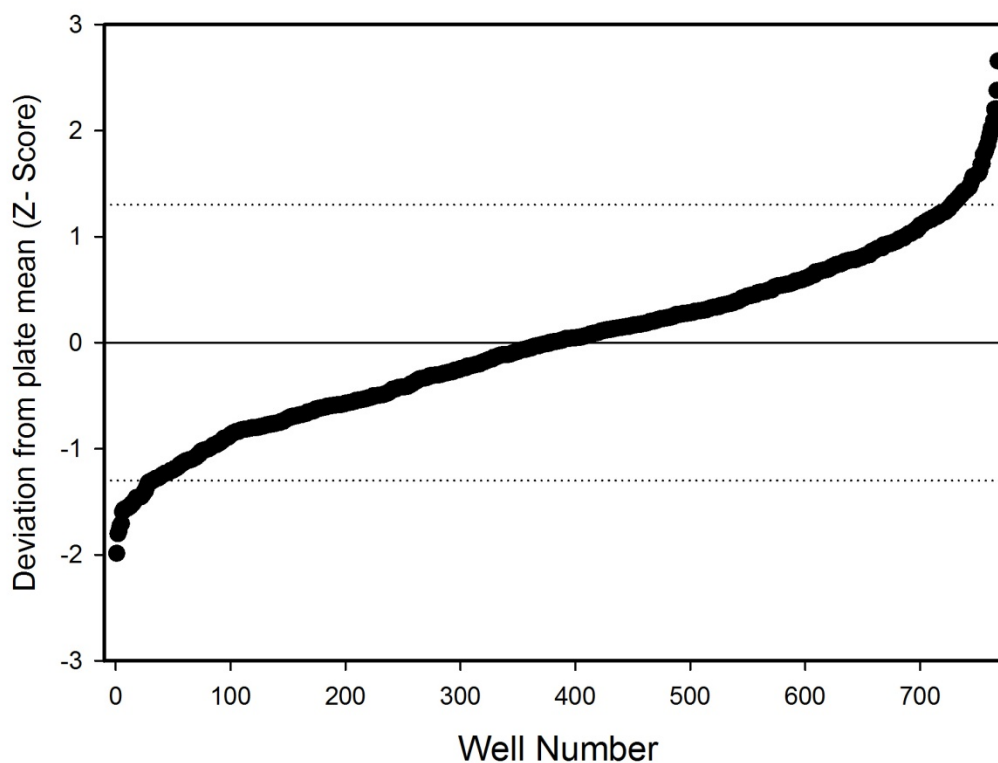
Figure 3. Z-Score data from HT-siRNA screen. Shown is a plot of the mean rank-ordered Z-score data (deviation in standard deviation units from the plate mean) for the HT-siRNA screen. A Z-score deviation of <-1.3 from the plate mean was used to identify candidate kinases, based on the Z-score deviation of the positive control siRNA for IKKγ included on each plate.

Name	Name	RefSeqGene	Avg Z score
Activin receptor type II	ACVR2	NC_000002.11	-2.0
Serine protein kinase ATM	ATM	NC_000011.9	-1.8
Cyclin dependent kinase (CDK)- 7	CDK7	NC_000005.9	-1.8
CDK2	CDK2	NC_000012.11	-1.7
CDK5	CDK5	NC_000007.13	-1.7
SCY-like 2	SCYL2	NC_000012.11	-1.6
Calmodulin 3	CALM3	NC_000019.9	-1.6
MAPKAPK5	MAPKAPK5	NC_000012.11	-1.6
RIO Kinase	RIOK1	NC_000006.11	-1.6
Deoxyguanosine kinase	DGUOK	NC_000002.11	-1.6
Megakaryocyte associated TK	MATK	NC_000019.9	-1.6
CDC-like kinase 2	CLK2	NC_000001.10	-1.5
Uridine-cytidine kinase 2	UCK2	NC_000001.10	-1.5
Discs, large homolog-1	DLG1	NC_000003.11	-1.5

Fyn-related kinase	FRK	NC_000006.11	-1.5
Tyrosine kinase, non-receptor	TNK2	NC_000003.11	-1.5
CaM kinase II	CAMK2B	NC_000007.13	-1.5
Discs, large homolog4	DLG4	NC_000017.10	-1.5
Discs, large homolog 3	DLG3	NC_000023.10	-1.5
AMP activated PK	NUAK1	NC_000012.11	-1.5
Insulin receptor	INSR	NC_000019.9	-1.5
PKC zeta	PRKCZ	NC_000001.10	-1.5
MAPK3K3	MEKK3	NC_000017.10	-1.4
CITRON	CIT	NC_000012.11	-1.4
Ribokinase	RBKS	NC_000002.11	-1.4
S/T kinase 23	SRPK3	NG_016329.1	-1.4
Phosphorylase kinase	PHKG2	NC_000016.9	-1.4
CDC kinase 11B	CDK11B	NC_000001.10	-1.3
Adenylate kinase 3	AK3	NC_000009.11	-1.3
EPH receptor	EPHA3	NC_000003.11	-1.3
Casein kinase 1	CSNK1A1	NC_000005.9	-1.3
Chemokine ligand 2	CCL2	NC_000017.10	-1.3
Eukaryotic elongation factor kinase	EEF2K	NC_000016.9	-1.3
TTK protein kinase	TTK	NC_000006.11	-1.3
BMP receptor	BMPR1B	NC_000004.11	-1.3
Phophofructo-2 kinase	PFKFB2	NC_000001.10	-1.3
MAPK3K12	MAP3K12	NC_000012.11	-1.3
IKKγ	IIKBKG	NC_000023.10	-1.3

Table 2. Candidate kinases. Shown are kinase name, mean Z-score and GenBank ID number for unique candidate kinases selected in the HT-siRNA screen that had an average Z score of <-1.3 corresponding to IKKγ, the spiked positive control for each plate.

To validate this candidate set, 11 kinases were randomly selected for independent validation by knockdown and examination of the effect on NF-κB canonical pathway. These kinases included ataxia telangiectasia mutated (ATM), CDK isoforms -2, -5 and -7, eukaryotic elongation factor-2 (EEF2), MAPKAPK5, MAP3K12, bone morphogenic protein R 1A (BMPR1A), calmodulin kinase -3 (CALM3), phosphorylase kinase (PHKG2), and PRKCζ. A new set of duplex siRNAs (separate synthesis of the same siRNA sequences used in the HTP screen) for each gene were reverse transfected into wild-type A549 cells. We

found that greater than 50% inhibition was observed for ATM, MAPKAPK5, CALM-3, CDK-7,-5 and -2 (Figure 4A). Efficiency of siRNA knockdown of the selected kinases at the protein levels were quantified by Western blot analysis. Here the abundance of CDK-2, -5 and ATM proteins were almost completely abolished by siRNA. CDK7 was reduced by ~ 50% (Figure 4B).
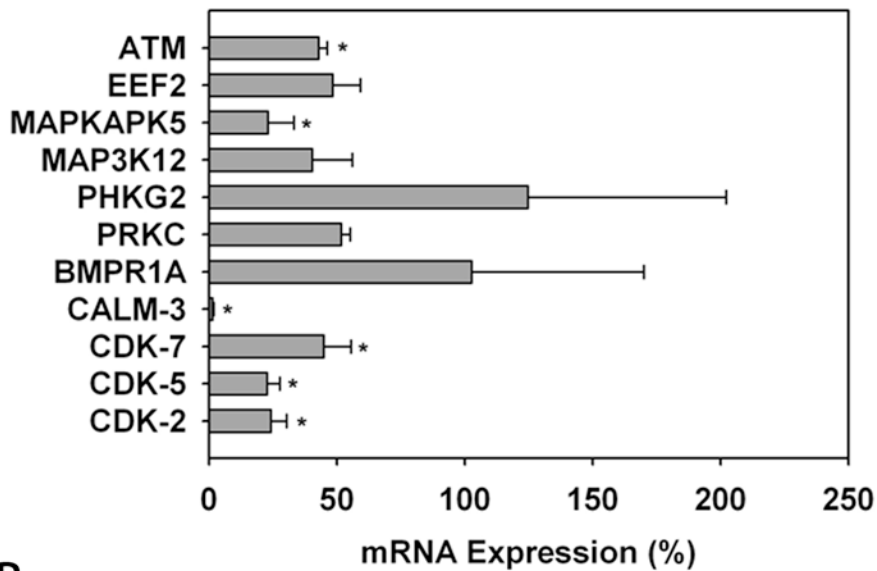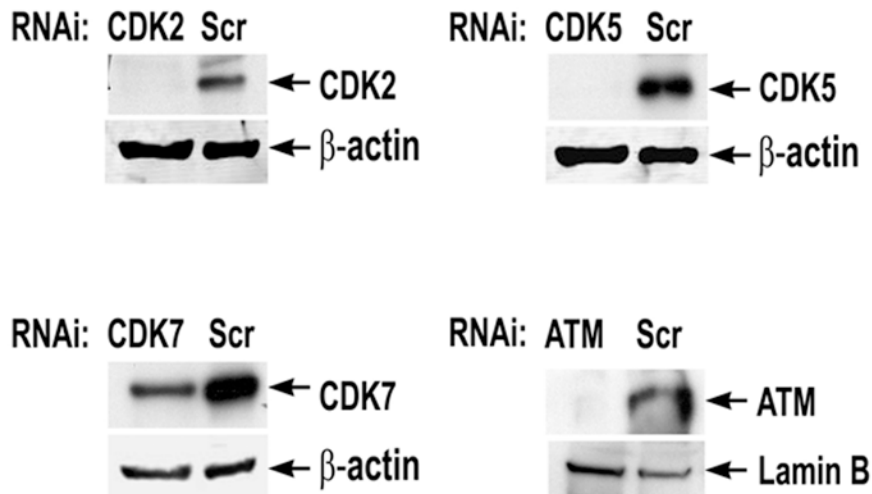
Figure 4. Validation of SiRNA knockdown. (A). siRNA knockdown of validation set. A549 cells were transfected with indicated siRNAs (EEF2, BMP1A, CALM3, CDK 7, ATM, CDK 2, CDK 5, PRKCζ, PHKG2, MAP3K12 and MAP3K5, as indicated at right). 72 h later, total RNA was extracted and level of each target was measured by Q-RT-PCR. Shown is the mRNA expression for each gene expressed as percentage of untransfected control (mean ± SD of triplicate plates). Data was analyzed by student t-test. *$p<0.05$, significantly different from scrambled siRNA treated samples. **(B)** Western blot to validate protein knockdown by their respective siRNA after 72 hr of transfection. β-actin was probed as a protein loading control; Lamin B was protein loading control for ATM due to its large size. Scr, scrambled siRNA.

The effect of successfully downregulated kinases was assessed on endogenous NF-κB induced gene expression. A549 cells were transfected with specific siRNAs to ATM, EEF2, MAPKAPK5, MAP3K12, CALM-3, CDK isoforms -2, -5, and -7. 48 h later, cells were stimulated in the absence or presence of TNF and the expression of TNFAIP3/A20, a highly inducible NF-κB dependent gene (160), was measured via Q-RT-PCR. Relative to scrambled controls, 25% inhibition of inducible TNFAIP3/A20 was observed after ATM knockdown, 50% inhibition was produced by MAP3K12, PRKCζ, IKKγ, and a >75% inhibition was observed for CDK-5, 7 and CALM3, respectively (Figure 5). No significant inhibition of inducible TNFAIP3/A20 expression was observed for MAPKAPK5 or EEF2, and an apparent induction was observed for CDK-2, indicating that these latter kinases may have been false positives generated from the screening assay.
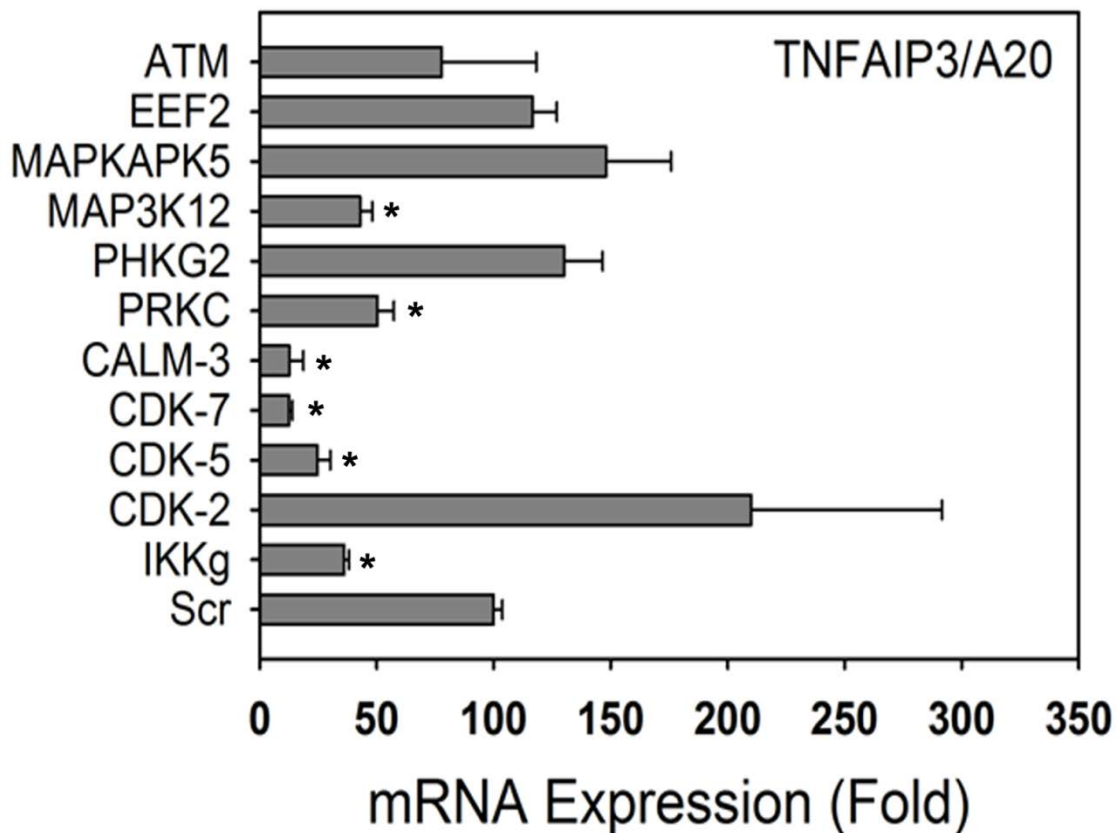
Figure 5. siRNA knockdown on TNF inducible endogenous NF-κB dependent gene expression. A549 cells were reverse transfected with siRNAs to the indicated kinases for 72 h prior to TNF stimulation and RNA extraction. The X- axis is fold change of TNF-stimulated relative to unstimulated value (mean ± SD of triplicate plates), and the Y axis, the target gene (TNFAIP3A20 mRNA) mRNA. Data was analyzed by student t-test. *$p < 0.05$ significantly different from scrambled siRNA treated samples. Scr, scrambled siRNA.

Similar qualitative effects on TNF-induced TNFAIP3/A20 expression was observed in HEK293 cells, with the exception of CDK2 and MAP3K12, which did not affect TNFAIP3/A20 expression in HEK293 cells (data not shown). These results suggest that the role of ATM, MAP3K12, PRKC, CALM-3, CDK -7, -5, and -2 in TNF signaling is not specific to A549 cells.

To determine whether these kinases were important in inducible transcription of any stimulus type, we examined the effect of siRNA knockdown on IL-6-Jak_STAT3 signaling. Silencing ATM, MAP3K12, PRKC, CALM-3, CDK -7, -5, and -2 did not affect IL6-induced SOCS3 expression (data not shown).

We next sought to initially identify the regulatory step that each kinase had in NF-κB canonical activation. For this purpose, the magnitude of RelA translocation was assayed after siRNA mediated silencing of CDK-2,-5,-7, CALM3, PRKCζ and ATM. TNF inducible RelA translocation was significantly inhibited for the CDK-2,-5 and -7 isoforms, with a smaller effect seen for CALM3, PRKCζ and ATM (data not shown).

The finding that ATM had a weak inhibitory activity on TNFAIP3/A20 expression was difficult to interpret, but may have occurred because the level of ATM knockdown produced by the siRNA transfection was only ~50% (Figure 4). ATM is a member of the PI3K family that has been implicated in double-stranded break-induced NF-κB activation in response to genotoxic stress; this mechanism involves its nuclear activation (phosphorylation at serine 1981), association with IKKγ and consequent export into the cytoplasm (141).

Because the role of ATM in extracellular TNF signaling is unknown, we therefore sought to further explore its role the canonical NF-κB signaling pathway. We first

sought to ask whether TNF activates ATM by measuring formation of phospho-ATM in a time course of TNF stimulation. Figure 6A shows that TNF (30 ng/ml) treatment increases ATM phosphorylation starting from 15 min and peaking at 30 min in A549 cells. Moreover, the magnitude of ATM activation is qualitatively similar to that produced by the etoposide-induced DNA damage pathway (Figure 6A). To understand which regulatory step ATM affects in the canonical NF-κB activation pathway, we asked if ATM is required for IκBα degradation and/or RelA nuclear translocation, the two key steps in the NF-κB activation pathway. Although TNF stimulation resulted in an increased IκBα degradation and RelA nuclear translocation in ATM wild-type mouse embryonic fibroblasts (MEFs) however, both of these processes were significantly reduced in ATM$^{-/-}$ MEFs, especially at 15 min of TNF treatment (Figures 6B and C). Additionally, ATM deficiency leads to decreased RelA phosphorylation. Here, TNF induced RelA Ser 536 phosphorylation at 15 min in both ATM$^{+/+}$ and ATM$^{-/-}$ MEFs, only RelA Ser 276 phosphorylation was only detected in ATM$^{+/+}$ cells (Figure 6D). Taken together, these results clearly suggest that ATM is involved in a regulatory step controlling the initial phase of IκBα degradation, RelA release and Ser 276 phosphorylation in the TNF-induced NF-κB activation pathway.
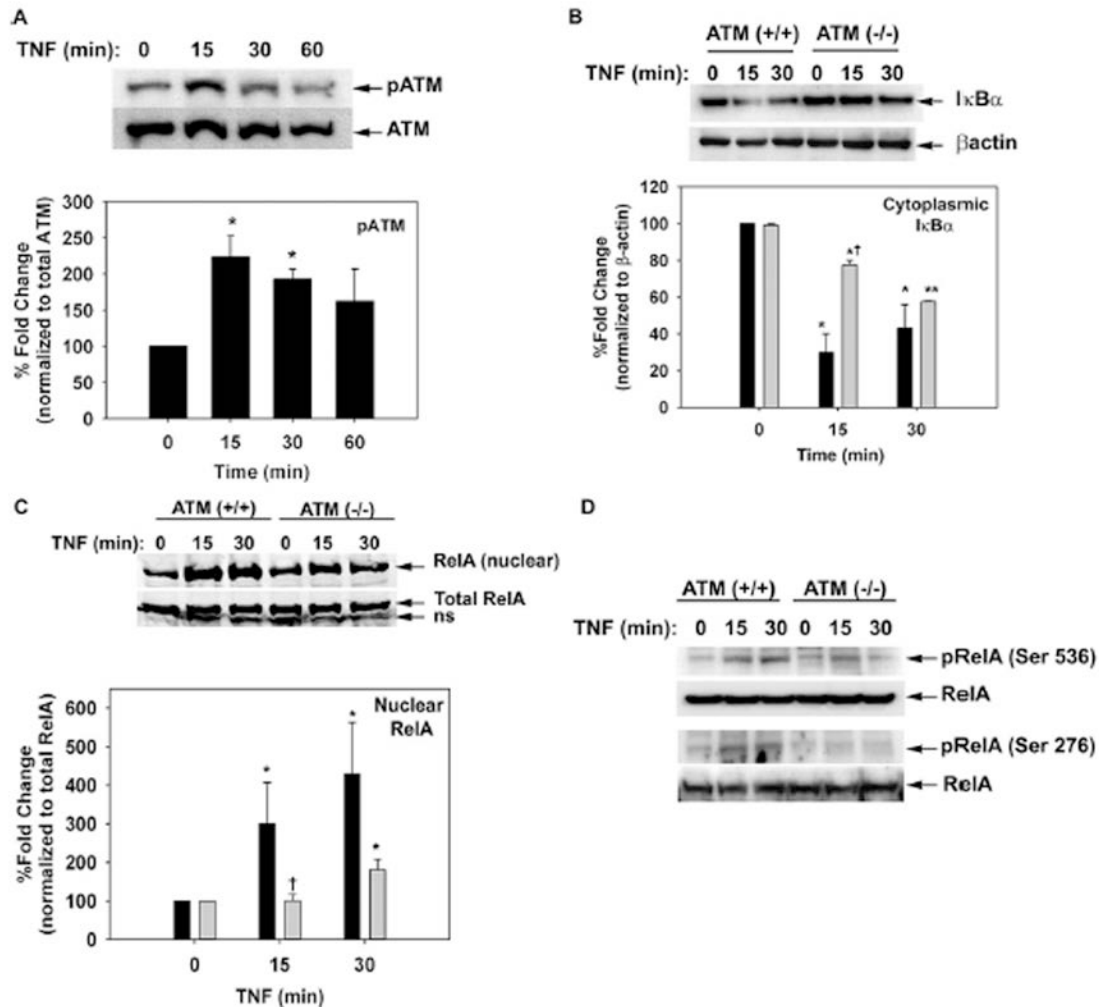
Figure 6. TNF-induced ATM activationand role in NF-κB signaling. (A) A549 cells treated with TNF (30 ng/ml) for various time intervals and immunoblotted for pATM (Ser1981). Western blot analysis showing increased ATM phosphorylation after TNF treatment. Cells treated with etoposide (10 μM), a known DNA damage-inducing agent served as a positive control. **(B)** Wild type (ATM^{+/+}) and ATM-deficient (ATM^{-/-}) MEFs were stimulated in the absence or presence of TNF (30 ng/ml) for indicated times followed by nuclear and cytoplasmic extraction. Relative amounts of cytoplasmic IκBα were quantified by Western blot; shown is normalized signal of the specific band to β-actin loading control. Upper panel shows TNF-induced IκBα degradation in ATM^{+/+} (dark bars) and ATM^{-/-} (light bars) cells whereas lower panel shows a representative blot. **(C)** TNF-induced nuclear translocation of RelA in ATM^{+/+} (dark bars) and ATM^{-/-} (light bars) cells. Data represents % fold changed as compared to untreated cells after normalizing to total RelA. Lower panel is a representative Western blot. Shown is the mean ± SD of three independent experiments. Overall significance was determined using 2 way ANOVA. *$p < 0.05$ significantly different from untreated (0 hr) samples;

42

whereas †p<0.01 significantly different from ATM$^{+/+}$ using post-hoc t-test **(D)** A representative Western blot showing effect of ATM knockout on RelA phosphorylation. ATM$^{+/+}$ and ATM$^{-/-}$ cells were treated with TNF (30 ng/ml) for specified time intervals,lysed in RIPA buffer and immunoblotted for Ser phosphorylated RelA (Ser 536, top, or Ser 276, bottom). Total RelA was quantified as a loading control.

To separately confirm the effect of ATM siRNA, A549-Luc cells were pre-treated

with the PI3K inhibitor wortmanin or Ku-55933, a specific ATM inhibitor (161). We

observed that a TNF-inducible NF-κB reporter activity (750-fold) was now almost

completely inhibited by either Ku-55933 or wortmanin (Figure 7).
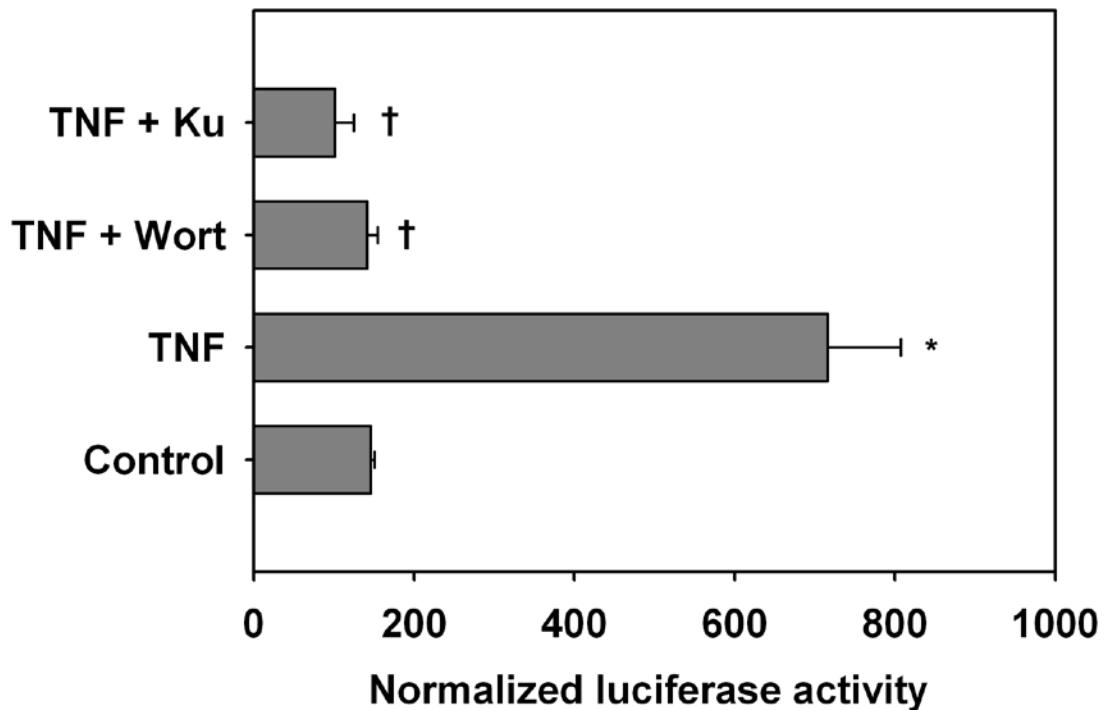
Figure 7. ATM kinase inhibition on TNF inducible reporter activity. NF-κB/Luc cells were pre-treated in the absence or presence of Ku55933 (40 µM) or Wortmanin (30 µM). Cells were then stimulated in the absence or presence of TNF (30 ng/ml, 6 h), lysed and normalized luciferase reporter activity (to protein) was measured. Shown is the mean ± SD of replicate plates. Overall significance

determined using 1 way ANOVA. *p<0.01 significantly different from control samples; whereas †p<0.01 significantly different from TNF-treated samples.

To quantify the transcriptional effect of ATM on the canonical pathway, ATM$^{+/+}$ and ATM$^{-/-}$ MEFs were stimulated with TNF for 0-1 h prior to the analysis of NF-κB dependent gene expression by Q-RT-PCR. We observed that 1 h of TNF treatment induced a 16-fold induction of TNFAIP3/A20 mRNA expression in ATM$^{+/+}$ MEFs, but was induced less than 4-fold in ATM$^{-/-}$ MEFs (Figure 8A). TNF stimulation induced a 5-fold increased expression of IκBα, a level that was not significantly different between the ATM$^{+/+}$ and ATM$^{-/-}$ cells (Figure 8B). Similar to the findings for TNFAIP3/A20, Groβ and KC gene expression was increased, in a TNF dependent fashion to, respectively, 28-fold and 9-fold, but the expression was significantly reduced in the TNF stimulated ATM$^{-/-}$ MEFs (Figures 8C and D). Previous work from our group has shown that the NF-κB dependent genes are inducible by several distinct mechanisms, with a subgroup of early response genes requiring activating phosphorylation of NF-κB/RelA at Ser 276, a site required for activation of a subgroup of inflammatory genes (158). Together, these data indicate that ATM is a regulator of NF-κB, mediating the canonical NF-κB activation pathway that activates a subset of dependent genes.
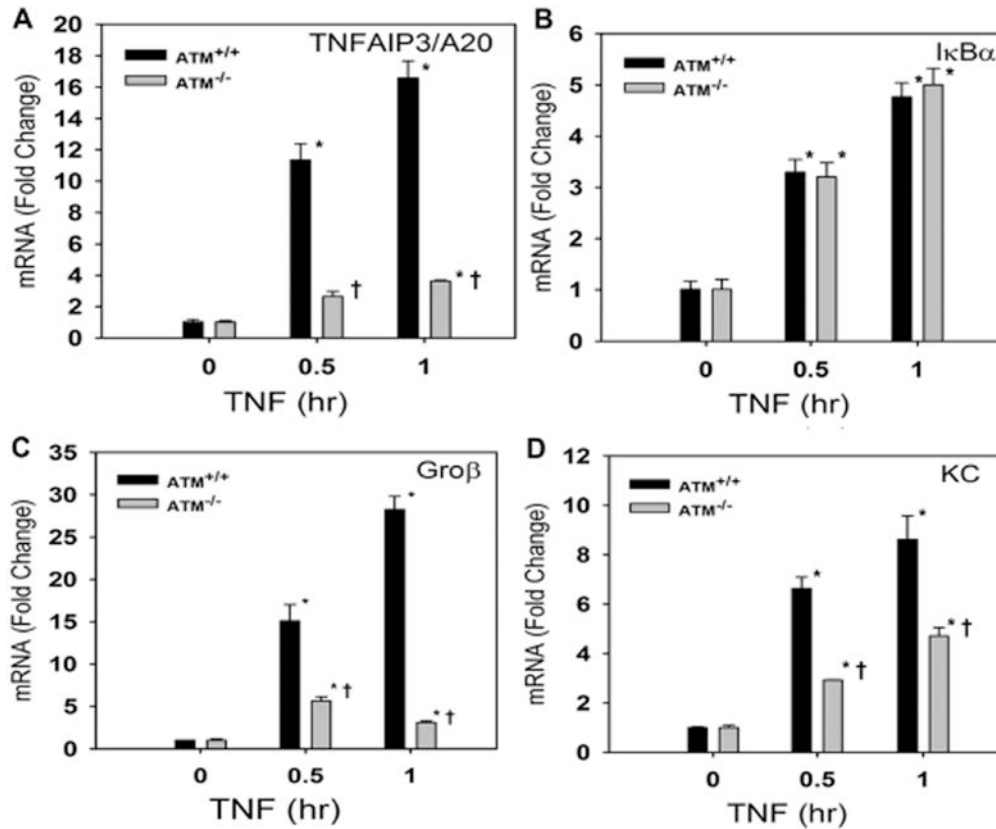
Figure 8. Effect of TNF stimulation in ATM$^{-/-}$ MEFs. Wild type (ATM$^{+/+}$) and ATM-deficient (ATM$^{-/-}$) MEFs were stimulated in the absence or presence of TNF (30 ng/ml) for indicated times, or with VP16. Total RNA was extracted and the expression of TNFAIP3/A20 (Panel A), IκBα (Panel B), Groβ (Panel C) and KC (Panel D) determined by Q-RT-PCR. Shown is fold change mRNA expression relative to unstimulated ATM$^{+/+}$ cells as calibrator. Data was analyzed by 2 way ANOVA with multiple comparison (time and treatment) and Tukey's post-hoc test for significance between time intervals and the treatment groups. Significantly different from control samples: $^*p<0.01$; and significantly different from TNF-treated samples: $†p<0.05$.

CHAPTER 4. ATM AND REGULATION OF THE NF-κB PATHWAY

4.1 TNF-induced ATM nuclear export requires IKKγ ubiquitination.

From the high throughput work, we discovered that 11 kinases potentially play important roles in TNF induced NF-κB activation. We also extended our study on ATM, and discovered its essential role in TNF induced NF-κB activation pathway in MEFs. Using ATM$^{+/+}$ and ATM$^{-/-}$ MEFs for these experiments has two obvious weaknesses: 1.Genetically engineered ATM knockout MEFs may have additional genes important to the inflammatory response altered. 2. MEFs are not fully mature and do not classically play a role in immune response systems. Therefore, to further validate our findings and investigate the details of mechanism, we conducted our research on A549 cell, an alveolar basal epithelial cell line, which provides a more representative in vitro model of the immune response.

In unstimulated cells, ATM resides in the nucleus as an inactive form. Following DNA double-strand breaks (DSBs), it undergoes autophosphorylation at Ser 1981 (123). ATM activation has been reported to be coupled with nuclear export in the DSBs DNA repair pathway (141). Therefore, we investigated whether a similar phenomenon happens upon TNF stimulation. Nuclear (NE) and cytoplasmic extracts (CEs) were prepared from cells stimulated with TNF and

assayed by Western immunoblot. First, Lamin B and β-tubulin were detected to characterize subcellular enrichment. Here, we observed that although the nuclear fractions stained strongly with Lamin B, the cytosolic fractions were largely devoid of nuclear contamination (Figure 9A). We next examined the distribution of ATM using anti-ATM Ab. Under unstimulated conditions, a ~350 kDa ATM band is primarily located in the nucleus and present in lower abundance in the cytosol. By contrast, after 0.25 hr of TNF stimulation, ATM is detected in the cytoplasmic fraction where it continues to accumulate until 1 hr of stimulation (Figure 9A). From this experiment, we concluded that TNF induces ATM nuclear-to-cytoplasmic transport.

In order to determine whether ATM auto-phosphorylation is required for TNF-induced nuclear export, we utilized the specific ATM kinase inhibitor, KU-55933 (161). A549 cells were pre-treated with the KU-55933 (10 μM, 1 hr) before TNF exposure. NE and CE were prepared and assayed by Western immunoblot. In the NE, phospho-Ser 1981 ATM (pATM) was observed in the absence of stimulation, whose abundance was strongly induced within 0.25 hr of TNF stimulation (Figure 9B). By contrast, a less basal level along with non-induction by TNF of pATM was observed upon the pretreatment of KU-55933 (Figure 9B). Correspondingly, the appearance of ATM in the CE was detected upon TNF stimulation while KU-55933 pretreatment completely blocked its cytoplasmic accumulation. Our observations that KU-55933 pretreatment completely blocks

TNF-induced pATM formation as well as cytoplasmic accumulation suggest that ATM auto-phosphorylation is prerequisite for its TNF-inducible nuclear export.

We have reported a significant and transient induction of ROS generation after TNF treatment as measured by H2DCF oxidation, increased in 8-oxoguanine (8-oxoG) DNA lesions, and by protein carbonylation (112). Although elevated ROS and 8-oxoG formation is usually associated with ssDNA breaks, we evaluated the possibility whether TNF treatment is sufficient to induce DNA double strand breaks (DSBs) and provide a potential mechanism of TNF-induced ATM activation and nuclear export. A549 cells were TNF treated for various times intervals followed by Neutral Comet assay, an assay that specifically detects DSBs (162). Etoposide (VP-16), which is a traditional drug to induce significant DSBs (144), is used as a positive control. A significant, but transient, increase in DSB level was observed after TNF exposure. A 2-fold increase in formation of DSB incidence was observed after 0.25 hr of TNF exposure that further increased to 2.5-fold at 0.5 hr before declining to untreated levels by the end of 1 hr exposure (Figure 9C, top panel). On the other side, VP-16 induced much higher level of DSBs, which indicate that TNF induced low-level of DSBs, but still enough to activate ATM. Representative microscopic images of comet moments after TNF stimulation is shown in Figure 9C (bottom panel). These data suggest that TNF induces DSBs.

To ascertain whether TNF-induced ROS generation is essential for pATM formation and its subsequent nuclear export, A549 cells were pretreated with the free radical scavenger, DMSO (2% for 0.5 hr), that we have previously shown to be sufficient to block ROS formation without apparent cytotoxicity (112). CE and NE were prepared from a TNF time course in the presence or absence of DMSO. For NE, we observed an induction on pATM upon TNF stimulation, but surprisingly, DMSO pretreatment did not affect pATM formation (Figure 9D, top panel). By contrast, DMSO pretreatment blocked the rapid kinetics of cytoplasmic accumulation of ATM. Here, we noted that in the absence of DMSO, cytoplasmic ATM is detectable within 0.25 hr, whereas in the presence of DMSO, cytoplasmic ATM does not peak until 1 h (Fig. 9D, middle panel).). To further validate our surprising findings, we utilized another chemically unrelated ROS inhibitor, NAC (N-acetyl cysteine) (163), to see whether pretreatment affects ATM phosphorylation and ATM export. Similar to the results of the DMSO pretreatment, NAC pretreatment blocked ATM export without affecting pATM formation (Figure 9E). This result suggests that TNF-induced ATM phosphorylation is ROS-independent. This data also suggests that ROS affects ATM cytoplasmic translocation in a step downstream of pATM formation (131).

Previous work showed that DSB-induced ATM export is IKKγ-dependent, where nuclear complex formation of pATM and IKKγ is prerequisite for NF-κB activation. In this mechanism, activated ATM phosphorylates IKKγ on Ser 85 to promote its ubiquitination (Ub) and nuclear export (141). Cytoplasmic export of the ATM·Ub-

IKKγ complex allows it to associate with and activate IKK, the rate-limiting step in NF-κB liberation from cytoplasmic stores. Therefore, we assessed if TNF-induced ATM nuclear export also is IKKγ-dependent. For this purpose, IKKγ$^{+/+}$ and IKKγ$^{-/-}$ MEFs were stimulated by TNF for various length times, CE were prepared and immunoblotted with anti-ATM Ab. ATM translocation into the cytosol was observed in IKKγ$^{+/+}$ MEFs, ATM export was completely blocked in IKKγ$^{-/-}$ cells suggesting that IKKγ is essential for TNF-induced nuclear export of ATM (Figure 9F).

Next we evaluated the effect of ROS on ATM·IKKγ complex formation. IKKγ was immunoprecipitated from NEs obtained from TNF treated A549 cells in the absence or presence of DMSO pretreatment. Levels of IKK-associated ATM were quantitated in the immunoprecipitates by Western blot. We noted that TNF induced ATM·IKKγ complex formation in a kinetic that matches with pATM phosphorylation and nuclear export. However, a distinct pattern was observed with DMSO pretreatment. Here, the ATM·IKKγ association was observed in DMSO only treated cells, and upon TNF stimulation, the abundance of the ATM•IKKγ complex reduced over time (Figure 9G). These data suggests that TNF-inducible ATM•IKKγ interaction is ROS dependent (Figure 9G). Previous studies have shown that IKKγ ubiquitination at Lys 285 is essential for ATM-NF-κB pathway (164). The ore, to further understand the role of TNF-induced ROS on ATM•IKKγ binding and subsequent nuclear export, we assessed its effect on

IKKγ ubiquitination. For this measurement, NEs from A549 cells stimulated with TNF with or without DMSO pretreatment were used. Ubiquitinated nuclear proteins were enriched by immunoprecipitation in native extracts using an ubiquitin-specific Ab. IKKγ was quantified by a quantitative, selected reaction monitoring-mass spectrometry (SID-SRM-MS) assay using a prototypic peptide that detects unmodified IKKγ. Within 0.25 h of TNF treatment, Ub-associated IKKγ levels increased by 2.5-fold over untreated cells and persisted for 1 h. However, DSMO pretreatment completely blocked Ub association with IKKγ (Figure 9H). Previous studies have shown that unanchored polyubiquitin chains existing in the cells play essential roles in innate cell signaling pathways (165,166). We therefore investigated whether the increased level of Ub associated with IKKγ comes from conjugated or unconjugated polyubiquitin. NEs were immunoprecipitated with anti-IKKγ Ab and the formation of ubiquitin adducts measured by Western blot using anti-ubiquitin Ab. No adducts could be detected (data not shown). We additionally probed the Western blot using anti-IKKγ Ab. Only a single IKKγ band was detected without any additional higher molecular weight species (Figure 9I). These data suggest that ROS induce IKKγ binding to free polyubiquitin chains, or the abundance of the covalently linked IKKγ is below the limit of detection of our assay. Overall, our data suggests that TNF-induced DNA DSBs activates ATM and nuclear export. Additionally our data suggest that TNF-induced ROS is required for ATM export through affecting Ub-IKKγ-complex formation and ATM association.
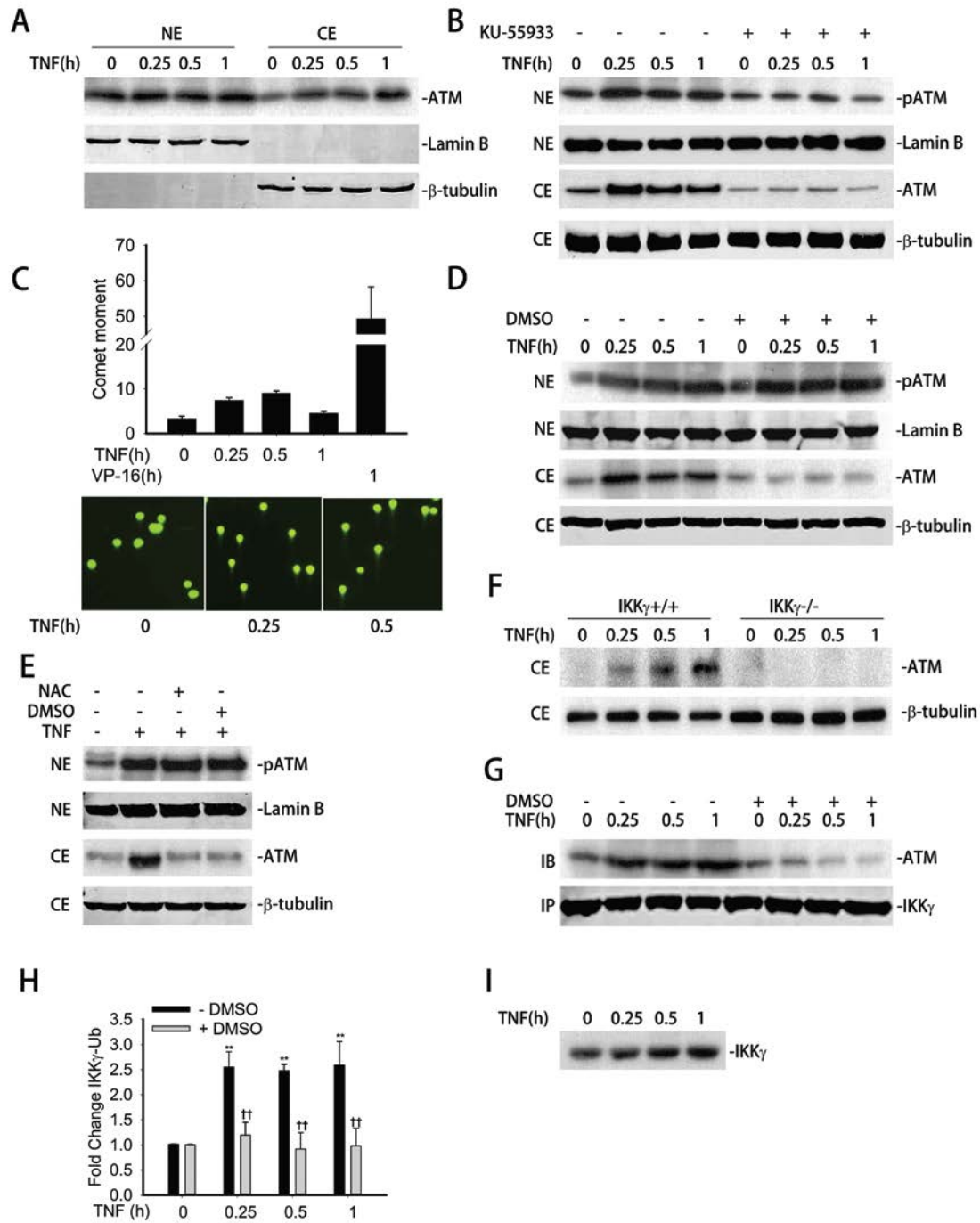
51

Figure 9. TNF-induced ATM activation and nuclear export. (A) A549 cells were treated with TNF (30 ng/ml) for the indicated time. Equal amounts of nuclear extract (NE) and cytoplasmic extract (CE) were analyzed by WBs to detect the level of ATM in both NE and CE. Lamin B and β-tubulin were also detected as internal control for NE and CE, respectively. **(B)** A549 cells were

treated with TNF (30 ng/ml) for the indicated time with or without the pretreatment of KU-55933 (10 μM, 1 h). Equal amounts of NE and CE were analyzed by WBs to detect the level of pATM and ATM, respectively. Lamin B and β-tubulin were also detected as internal control for NE and CE, respectively. **(C)** Top panel. A549 cells were treated with TNF (30 ng/ml) or VP-16 (10 μM) for the indicated time and then assayed by neutral comet assay. 100 cells from each time interval were quantitated. Bottom panel. Representative images of comet moments. **(D)** A549 cells were treated with TNF (30 ng/ml) for the indicated time with or without the pretreatment of DMSO (2% in vol, 0.5 h). Equal amounts of NE and CE were analyzed by WBs to detect the level of pATM and ATM, respectively. Lamin B and β-tubulin were also detected as internal control for NE and CE, respectively. **(E)** A549 cells were treated with TNF (30 ng/ml) for 1 h with or without DMSO (2% in vol, 0.5 h) or NAC (15 mM, 1 h) pretreatment. Equal amounts of NE and CE were extracted and analyzed by WBs to detect the level of pATM and ATM, respectively. Lamin B and β-tubulin were also detected as internal control for NE and CE, respectively. **(F)** IKK$\gamma^{+/+}$ and IKK$\gamma^{-/-}$ MEFs were treated with TNF (30 ng/ml) for the indicated time. Equal amounts of CE were analyzed by WB to detect the level of ATM. β-tubulin were detected as internal control. **(G)** A549 cells were treated with TNF (30 ng/ml) for the indicated time with or without the pretreatment of DMSO (2% in vol, 0.5 h). Equal amount of NE were immunoprecipitated by IKKγ antibody. Interacting ATM were measured by WBs. **(H)** A549 cells were treated with TNF (30 ng/ml) for the indicated time with or without the pretreatment of DMSO (2% in vol, 0.5 h). Equal amount of NE were immunoprecipitated by Ubiquitin antibody and subjected to SID-SRM-MS analysis of IKKγ protein level. All of the values are presented as the ratios of native to SIS peptides. **(I)** A549 cells were treated with TNF (30 ng/ml) for the indicated times, Equal amount of NE were immunoprecipitated by anti-IKKγ Ab and assayed by Western blot using anti-IKKγ Ab. * Significantly different from TNF (0 h)-treated samples, $p<0.05$;** Significantly different from TNF (0 h)-treated samples, $p<0.01$; † Significantly different from ATM$^{+/+}$ samples, $p<0.05$; †† Significantly different from ATM$^{+/+}$ samples, $p<0.01$.

4.2 Cytoplasmic ATM is essential for TNF-α induced IκBα degradation through β-TrCP recruitment.

In our earlier report we observed a delay in TNF-inducible IκBα proteolysis and decreased RelA nuclear translocation in ATM$^{-/-}$ MEFs, suggesting a novel role of cytoplasmic ATM in facilitating IκBα degradation (167). Here, we further

extended this observation and sought to elucidate the mechanism by which ATM alters IκBα degradation. We first sought to reproduce the findings in human epithelial cells. ATM-directed shRNA decreased ATM expression by 80% (Figure 10A). IκBα degradation was measured in CEs using Western immunoblot. In control A549 cells, there was no marked IκBα degradation after 0.25 h; however, a rapid disappearance was observed 0.5 h after TNF treatment followed by IκBα resynthesis within 1 h. By contrast, in the ATM depleted cells IκBα degradation was significantly delayted, not being apparent until after 1 hr of TNF treatment (Figure 10B). Similar findings were observed in experiments using shRNA mediated ATM knockdown in Hela cells. IκBα was not affected after 0.25 h, but rapidly degraded 0.5 h in control shRNA-transfected cells. This proteolysis was blocked after ATM knockdown (Figures 10C and 10D). Together we conclude that ATM affects TNF-induced IκBα degradation.

Previous work has shown that TNFα activates the IKK complex, a rate-limiting kinase responsible for IκBα phosphorylation at Ser residues 32 and 36 in its NH2 terminal regulatory domain. Phospho-Ser 32/36 IκBα (pIκBα) is specifically bound by the β-TrCP ubiquitin ligase, triggering recruitment to the 26S proteasome and its degradation (168,169). We first investigated if ATM affects IκBα phosphorylation. pIκBα was detected in whole cell extracts (WCE) from time course of TNF stimulation in control or ATM knockdown A549 cells. In control shRNA-transfected cells pIκBα was detectable in unstimulated cells and

was depleted by 0.5 h, similar to the profiles for total IκBα degradation (Figure 10B). In contrast, pIκBα accumulates immediately after TNF stimulation in ATM shRNA-transfected cells, and persists throughout the time course (Figure 10B). Similar findings were observed in shRNA mediated HeLa cells (Figure 10D). These results demonstrate that pIκBα is stabilized in ATM-deficient cells.

To confirm the effects of ATM on stabilizing pIκBα levels, WCEs from a time course of TNF stimulation in ATM$^{+/+}$ and ATM$^{-/-}$ MEFs were prepared and total IκBα was immunoprecipitated. The level of IκBα was then detected by Western immunoblot. ATM$^{+/+}$ MEFs showed a low level of pIκBα in untreated cells. By contrast, there was an accumulation of pIκBα in ATM$^{-/-}$ MEFs (Figure 10E). Although the level of pIκBα was difficult to detect in ATM$^{+/+}$ cells due to its proteolysis, the abundance of pIκBα in ATM$^{-/-}$ MEFs showed marked accumulation compared to that of ATM$^{+/+}$ MEFs (Figure 10E). To further extend these findings, the same experiment was done using control shRNA- and ATM shRNA-transfected A549 cells. A similar result was observed (data not shown). These data further suggest that pIκBα stabilization is a consistent finding for ATM$^{-/-}$ MEFs and ATM knockdown human cell lines.

To exclude the potential role of ATM in upstream effects on the TNF signaling pathway, we examined pIKKβ activation, the kinase directly upstream of IκBα (43). WCE from TNF stimulated control- and ATM knockdown A549 cells

were assayed by Western blot using anti-pIKKβ Ab. We observed indistinguishable induction of pIKKβ in both cell lines (Figure 10F). We therefore conclude that TNF induced pIKKβ formation is ATM-independent.

Recruitment of β-TrCP to pIκBα is essential for its ubiquitination and proteolysis. One explanation could be that the differences in IκBα proteolysis were due to differences in β-TrCP expression. To address this possibility, CEs from TNF stimulated ATM$^{+/+}$ and ATM$^{-/-}$ MEFs were prepared and assayed for steady-state β-TrCP levels. We observed that the level of β-TrCP protein expression was identical in ATM$^{+/+}$ and ATM$^{-/-}$ (Figure 10F). Therefore, we assessed whether ATM influenced formation of the IκBα·β-TrCP complex. In this experiment ATM$^{+/+}$ and ATM$^{-/-}$ MEFs pre-treated with MG132 (to block proteosomal activity) were stimulated with TNF. IκBα complexes were enriched by immunoprecipitation and β-TrCP level detected by immunoblot. In ATM$^{+/+}$ cells, β-TrCP was engaged with IκBα at a low level in the absence of stimulation, and transiently increased after 0.25 hr of treatment (Figure 10G). A subsequent decline in the abundance of the complex was seen after 0.5 hr. By contrast, the basal IκBα·β-TrCP interaction was significantly decreased in ATM$^{-/-}$ MEFs, and was not detectable until after 1 hr of stimulation (Figure 10H). To extend these findings, this experiment was also conducted in control- and ATM shRNA-transfected HeLa cells, where different kinetics of β-TrCP and IκBα association was observed (data not shown).

56

Since β-TrCP also targets NF-κB2/p100 for ubiquitin-mediated proteolysis, we asked whether ATM deficiency affects NF-κB2/p100 binding in response to noncanonical pathway activation (170). For this purpose, control- or ATM shRNA-transfected A549 cells were pre-treated with the proteasome inhibitor MG132 and subsequently TNF stimulated for 1 and 3 h, time points reported to induce p100 processing and non-canonical pathway activation in A549 cells (60). NF-κB2/p100-β-TrCP association was measured by NF-κB2/p100 Western blot of β-TrCP immunoprecipitates. We detected induction of NF-κB2/p100-β-TrCP association at equivalent levels in both ATM replete and ATM knockdown cells (data not shown). Taken together, we conclude that cytoplasmic ATM is specifically required for β-TrCP-pIκBα complex formation, essential for rapid pIκBα proteolytic degradation in response to TNF treatment.

We next tested whether ATM participates in the IκBα·β-TrCP complex. β-TrCP was immunoprecipitated from CEs from TNF-exposed A549 cells and the bound ATM was detected by Western blot. In the absence of stimulation, little ATM is associated with β-TrCP. However, TNF induced a rapid induction of ATM binding (Figure 10I). In this assay, p53, a protein known to bind ATM upon VP-16 addition (171), served as a positive control. The same experiment was also conducted in ATM-replete HeLa cells; similar results were obtained (data not shown).

Since different kinetics of IκBα degradation was observed in control shRNA- and ATM shRNA-transfected A549 cells, we further investigated the effects of ATM depletion on RelA nuclear translocation. For this experiment, NE from TNF stimulated control- or ATM shRNA-transfected A549 cells were prepared and assayed for RelA by Western blot. In control shRNA-transfected A549 cells, a significant induction of RelA translocation was observed within 0.25 h, peaking within 0.5 h. By contrast, in ATM shRNA-transfected A549 cells, a decreased, but still obvious induction was observed (Figure 10J). The different kinetics of RelA nuclear translocation is consistent with the different kinetics of IκBα degradation in these cell lines (Figures 10B, D).

Taken together, these findings clearly suggest a novel role of cytoplasmic ATM to bind and recruit β-TrCP to pIκBα. This finding explains the differences of kinetics in IκBα degradation, reduced β-TrCP·IκBα binding, and stabilization of pIκBα in ATM-deficient cells.
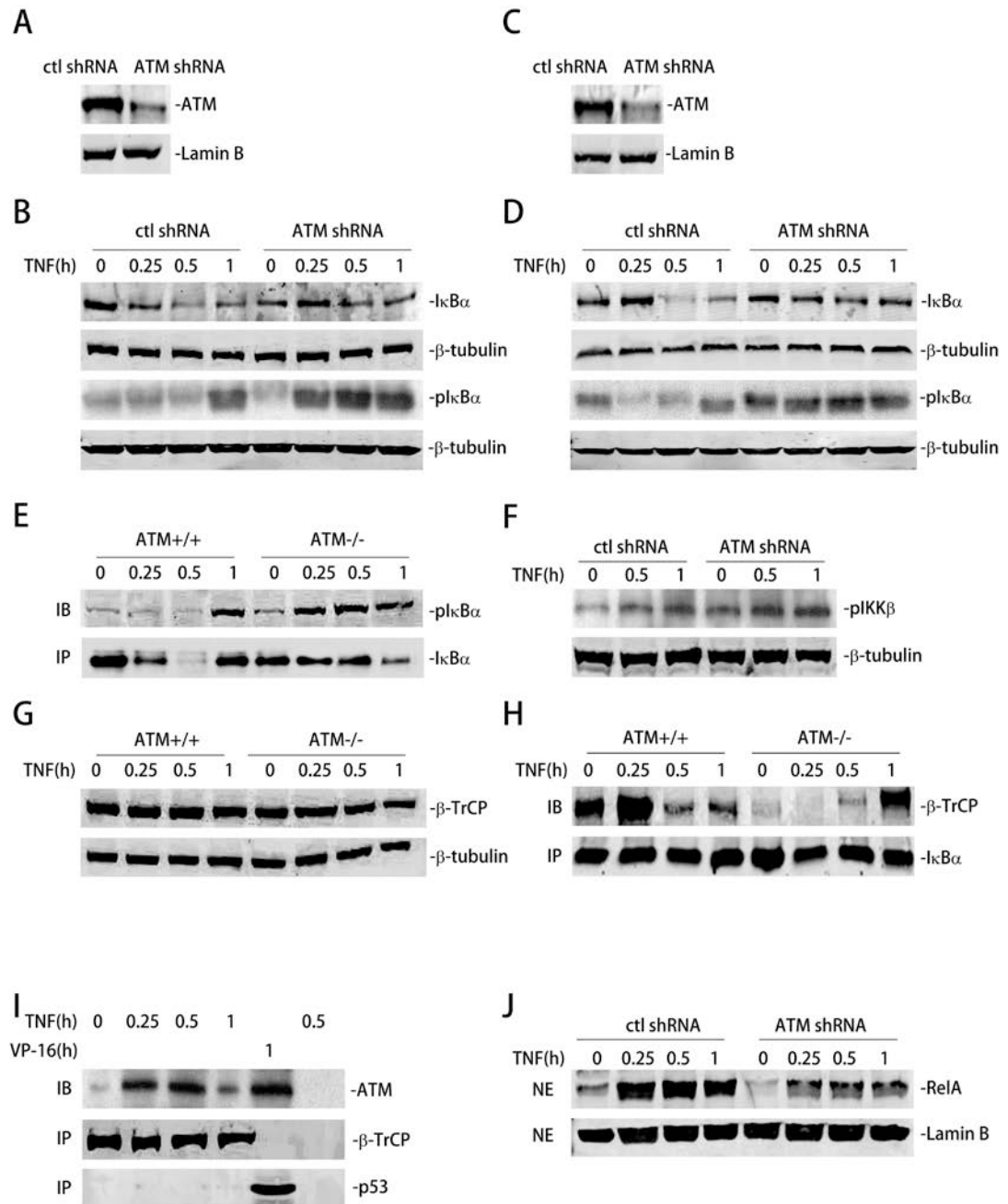
Figure 10. ATM is essential for IκBα degradation by recruiting β-TrCP. (A) A549 cells were transfected with ATM shRNA. 72 h later, equal amounts of NE were analyzed by WB to detect ATM. Lamin B were detected as internal control. **(B)** Control shRNA and ATM shRNA knockdown A549 cells were treated with TNF (30 ng/ml) for the indicated time. Equal amounts of CE were analyzed by

WBs to detect the level of total IκBα and pIκBα. β-tubulin were detected as internal control. **(C)** HeLa cells were transfected with ATM shRNA. 72 h later, equal amounts of NE were analyzed by WB to detect ATM. Lamin B were detected as internal control. **(D)** Control shRNA and ATM shRNA knockdown HeLa cells were treated with TNF (30 ng/ml) for the indicated time. Equal amounts of CE were analyzed by WBs to detect the level of total IκBα and pIκBα. β-tubulin were detected as internal control. **(E)** ATM$^{+/+}$ and ATM$^{-/-}$ MEFs were treated with TNF (30 ng/ml) for the indicated time. Equal amount of CE were immunoprecipated by IκBα antibody. pIκBα levek were measured by WBs. (**F**) Control shRNA and ATM shRNA-transfected A549 cells were TNF treated (30 ng/ml) for the indicated times. Equal amounts of WCE were analyzed by Western blot using anti-pIKKβ Ab. β-tubulin was used as an internal control. **(G)** ATM$^{+/+}$ and ATM$^{-/-}$ MEFs were treated with TNF (30 ng/ml) for the indicated time. Equal amount of CE were were analyzed by WB to detect β-TrCP. β-tubulin were detected as internal control. **(H)** ATM$^{+/+}$ and ATM$^{-/-}$ MEFs were pre-treated with MG132 prior to treatment with TNF (30 ng/ml) for the indicated time. Equal amount of CE were immunoprecipated by IκBα antibody. Interacting β-TrCP were measured by WBs. **(I)** A549 cells were treated with TNF (30 ng/ml) or VP16 (10 μM) for the indicated time. Equal amount of CE were immunoprecipated by β-TrCP antibody (lane 1-4), p53 antibody (lane 5) or rabbit preimmune serum (lane 6). Interacting ATM were measured by WBs. **(J)** Control shRNA and ATM shRNA-transfected A549 cells were treated with TNF (30 ng/ml) for the indicated times. Equal amounts of NE were analyzed by Western to detect the level of RelA. Lamin B was detected as internal control.

4.3 ATM is required for TNF induced NF-κB phosphorylation on Ser[276] through the PKAc pathway.

Once released from IκBα inhibition, RelA is required for induction of downstream genes (45,112). In this process, RelA is phosphorylated at Ser^{276} and/or Ser^{536} by distinct pathways (172,173). In particular we have observed that TNF induced phospho-Ser 276 RelA formation is ROS dependent, whereas phospho-Ser 536 RelA formation is ROS-independent (112). In order to examine whether ATM affects RelA phosphorylation on either Ser 276 or Ser 536, A549 cells were TNF-

stimulated in the absence or presence of KU-55933 pretreatment. WCE were prepared and total RelA enriched by immunoprecipitation. Phospho-RelA was then quantitated in the immunoprecipitates by SID-SRM-MS. We observed that TNF induced an 8-fold induction of phospho-Ser 276 RelA formation after 0.5 hr of treatment in control cells, whereas KU-55933 pretreatment significantly blocked phospho-Ser 276 RelA formation at all time points (Figure 11A). Quantitation of phospho-Ser 536 RelA formation showed that TNF induced a ~4.5-fold induction of phospho-Ser 536 RelA in a manner that was not KU-55933 sensitive (Figure 11B). A western blot also showed the same result upon TNF stimulation with or without the pretreatment of KU-55933 (Figure 11C).

To further validate the role of ATM in RelA phosphorylation, we measured phospho-Ser 276 RelA levels in ATM knockdown cells. Either empty shRNA-transfected or ATM shRNA-transfected A549 cells were treated with TNF for indicated times. WCE were collected and RelA was immunoprecipitated. Phospho-Ser 276 RelA formation was quantitated by immunoblot. As expected, TNF treatment increased phospho-Ser 276 RelA formation in control shRNA transfectants starting from 0.25-1 hr. However, TNF-induced phospho-Ser 276 RelA formation was significantly reduced in the ATM shRNA-transfected cells (Figure 11D).

To ensure the antibody specificity for detection of phospho-Ser 276 RelA(174), WCE from control or TNF stimulated RelA$^{+/+}$ and RelA$^{-/-}$ MEFs were prepared

and assayed by Western blot. We noted a significant induction of phospho-Ser 276 RelA band in ATM$^{+/+}$ MEFs while no signal was detected in ATM$^{-/-}$ MEFs. The blot with anti-RelA Ab proved the knockout of RelA in ATM$^{-/-}$ MEFs (Figure 11E).

Furthermore, we used RelA$^{+/+}$ and RelA$^{-/-}$ MEFs to validate the specificity of the IP-SRM assay for phospho-Ser 276 RelA. WCE from control or TNF stimulated RelA$^{+/+}$ and RelA$^{-/-}$ MEFs were prepared and immunoprecipitated by pan anti-RelA Ab. The abundanace of RelA and phospho-Ser 276 RelA were separately quantitated in the immunoprecipitates by SID-SRM-MS. Relative to that of RelA$^{+/+}$ MEFs, very little RelA signal was detected (<0.1%) in RelA$^{-/-}$ MEFs (Figure 11F, left panel). In RelA +/+ MEFs, phospho-Ser 276 RelA signal was detected and increased in response to TNF. Importantly, there was no signal of phospho-Ser 276 RelA detected in the RelA$^{-/-}$ MEFs (Figure 11F, right panel). These data support the specificity of IP-SRM to measure phospho-Ser 276 RelA.

Earlier we reported that RelA Ser 276 phosphorylation is mediated by redundant ribosomal S6 kinases, including mitogen-stress related kinase-1 (MSK1) and catalytic subunit of active cAMP-dependent protein kinase A (PKAc) (111,112). Since PKAc is an ROS- sensitive kinase that mediates phospho-Ser 276 RelA formation, we investigated if PKAc activity is regulated by ATM. For this purpose, a PKAc kinase activity assay was performed in TNF stimulated ATM$^{+/+}$ and ATM$^{-/-}$ MEFs. In ATM$^{+/+}$ MEFs, TNF induced a small, but significant increase in

incorporation into the PKAc peptide at 0.25 and 0.5 hr of stimulation (Figure 11G). When we examined the effect of ATM knockdown on MSK1 activation (phosphorylation at Ser 276), we did not observe any difference between wild type and ATM knockdown cells (data not shown). Together these data indicate that ATM is required for rapid induction of PKAc kinase activity in response to TNF treatment.

To investigate how ATM affects PKAc activity, we assessed whether ATM complexes with PKAc. PKAc was immunoprecipitated from control or TNF stimulated A549 cells and the immunoprecipitates were immunoblotted using anti-ATM Ab. In unstimulated cells, there was no detectable ATM. However, a strong ATM signal was observed 0.25 hr after TNF stimulation peaking at 0.5 hr (Figure 11H). p53, which is known to bind ATM upon VP-16 addition (171), serves as a positive control here. Overall, these data suggest that cytoplasmic ATM is essential for TNF-induced PKAc activation leading to RelA Ser 276 phosphorylation via a mechanism involving complex formation.
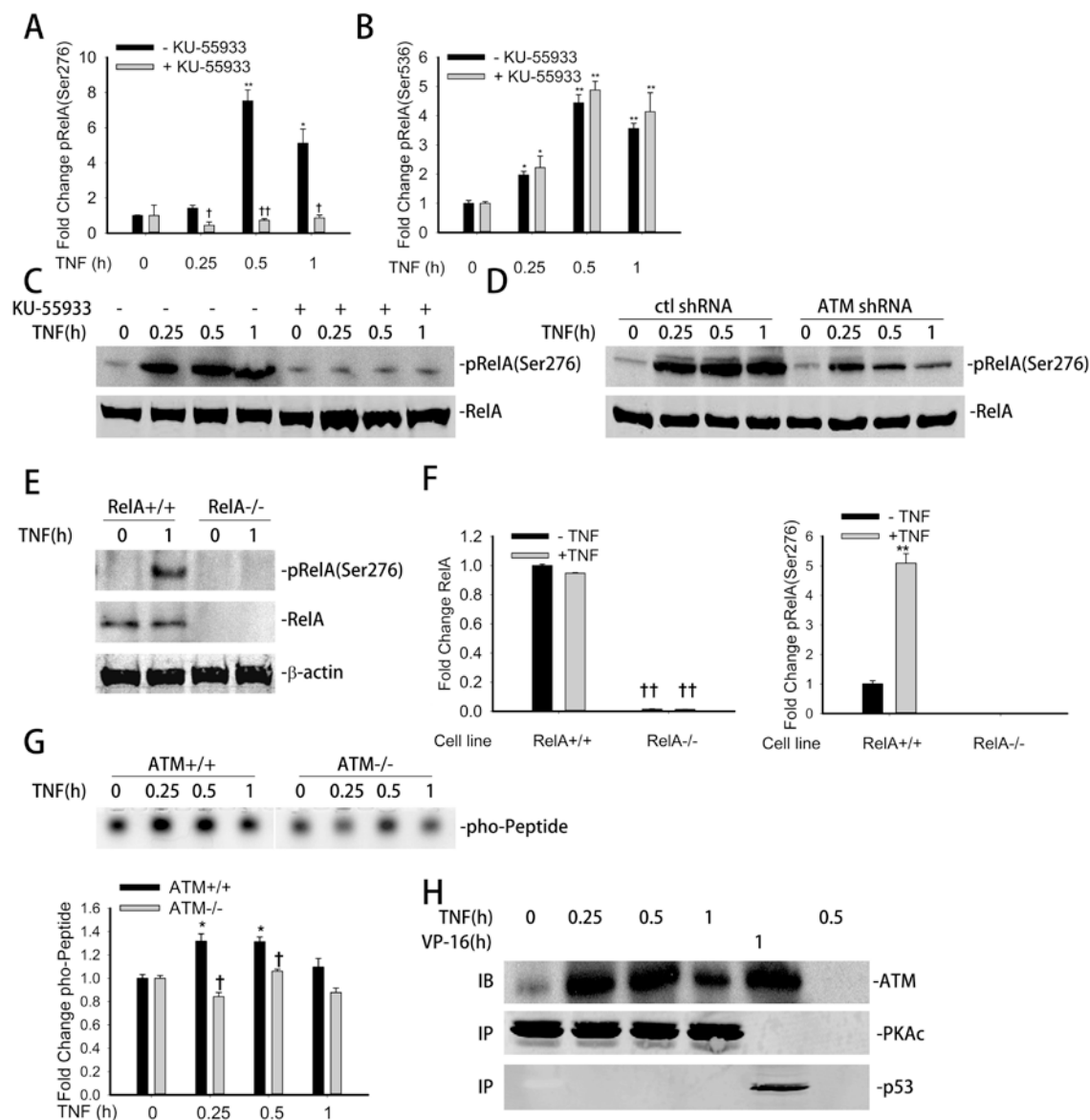
Figure 11. ATM is required for TNF induced RelA Ser 276 phosphorylation through PKAc pathway. (A) A549 cells were treated with TNF (30 ng/ml) for the indicated time with or without the pretreatment of KU-55933 (10 µM, 1 h). Equal amounts of WCE were immunoprecipitated by pan anti-RelA Ab and subjected for SID-SRM-MS analysis using a phospho-Ser 276 RelA proteotypic peptide. All

64

of the values are presented as the ratios of native to SIS peptides. **(B)** A549 cells were treated with TNF (30 ng/ml) for the indicated time with or without the pretreatment of KU-55933 (10 µM, 1 h). Equal amounts of WCE were immunoprecipitated by pan anti-RelA Ab and subjected for SID-SRM-MS analysis using a phospho-Ser 536 RelA proteotypic peptide. All of the values are presented as the ratios of native to SIS peptides. **(C)** A549 cells were treated with TNF (30 ng/ml) for the indicated time with or without the pretreatment of KU-55933 (10 µM, 1 h). Equal amounts of WCE were analyzed by WBs to detect the level of phospho-Ser 276 RelA. RelA were detected as internal control. **(D)** Control shRNA and ATM shRNA knockdown A549 cells were treated with TNF (30 ng/ml) for the indicated time. Equal amounts of WCE were analyzed by WBs to detect the level of phospho-Ser 276 RelA. RelA were detected as internal control. **(E)** RelA$^{+/+}$ and RelA$^{-/-}$ MEFs were treated with TNF (30 ng/ml) for 1 h. Equal amounts of WCE were assayed by Western blot using anti-RelA and anti-phospho-Ser 276 RelA Abs. β-actin was measured as internal control **(F)** Equal amounts of WCE from TNF treated RelA$^{+/+}$ and RelA$^{-/-}$ MEFs were immunoprecipitated by anti-RelA Ab and then applied for SID-SRM-MS analysis to determine the RelA and phospho-Ser 276 RelA abundance. All of the values are presented as the ratios of native to SIS peptides. **(G)** Top panel. ATM$^{+/+}$ and ATM$^{-/-}$ MEFs were treated with TNF (30 ng/ml) for the indicated time. WCE were collected and PKAc activity was measured with PepTag nonradioactive assay reagents as described in Materials and Methods. Bottom panel. Quantitation of the top panel. **(H)** A549 cells were treated with TNF (30 ng/ml) or VP16 (10 μM) for the indicated time. Equal amount of CE were immunoprecipitated by PKAc Ab (lane1-4), p53 Ab (lane 5) or rabbit preimmune serum (lane 6). Interacting ATM were measured by WBs.* Significantly different from TNF (0 h)-treated samples, p<0.05;** Significantly different from TNF (0 h)-treated samples, p<0.01; † Significantly different from ATM$^{+/+}$ samples, p<0.05; †† Significantly different from ATM$^{+/+}$ samples, p<0.01.

4.4 ATM is required for a NF-κB dependent immediate-early cytokine gene expression.

Previously, we have reported that ROS-inducible RelA phosphorylation on Ser 276 is a post-translationally modified state required for the transcription of a subset of rapidly inducible NF-κB dependent genes including the cytokines IL-8 and Gro-β, but not IκBα (112). Since ATM selectively affects RelA Ser 276

phosphorylation, we asked whether ATM is required for expression of these immediate- early genes. For this purpose, A549 cells were pre-treated in the absence or presence of KU-55933, TNF stimulated, and expression of NF-κB dependent gene expression performed by Q-RT-PCR. In the absence of KU-55933, TNF induced a 15-fold increase in Gro-β expression at 0.5- and 1 hr. This induction was significantly decreased by KU-55933 pretreatment (Figure 12A). A time dependent increase in IL-8 expression from 10 fold in 0.25 hr to 70 fold after 1 hr of TNF exposure was significantly blocked in cells pretreated with KU-55933 (Figure 12A). By contrast, IκBα, a gene whose expression is phospho-Ser 276 RelA independent (45), was induced to similar magnitude in control or KU-55933 treated cells (Figure 12A). A similar effect on Gro-β and IL-8 expression was observed in ATM shRNA-transfected A549 cells, with IκBα being unaffected (Figure 12B). An identical pattern was seen in HeLa cells transfected with ATM shRNA (Figure 12C).

Previous studies have shown that the physiological level of TNFα in human plasma is much lower than the levels used in our experimental design to produce maximum responses (175,176). Therefore we next tested the requirement for ATM on NF-κB dependent gene expression over a broad TNF dose-response range. For this experiment, control shRNA- or ATM shRNA-transfected A549 cells were stimulated by escalating TNF doses (0.3, 3, 30 ng/ml) and IL-8 gene expression measured by Q-RT-PCR. We observed a very sharp induction of IL-8 expression between 3 and 30 ng/ml, consistent with the known steep dose

response of TNF signaling. However, at all doses of TNF, IL-8 expression was reduced in ATM shRNA-transfected A549 cells (Figure 13). Therefore, we conclude that ATM is required for TNF induced NF-κB dependent gene expression over a broad physiological concentration range.

Overall, these studies demonstrated that ATM is required for the expression of a subset of phospho-Ser 276 RelA immediate early genes.
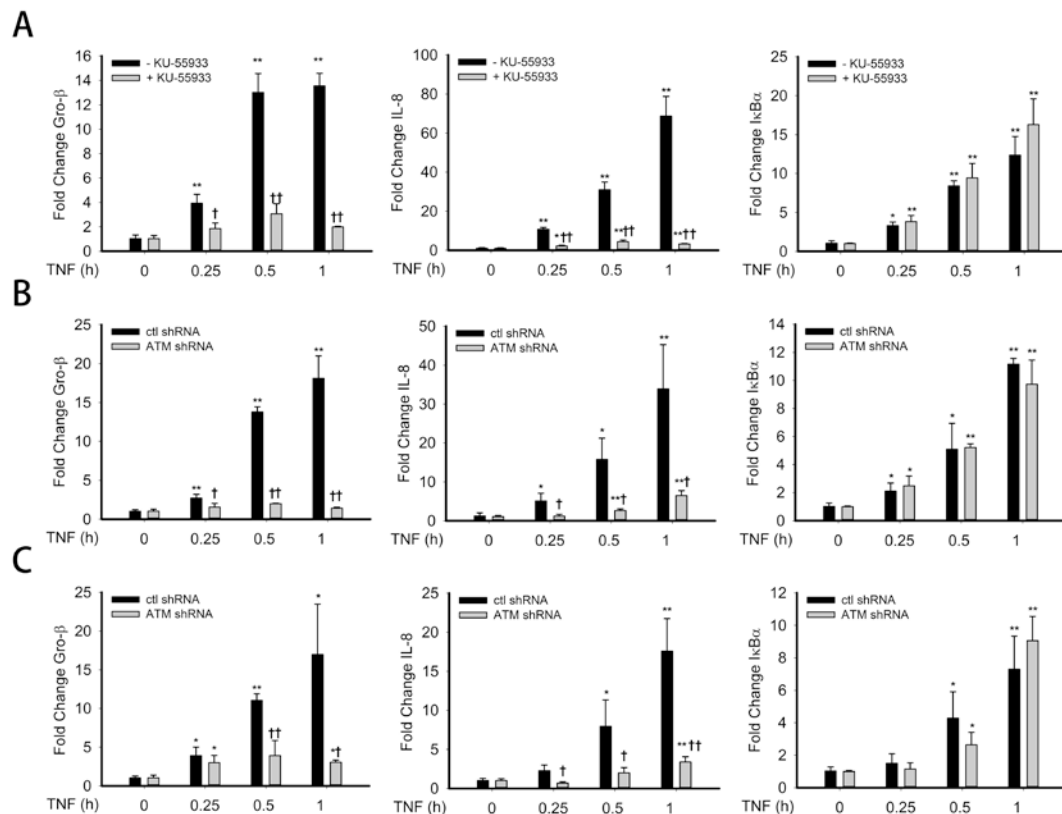
Figure 12. ATM in NF-κB dependent immediate-early cytokine gene expression. (A). A549 cells were treated with TNF (30 ng/ml) for the indicated time with or without the pretreatment of KU-55933 (10 µM, 1 h). Total RNA was extracted. The mRNA levels of Gro-β, IκBα, and IL-8 were measured. The results are expressed as fold change as compared with untreated cells after normalizing to internal controls, cyclophilin. Data represent the mean and STD of three independent experiments. **(B)**. Control shRNA and ATM shRNA knockdown

A549 cells were treated with TNF (30 ng/ml) for the indicated time with or without the pretreatment of KU-55933 (10 μM, 1 h). The experiment was performed as described for panel A. **(C)**. Control shRNA and ATM shRNA knockdown HeLa cells were treated with TNF (30 ng/ml) for the indicated time with or without the pretreatment of KU-55933 (10 μM, 1 h). The experiment was performed as described for panel A. * Significantly different from TNF (0 h)-treated samples, $p<0.05$;** Significantly different from TNF (0 h)-treated samples, $p<0.01$; † Significantly different from $ATM^{+/+}$ samples, $p<0.05$; †† Significantly different from $ATM^{+/+}$ samples, $p<0.01$.
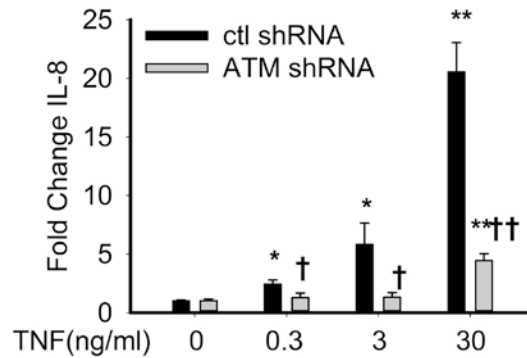
Figure 13. Dose titration of TNF induced IL-8 gene expression in ATM replete and knockdown cells. Control shRNA- and ATM shRNA-transfected A549 cells were treated with the indicated concentrations of TNF (1 h). Total RNA was extracted. The mRNA levels of IL-8 were measured. The results are expressed as fold change as compared with untreated cells after normalizing to cyclophilin as an internal control. * Significantly different from TNF (0 h)-treated samples, $p<0.05$;** Significantly different from TNF (0 h)-treated samples, $p<0.01$; † Significantly different from ATM WT samples, $p<0.05$; †† Significantly different from ATM WT samples, $p<0.01$.

4.5 ATM is required for recruiting RelA and co-activators to immediate-early gene promoters.

Earlier we have reported that phospho-Ser 276 RelA dependent gene expression is regulated via its interaction with CDK9 resulting in RNA polymerase II (RNA Pol II) phosphorylation on Ser 2 of the heptad repeat in the C terminal domain (CTD), a biochemical event necessary for expression of Gro-β and IL-8 (but not IκBα) genes (45). We therefore investigated role of ATM on targeting of CDK9 and RNA Pol II on IL-8, Gro-β and IκBα-containing chromatin by ChIP assay. For this purpose, A549 cells transfected with either control or ATM-specific shRNA were treated with TNF for the indicated times; chromatin was cross-linked and subjected to immunoprecitpitation with anti-RelA, CDK9 or phospho-Ser 2 Pol II Abs. Anti-rabbit IgG was used as a negative control. As expected, in control shRNA-transfected A549 cells, TNF induced a 6-fold recruitment of RelA (after 0.5 hr) and a 12-fold recruitment (after 1 hr) on the Gro-β promoter. However, in cells transected with ATM shRNA, RelA recruitment was significantly inhibited (less than 2-fold at these time points, Figure 14A). Similarly, TNF induction of CDK9 and phospho-Ser 2 RNA pol II recruitment was significantly induced in control shRNA transfectants and significantly inhibited in the ATM-shRNA transfectants (Figure 14A, middle and right panels).

A similar pattern of inhibition was observed for the IL-8 gene, whereas protein recruitment to the IκBα promoter was not affected (Figures 14B and 10C). These results provide a potential mechanism by which ATM-induced RelA posttranslational modifications regulate expression of a highly inducible subset of NF-κB-dependent genes.
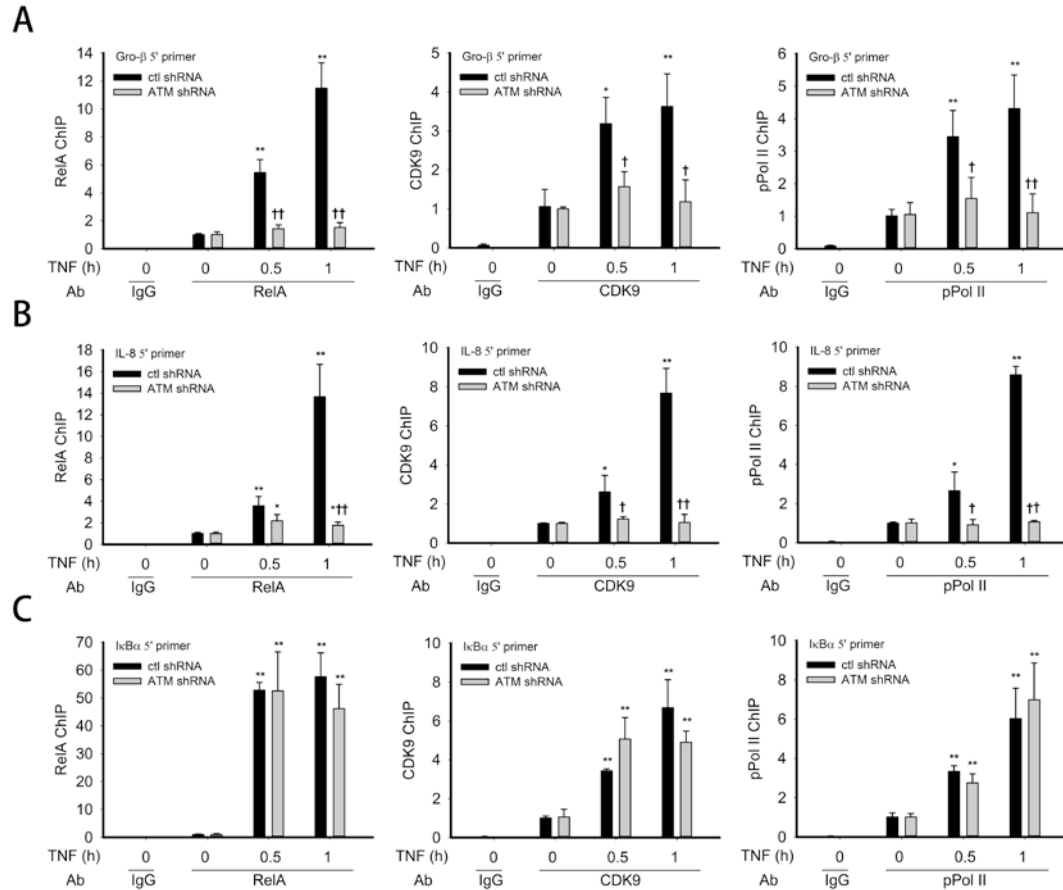
Figure 14. ATM in recruitment of RelA and co-activators to immediate-early gene promoters. **(A)** Control shRNA and ATM shRNA knockdown A549 cells were treated with TNF (30 ng/ml) for the indicated time. The corresponding chromatin was immunoprecipitated with anti-RelA, CDK9 and pPol II Abs. IgG was the negative control. Q-RT-PCR was performed using the Gro-β 5'primer set, and the fold change was calculated compared with unstimulated samples. **(B)** The experiment was performed as described for panel A. Q-RT-PCR was performed using the IL-8 5' primer set, and the fold change was calculated compared with unstimulated samples. **(C)** The experiment was performed as described for panel A. Q-RT-PCR was performed using the IκBα 5'primer set, and the fold change was calculated compared with unstimulated samples. * Significantly different from TNF (0 h)-treated samples, $p<0.05$;** Significantly different from TNF (0 h)-treated samples, $p<0.01$; [†] Significantly different from ATM$^{+/+}$ samples, $p<0.05$; [††] Significantly different from ATM$^{+/+}$ samples, $p<0.01$.

CHAPTER 5. ATM REGULATES ANTIVIRAL PATHWAY

5.1 The replication of RSV and Sendai virus is increased in ATM$^{-/-}$ A549 cells

Ataxia telangiectasia (A-T) is an autosomal recessive neurodegenerative disease results from the inactivation of the ATM kinase. The symptom of A-T patients includes immune deficiency. Therefore, we investigated whether ATM plays an essential role in antiviral response.

Human type II-like A549 airway epithelial cells productively replicate RSV and are a well-established model for the lower airway epithelial cell response to RSV infection study (80,177,178). Here we investigated the RSV replication in control shRNA- and ATM shRNA-transfected A549 cells. These 2 cell lines were inoculated with RSV and the protein level was measured by Western blot. 15 and 24 h after infection, a much more significant increase of RSV protein was observed in ATM shRNA-transfected A549 cells than control shRNA-transfected A549 cells (Figure 15A). To confirm our findings, RSV protein expressions were also evaluated by Q-RT-PCR. A 3-4 fold difference was observed in these 2 cell lines in both time intervals (Figure 15B). These results demonstrated an increased RSV replication in ATM shRNA-transfected A549 cells, which indicated a deficiency of immune response to RSV infection upon ATM depletion.

To investigate whether defective immune response is specific to RSV, or is a general deficiency to virus infection, we employed another ssRNA virus, Sendai virus (SeV), to further test the role of ATM in antiviral response. Similarly, more SeV protein was detected in ATM shRNA-transfected A549 cells than control shRNA-transfected A549 cells (Figure 15B) 12 h and 24 h after SeV infection. This result was also confirmed by Q-RT-PCR measurement (Figure 15D). Taken together, these results demonstrated an increased virus replication in ATM depleted A549 cells, which indicated an essential role of ATM in antiviral response.
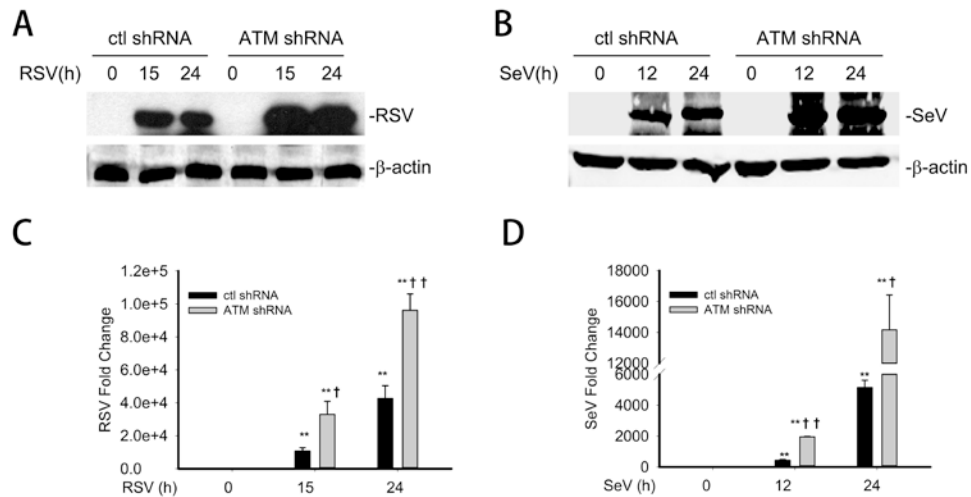
Figure 15. Enhanced RSV and Sendai virus protein expression in ATM knockdown cells. (A) Control shRNA and ATM shRNA knockdown A549 cells were infected with RSV (MOI, 1.0) for 0, 15, 24 h. Equal amount of WCE were analyzed by WBs to detect the level of RSV protein expression. β-actin were detected as internal control. (B) Control shRNA and ATM shRNA knockdown

A549 cells were infected with Sendai virus (MOI, 1.0) for 0, 12, 24 h. Equal amount of WCE were analyzed by WBs to detect the level of Sendai virus protein expression. β-actin were detected as internal control. (C) Control shRNA and ATM shRNA knockdown A549 cells were infected with RSV (MOI, 1.0) for 0, 15, 24 h. Total RNA was extracted. mRNA level of RSV N protein was measured. (D) Control shRNA and ATM shRNA knockdown A549 cells were infected with Sendai virus (MOI, 1.0) for 0, 12, 24 h. Total RNA was extracted. mRNA level of Sendai virus protein was measured. * Significantly different from RSV or SeV (0 h)-treated samples, $p<0.05$;** Significantly different from RSV or SeV (0 h)-treated samples, $p<0.01$; † Significantly different from ATM+/+ samples, $p<0.05$; †† Significantly different from ATM+/+ samples, $p<0.01$

5.2 RSV and poly(I•C) induced interferon and ISG expressions are ATM dependent

Our findings indicate a deficiency of innate immune response in ATM depletion cells upon RNA virus infection. To evaluate it, we examined the gene expression of interferon and ISG, which play a key role in antiviral response, in both control shRNA- and ATM shRNA-transfected cells after virus infection. Type I (INFα6 and IFNβ1) and type III interferon (IL28A) as well as ISG (ISG54) gene expression was examined.

In control shRNA-transfected cells, we found that mRNA transcript levels of INFα6, IFNβ1, IL28A and ISG54 genes were significantly increased 24 h after RSV infection to 80-fold, 90-fold, 45-fold and 50-fold, respectively. By contrast, in ATM shRNA-transfected cells, much less inductions of all these 4 genes were

observed 15 and 24 h after RSV infection (Figure 16A). These results indicate an essential role of ATM in RSV-induced IFN and ISG expressions.

We next quantified the dependence of ATM on poly(I•C)-induced IFN and ISG expressions. Similarly, in response to poly(I•C) stimulation, IFNα6, IFNβ1, IL28A and ISG54 mRNA transcript levels were significantly induced 6 h after electroporation of poly(I•C) by 120-fold, 140-fold, 40-fold and 10-fold changes, respectively in control shRNA-transfected cells. However, the inductions were significantly blocked in ATM shRNA-transfected cells (Figure 16B). Taken together, these results demonstrate the dependence of ATM in RSV- and poly(I•C)-induced INF and ISG expressions.
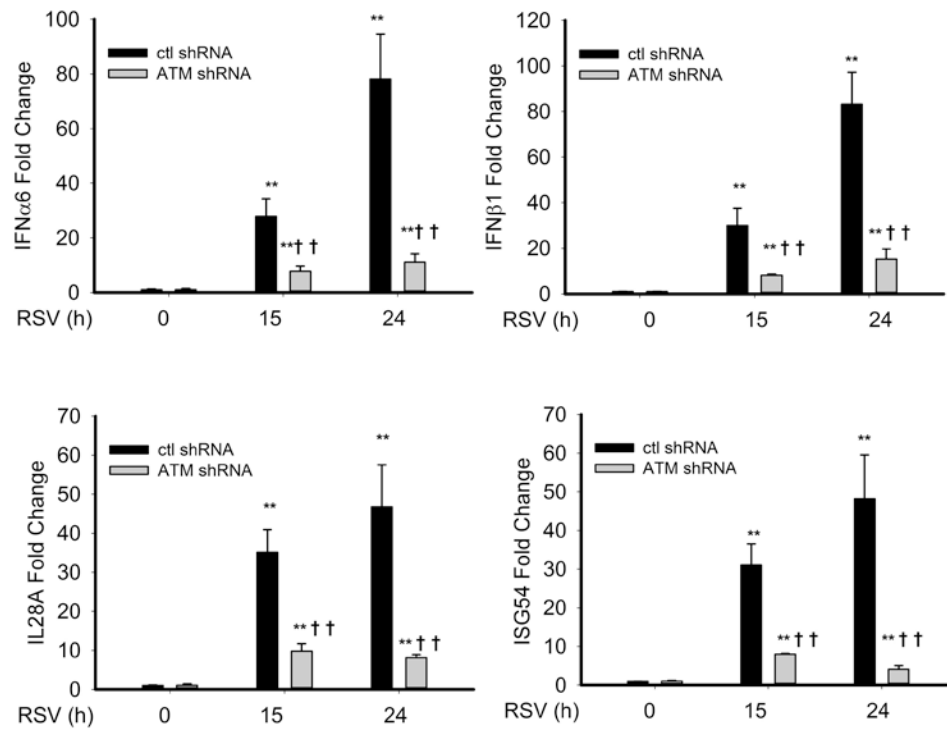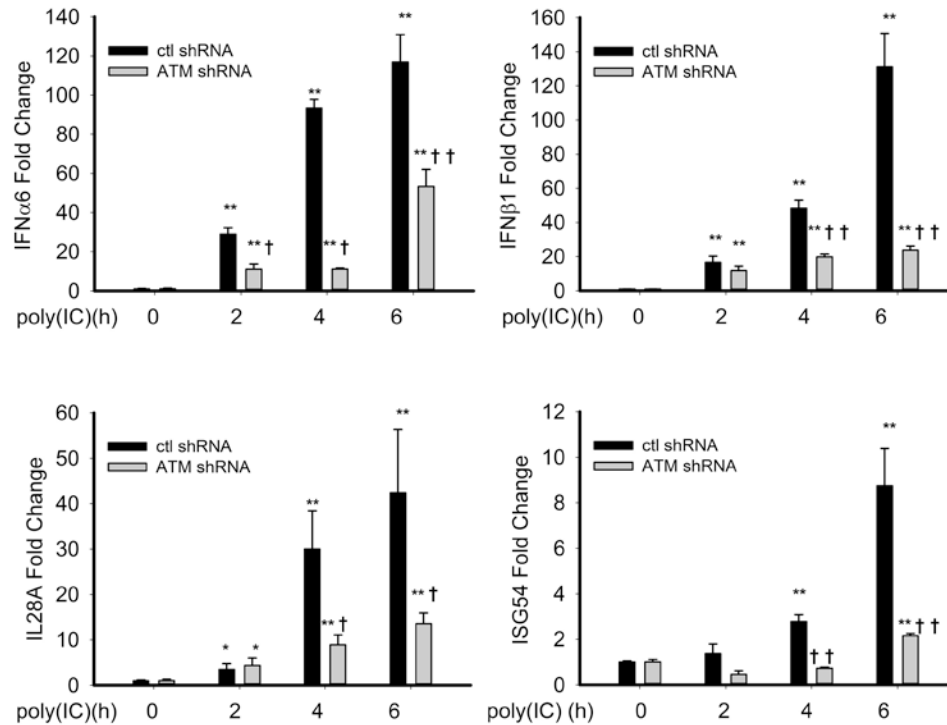
Figure 16. Suppressed IFNs and ISG expression upon RSV infection and poly(I•C) treatment in ATM knockdown cells. (A) Control shRNA and ATM shRNA knockdown A549 cells were infected with RSV (MOI, 1.0) for 0, 15, 24 h. Total RNA was extracted. mRNA level of IFNα6, INFβ1, IL28A and ISG54 were measured. **(B)** Control shRNA and ATM shRNA knockdown A549 cells were electroporated wit 10 μg poly(I•C) for 0, 2, 4, 6 h. Total RNA was extracted. mRNA level of IFNα6, INFβ1, IL28A and ISG54 were measured. * Significantly different from RSV or poly(I•C) (0 h)-treated samples, $p<0.05$;** Significantly different from RSV or poly(I•C) (0 h)-treated samples, $p<0.01$; † Significantly different from ATM+/+ samples, $p<0.05$; †† Significantly different from ATM+/+ samples, $p<0.01$

5.3 RSV infection activates ATM

Previous studies have direct evidences that some DNA virus, like Simian virus, can activate DNA damage response and ATM kinase (179,180). Other studies also demonstrate that RSV can affect lung epithelial cell cycle through a p53-dependent pathway (181,182), which indicate an active role of ATM after RSV infection. Besides these facts, our data demonstrate a significant role of ATM in antiviral response upon RSV stimulation. Therefore, we sought to further explore the mechanism how ATM is involved in the process. For this purpose, we first examined whether RSV inoculation activates ATM by measuring formation of phospho-ATM in a time course of RSV stimulation. RSV treatment siginificantly increases ATM phosphorylation 15 and 24 h after RSV infection while almost no pATM level was detected without RSV stimulation (Figure 17). From this result, we conclude that RSV stimulation can activate ATM.
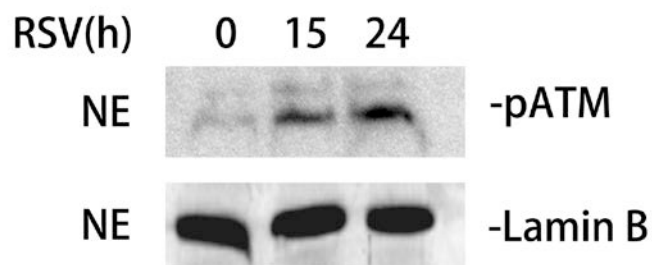
Figure 17. ATM is activated by RSV inoculation. A549 cells were infected by RSV (MOI, 1.0) for 0, 15, 24 h. NE were collected and assayed by WBs using pATM antibody. Lamin B was also detected as internal control.

5.4 RSV induced RelA Ser 276 phosphorylation is ATM dependent.

Previously, we have demonstrated that upon RSV stimulation, RelA is phosphorylated on Ser 276, an essential posttranslational modification that is important for a subset of NF-κB dependent gene expression. In parallel, ROS stress is enhanced by RSV infection and the elevated ROS level is prerequisite for RelA Ser 276 phosphorylation (111). Since TNF-induced ROS is required for ATM nuclear-to-cytoplasm export and cytoplasmic export is required on RelA Ser 276 phosphorylation through PKAc pathway, we further examined whether RSV-induced RelA Ser 276 phosphorylation is ATM-dependent. For this purpose, control shRNA-transfected A549 cells and ATM shRNA-transfected A549 cells were inoculated with RSV for 15 and 24 h. WCE were collected and total RelA was immunoprecipitated. Phospho-Ser 276 RelA formation was measured by western blot. RSV infection increased phospho-Ser 276 RelA formation in control

shRNA- transfectants starting at 15h and lasting until 24h. However, RSV-induced phospho-Ser 276 RelA formation was significantly reduced in the ATM shRNA-transfected cells (Figure 18). To sum up, we conclude that ATM is required for RSV-induced RelA Ser 276 phosphorylation.
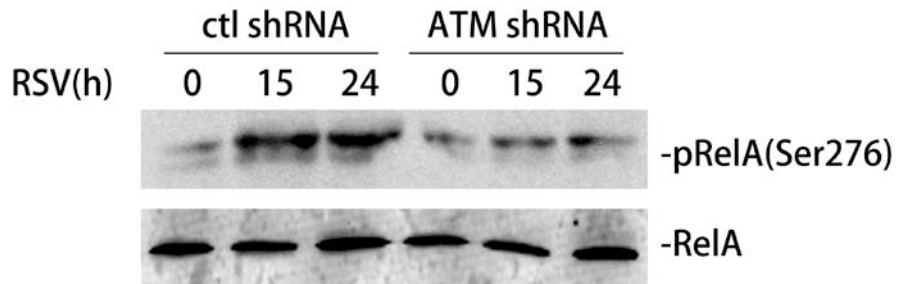
Figure 18. RSV induced RelA Ser 276 phosphorylation is inhibited in ATM knockdown cells. Control shRNA and ATM shRNA knockdown A549 cells were infected with RSV (MOI, 1.0) for 0, 15, 24 h. WCE were collected and assayed by WBs using pRelA (Ser 276) and RelA antibodies.

5.5 RSV and poly(I•C) induced IRF7 and RIG-I expression are ATM dependent

Earlier, several studies have shown that IRF7 gene expression is NF-κB dependent, and IRF7 is a primary regulator of RIG-I expression (183,184). Our previous data demonstrated that ATM is required for RSV induced RelA Ser 276 phosphorylation. Therefore, we examined whether ATM affect RSV-induced IRF7 gene expression and downstream RIG-I gene expression. For this purpose,

control shRNA- and ATM shRNA-transfected A549 cells were inoculated with RSV for 15 h and 24 h, and the expression of IRF7 and RIG-I mRNA was measured by Q-RT-PCR. In control shRNA-transfected cells, RSV induced 20- and 100- fold change of IRF7 gene expression 15 or 24 h after RSV infection, respectively. In ATM shRNA-transfected cells, the induction was significantly blocked. For the RIG-I gene expression, the pattern is similar to IRF7 genes (Figure 19A).

To further validate our findings, we stimulated these cell lines with poly (I•C) and measured IRF7 and RIG-I gene expressions. Similar result was observed compared with RSV stimulation. The depletion of ATM significantly blocked poly (I•C) induced IRF7 and RIG-I gene expressions (Figure 19B).

Taken together, these results demonstrated the requirement of ATM in RSV induced IRF7 and RIG-I gene expression.
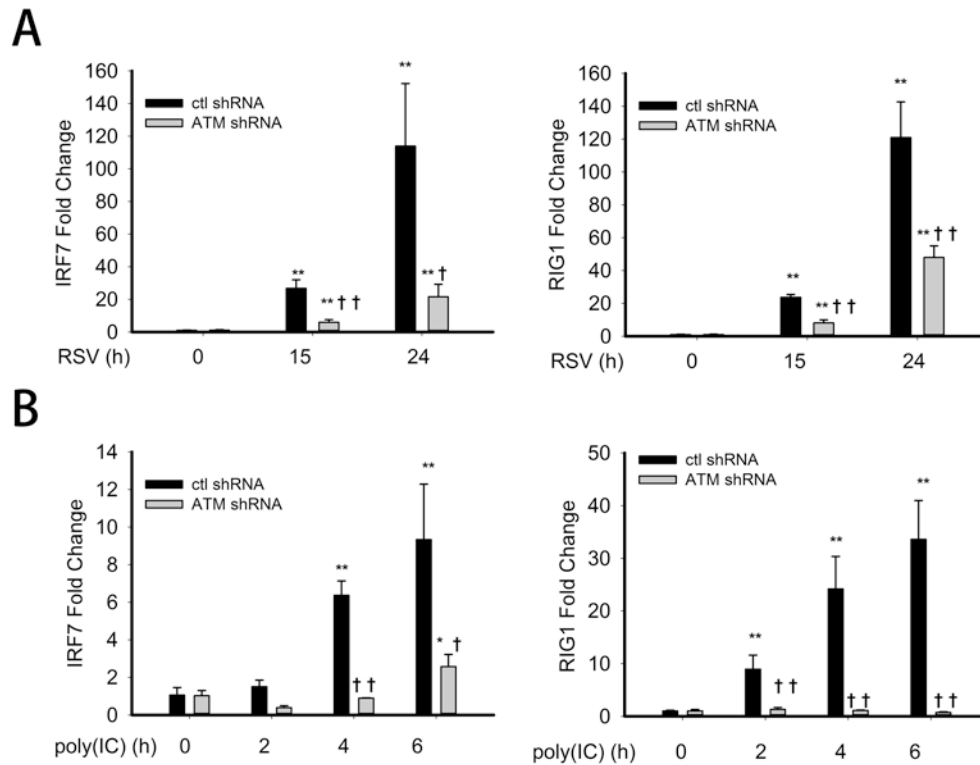
Figure 19. Suppressed IRF7 and RIG-I expression upon RSV infection and poly(I•C) treatment in ATM knockdown cells. (A) Control shRNA and ATM shRNA knockdown A549 cells were infected with RSV (MOI, 1.0) for 0, 15, 24 h. Total RNA was extracted. mRNA level of IRF7 and RIG-I were measured. **(B)** Control shRNA and ATM shRNA knockdown A549 cells were electroporated wit 10 μg poly(I•C) for 0, 2, 4, 6 h. Total RNA was extracted. mRNA level of IRF7 and RIG-I were measured. * Significantly different from RSV or poly(I•C) (0 h)-treated samples, $p<0.05$;** Significantly different from RSV or poly(I•C) (0 h)-treated samples, $p<0.01$; † Significantly different from ATM+/+ samples, $p<0.05$; †† Significantly different from ATM+/+ samples, $p<0.01$

5.6 phospho-Ser 276 RelA is required for antiviral immune response

To further examine the role of phospho-Ser 276 RelA in RSV-induced antiviral immune response pathway, we employed RelA WT and RelA Ser276A MEFs.

80

These two cell lines were infected by RSV for 24 h and the corresponding genes expression was measured.

As expected, in RelA WT MEFs, we observed significant induction of IRF3, IRF7 and RIG-I gene expression upon RSV infection. However, in RelA Ser276A MEFs, the inductions of IRF7 and RIG-I gene expression were significantly blocked while IRF3 gene expression is unaffected (Figure 20A). These findings indicate that IRF7 and RIG-I, but not IRF3, is dependent of RSV induced RelA phosphorylation on Ser 276.

Furthermore, we investigated the requirement of phospho-Ser 276 RelA in RSV induced IFN and ISG gene expression. In RelA WT cells, we found that mRNA level of IFNα6, INFβ1, IL28A ISG54 and ISG56 genes were dramatically increased 24 h after RSV infection to 20-, 50-, 40-, 20-, 15-fold, respectively. We further observed that RSV induced gene expressions were significantly blocked in RelA Ser276A MEFs (Figure 20B). A previous study has demonstrated that IFN and ISG gene expression are IRF3-dependent (46). Here we observed that, although IRF3 gene expression is not affected by the mutation of RelA Ser 276, the IFN and ISG gene expression were still blocked due to the disruption in IRF7-RIG-I pathway. One explanation for this finding is, resynthesized RIG-I that is regulated by IRF7 is essential for RSV-induced IFN and ISG gene expression.

Taken together, these results demonstrated the requirement of phospho-Ser 276 RelA-IRF7-RIG-I pathway in antiviral response.
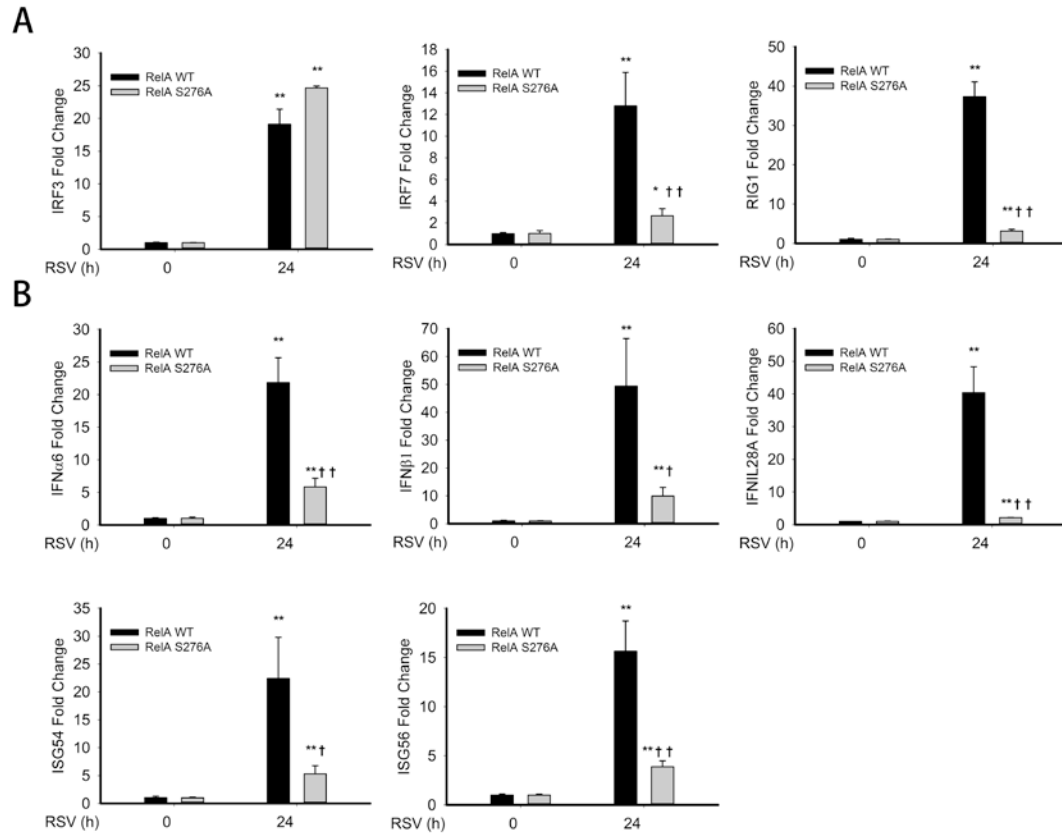
Figure 20. Suppressed gene expression upon RSV infection in RelA Ser276A cells. (A) RelA WT and Rel Ser276A MEFs were were infected with RSV (MOI, 1.0) for 0 and 24 h. Total RNA was extracted. mRNA level of IRF3, IRF7 and RIG-I were measured. **(B)** RelA WT and Rel Ser276A MEFs were were infected with RSV (MOI, 1.0) for 0 and 24 h. Total RNA was extracted. mRNA level of IFNα6, INFβ1, IL28A ISG54 and ISG56 were measured. * Significantly different from RSV or poly(I•C) (0 h)-treated samples, $p<0.05$;** Significantly different from RSV or poly(I•C) (0 h)-treated samples, $p<0.01$; † Significantly different from ATM+/+ samples, $p<0.05$; †† Significantly different from ATM+/+ samples, $p<0.01$

5.7 ATM is required for recruiting RelA to IRF7 gene promoter and IRF7 to RIG-I gene promoter

Earlier we have reported that phospho-Ser 276 RelA dependent gene expression is regulated via its interaction with cyclin-dependent kinase 9 (CDK9) resulting in RNA polymerase II (RNA Pol II) phosphorylation, a biochemical event necessary for expression of a subset of gene expression (45). Our previous data demonstrated the requirement of phospho-Ser 276 RelA on IRF7 and RIG-I gene expression as well as the requirement of ATM on RSV induced phospho-Ser 276 RelA formation. Therefore, we investigated whether ATM is required for the binding of proteins to IRF7 and RIG-I promoter by ChIP assay.

We first investigated whether ATM is required for RelA, CDK9 and phospho-Ser 2 Pol II's binding to IRF7 promoter. Cells transfected with either control or ATM shRNA were electroporated with poly(I•C) for the indicated times; chromatin was cross-linked and subjected to immunoprecitpitation with anti-RelA, CDK9 or phospho-Ser 2 Pol II Abs. Anti-rabbit IgG was used as a negative control. As expected, electroporation of poly(I•C) significantly induced RelA, CDK9 and phospho-Ser 2 Pol II's binding to IRF7 gene promoter in control shRNA-transfected A549 cells. However, in ATM shRNA-transfected A549 cells, the proteins' binding were significantly blocked (Figure 21A). These results illustrated the mechanism that how IRF7 gene expression is regulated by phospho-Ser 276 RelA.

83

From our previous experiment we knew that RIG-I gene expression is controlled by IRF7. However, the details of the mechanism are unknown to us. To address this question, we detected whether RIG-I promoter can be bound by IRF7 and RelA. Cells transfected with either control or ATM-specific shRNA were electroporated with poly(I•C) for the indicated times; chromatin was cross-linked and subjected to immunoprecitpitation with anti-IRF7, RelA or phospho-Ser 2 Pol II Abs. Anti-rabbit IgG was used as a negative control. In control shRNA-transfected A549 cells, we observed a significant induction of both IRF7 and RelA binding. However, in ATM shRNA-transfected A549 cells, binding of these proteins were blocked. A similar pattern was observed for phospho-Ser 2 Pol II binding (Figure 21B). These results demonstrated that both IRF7 and RelA can bind RIG-I gene promoter and regulate its gene expression. However, the relationship between these 2 proteins in binding RIG-I gene promoter need further investigation.
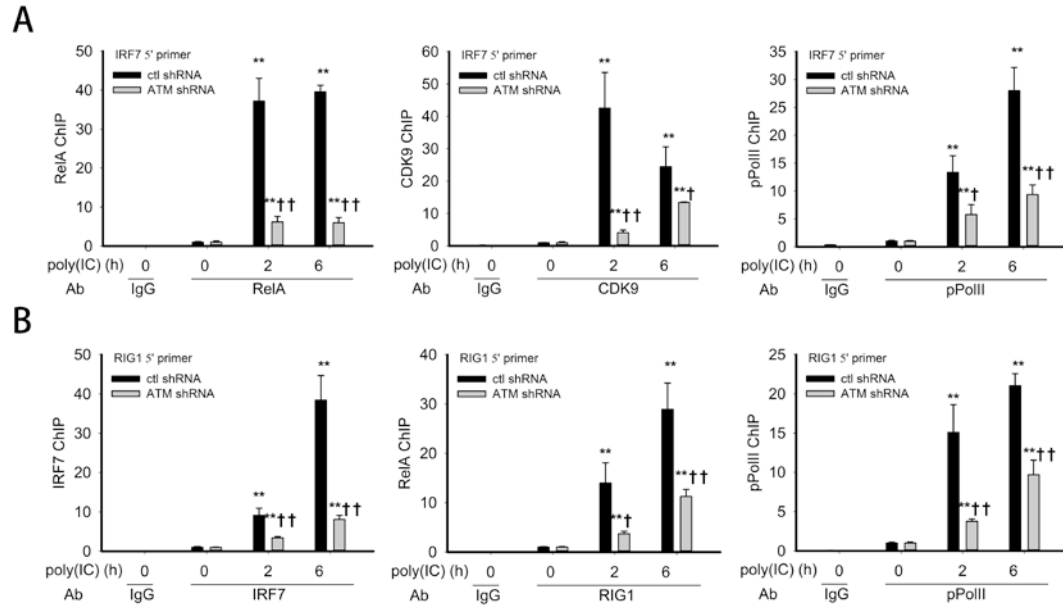
Figure 21. Requirement of ATM in recruitment of RelA, IRF7 and co-activators to IRF7 and RIG-I gene promoter. (A) Control shRNA and ATM shRNA knockdown A549 were electroporated with 10 μg poly(I•C) for 0, 2, 6 h. The corresponding chromatin was immunoprecipitated with anti-RelA, CDK9 and pPol II Abs. IgG was the negative control. Q-RT-PCR was performed using the IRF7 5'primer set, and the fold change was calculated compared with unstimulated samples. **(B)** The experiment was performed as described for panel A. The corresponding chromatin was immunoprecipitated with anti-IRF7, RelA, and pPol II Abs. IgG was the negative control. Q-RT-PCR was performed using the RIG-I 5'primer set, and the fold change was calculated compared with unstimulated samples. * Significantly different from TNF (0 h)-treated samples, $p<0.05$;** Significantly different from TNF (0 h)-treated samples, $p<0.01$; † Significantly different from ATM$^{+/+}$ samples, $p<0.05$; †† Significantly different from ATM$^{+/+}$ samples, $p<0.01$.

CHAPTER 6. CONCLUDING REMARKS

6.1 High throughput siRNA screening identifies ATN controlling the canonical NF-κB pathway

NF-κB is a major regulatory arm of the innate immune response in airway epithelial cells that mediates temporally coordinated expression of gene networks by a mechanism involving its nuclear translocation and activating phosphorylation on the Ser 276 residue (45,160). Despite intensive study of this pathway, the complete spectrum of kinases involved in its regulation is not fully understood. In this study, we standardized and applied a HT-siRNA screen to identify new kinase candidates that control the canonical NF-κB pathway; we further sought to validate a subset of the identified kinases. Thirty six serine-threonine kinases were identified within our screen that had effects significantly greater than that produced by siRNA-mediated knockdown of IKKγ/NEMO, which served as a positive control within our screen. Of the 11 kinases selected for validation, we were able to achieve sufficient knockdown of 8. From these 8, the knock-down of 6 kinases demonstrated significant effects on TNF-inducible and NF-κB-dependent gene expression, indicating that our duplicate screening strategy has uncovered several genuine candidates involved in the canonical NF-κB pathway.

Of the kinases identified in our screen a few have been implicated in NF-κB signaling in prior studies. For example, PKCζ, an atypical PKC isoform, has been reported as a regulator of NF-κB transcriptional activity in certain cell types (185). Consequently, PKCζ deficiency results in reduced cell proliferation and TNF-inducible NF-κB dependent gene expression (185). Furthermore, lack of PKCζ in B cells and embryonic fibroblasts (EFs) does not affect the ability of TNF or IgM to activate the IKK complex or the DNA-binding activity of NF-κB, respectively. However, PKCζ mediates Ser 311 phosphorylation of RelA and thus regulates diacylglycerol kinase (DGK)-induced TNF-dependent NF-κB activation (186). Thus, PKCζ can directly associate with and efficiently phosphorylate RelA and, more importantly, TNF-induced phosphorylation of RelA in vivo was shown to be dramatically inhibited in pkcζ$^{-/-}$ EFs (185). Moreover, PKCζ has also been implicated in LPS-induced NF-κB activation within human peripheral blood monocytes and macrophages through its association with both RhoA and activating transforming growth factor β-activated kinase-1(TAK1) (187).

Our findings also implicate a role for PKCζ in TNF signaling in airway epithelial cells. Several CDKs were also identified in our screen. The CDKs are a family of related serine-threonine kinases best known, perhaps, to be responsible for the orderly progression of cells through various phases of the cell cycle; nevertheless, they also play an important role in transcription and mRNA processing (188-190). The requirement of CDKs in several steps of NF-κB

dependent gene transcription has been already been appreciated (188). The enzymatic activity of CDKs is regulated by interactions with their cyclin protein partners to form an active heterodimer complex. CDK2 and Cyclin E have been shown to interact with RelA via p300/CBP and, thus, negatively regulate phorbol 12-myristate 13-acetate (PMA)-induced, and NF-κB dependent, gene expression (191). On the other hand, we and others have shown that recruitment of P-TEFb, a heterodimer of CDK9 and Cyclin T1, is essential for expression of selected subgroups of NF-κB dependent genes (45). Activated NF-κB associates and recruits P-TEFb to target genes; and CDK9 mediates increased phosphorylation of negative elongation factors and phosphorylation of Ser residue 2 of the heptad repeat in the RNA Polymerase II COOH terminal domain (CTD). In turn, there is an initiation of a transcriptional elongation phase in NF-κB dependent gene expression (192). Consistent with these findings, we have reported that flavopiridol, a pan-selective CDK inhibitor, potently inhibits NF-κB dependent gene expression (45). Additionally, murine 264.7 macrophages treated with olomoucine and roscovitine, selective inhibitors of CDK 1, 2, 5 and 7, exhibit a reduction in lipopolysaccharide-induced inflammatory responses by down regulating NF-κB dependent gene expression (193). Taken together, these studies suggest that CDKs regulate NF-κB dependent gene expression by various mechanisms and at multiple steps in the transcriptional activation process. However, with the exception of CDK-2 and -9, the roles of the other CDKs uncovered here have not been clearly implicated in TNF-induced NF-κB activation. Therefore, our finding that siRNA mediated knock down of CDKs-5

and 7 significantly inhibited TNF-induced NF-κB promoter activity suggest that additional CDKs may also have additional roles as a transcriptional regulators of TNF-induced, NF-κB signaling. The more profound effect of CDK7 knockdown on TNF-dependent transcription may be also explained by its additional role in general transcription as a component of universal transcription factor TFIIH (194).

Similarly, MAP3K3/MEKK3, and MAPKAPK5/p38-regulated and -activated kinase (PRAK) have been reported earlier to regulate NF-κB activity (157-159). Of these, MAP3K3/MEKK3 is required for lysophosphatidic acid signaling to the IκB kinase complex through the BCL10, MALT lymphoma translocation gene 1, and CARD and MAGUK domain-containing protein complex. Interestingly, this signaling pathway is independent of TAK1, the IKK effector kinase that mediates PKCζ-induced NF-κB signaling.

ATM is a serine-threonine kinase of the PI3K family involved in cell cycle regulation in response to DNA damage. ATM has been reported to activate NF-κB in response to DNA damage (141), identifying ATM as a requirement for NF-κB signaling by within our screen was a surprising finding. We therefore decided to explicitly validate this result. Previous work has shown that ATM mediates a nuclear stress response signaling pathway whereby activated ATM forms a complex with nuclear IKKγ, inducing its SUMO-lyation, and promoting nuclear export (141). In the cytoplasm, the ATM-IKKγ complex associate with the

cytoskeletal ELKS-IKKα/β complex, resulting in IκBα phosphorylation and releasing of NF-κB/RelA sequestered in the cytoplasm (195).

Our comparison of the kinetics of IκBα proteolysis and NF-κB translocation indicate that ATM participates in the initial steps of NF-κB release. Several reports previously suggested that ATM may not play a role in TNF-mediated NF-κB activation; these conclusions have been made after measuring the effect of ATM inhibition on its DNA binding ability using electrophoretic mobility shift assays (EMSA) (196). Because the EMSA assay does not measure the activated (Ser 276 phosphorylated) form of NF-κB, an effect on the separate transactivation pathway may have been missed. More detailed experiments are required to ascertain the precise role of ATM in the NF-κB transactivation pathway.

Although the predominant mechanism by which ATM is activated occurs in response to double stranded DNA breaks in the genome, it is also known that ATM is activated by an ancillary pathway in response to reactive oxygen stress (ROS), which is double strand break-independent (137). In this regard, we note that TNF stimulation induces ROS stress and oxidative DNA damage measured by the inducible formation of 8-oxoguanine adducts in stimulated cells (112). The kinetics of ROS formation in epithelial cells, peaking 15 min after TNF stimulation, are consistent with the activation profile of ATM we have observed in this study. More detailed work will be required to determine whether TNF

signaling induces a nuclear signal, or whether ATM is somehow involved in cytoplasmic IKK activation in response to extracellular TNF receptor signaling.

Another interesting finding from our study is that ATM affects only a subset of NF-κB dependent genes. Earlier we have observed that the subset of NF-κB dependent genes including Groβ, TNFAIP3/A20, and IL-8 are downstream from an ROS-PKAc-CDK9 pathway that controls phosphorylation of the CTD of RNA polymerase II (160,197). Here, Ser 276 RelA phosphorylation is a key activating step, enabling RelA to form a stable complex with CDK9, recruiting it to target chromatin. The findings that RelA Ser 276 phosphorylation is impaired in ATM$^{-/-}$ MEFs suggest that ATM participates in controlling transcriptional elongation of the Groβ, TNFAIP3/A20, and IL-8 genes. By contrast, IκBα is an NF-κB dependent gene that does not require RelA Ser 276 phosphorylation of CDK9 for its inducible expression (160,197). Here we note that IκBα is also insensitive to ATM deficiency (Figure 7). Together these findings suggest that ATM may participate in the ROS-PKAc-CDK9 pathway important in the activation of rapidly responding inflammatory genes.

In summary, by using a HT-siRNA screening approach, we identified and validated 6 kinases in TNF-induced NF-κB activation, including a novel role for PKCζ, CDK2, CDK5 and -7 and ATM (Figure 22). Our functional data complements the protein interaction map previously determined by tandem affinity purification proteomics for a more complete understanding of the regulatory kinases controlling this complex signaling network. We further

selected and validated the role of ATM in TNF signaling using selective inhibitors and ATM$^{-/-}$ MEFs. Although ATM is an established mediator of double stranded DNA break-induced signaling and NF-κB release from cytoplasmic sequestration, our findings in TNF signaling suggest that the role of ATM extends to other stimulus types, and affects the transactivation step of NF-κB during pathway activation. These exciting findings link the nuclear cell stress responsive ATM kinase to the canonical NF-κB pathway classically mediated by cytokine signaling through the TNF receptors.
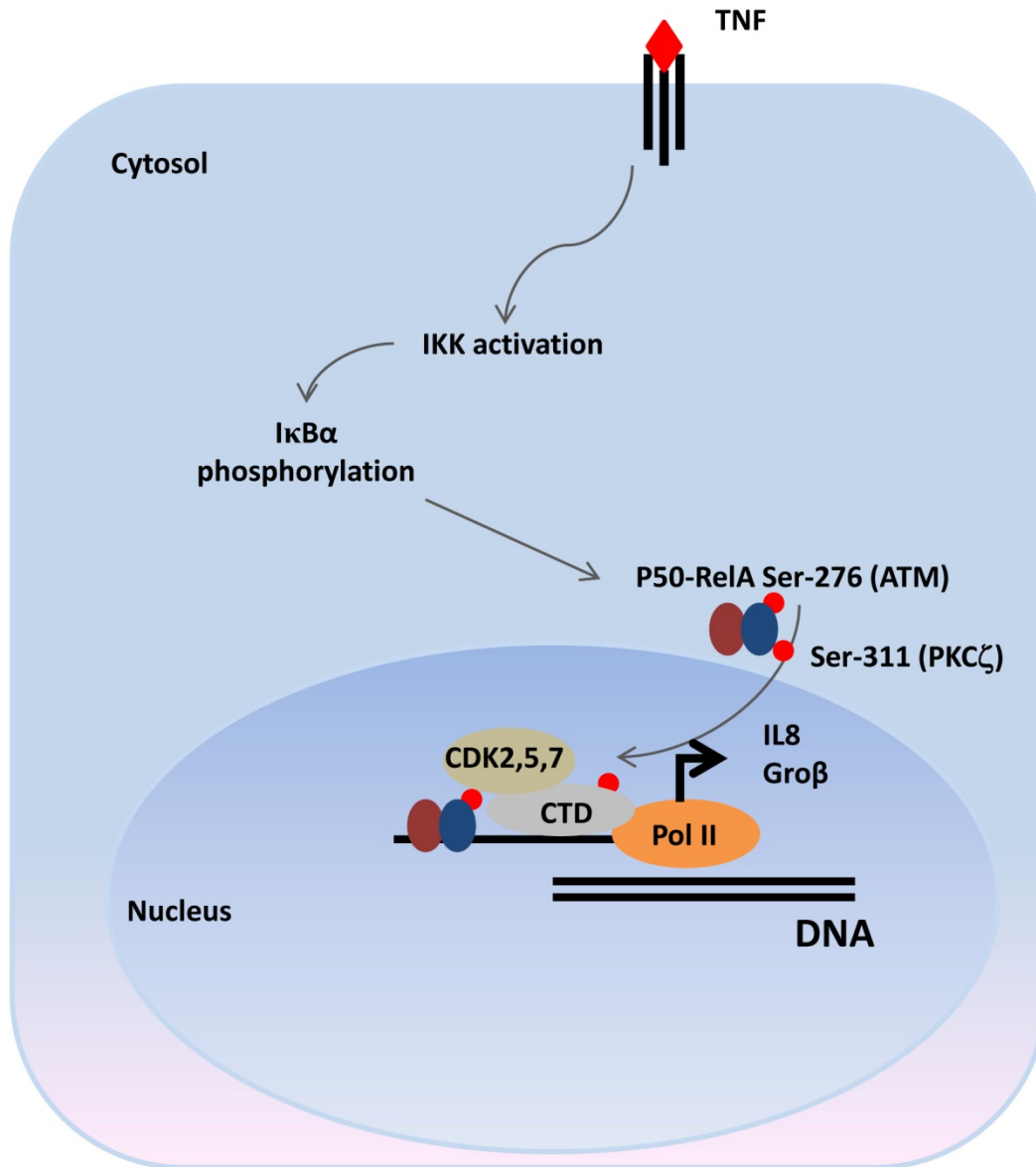
Figure 22. Potential role of kinases in TNF induced NF-κB pathway. The PKCζ mediates TNF induced RelA Ser 311 phosphorylation. ATM mediates TNF induced RelA Ser 276 phosphorylation. CDK2, CDK5 and -7 mediates transcriptional elongation of TNF induced NF-kB dependent genes.

6.2 The role of ATM in TNF induced NF-κB pathway

In this study, we extend our previous discovery-based observation for a role of ATM in outside-in signaling in the innate immune response. Our data suggests that ATM is rapidly exported from the nucleus in response to TNF stimulation via an ROS-dependent pathway that affects IKKγ-ubiquitin association and complex formation with ATM. Activated ATM functions in regulating the NF-κB pathway at two key steps- one, affecting the rate of IκBα degradation, and the second, affecting RelA activation by Ser 276 phosphorylation (schematically diagrammed in Figure 23). In ATM knockdown cells, we have observed a decreased recruitment of the β-TrCP ubiquitin ligase to pIκBα and its stabilization. In parallel, activated ATM forms a complex with PKAc, stimulating its activity and promoting phosphorylation of at RelA Ser 276. This event is required for CDK9 recruitment and expression of immediate early cytokine genes through phospho-Ser2 CTD Pol II formation and transcriptional elongation. Our studies suggest a coordinated signaling pathway involving "inside-out", nuclear DNA-damage response pathways, and "outside-in" plasma membrane located cytokine receptor signaling for full activation of the innate response.

Double-stranded DNA breaks are well-established to be the prototypical activating stimulus for ATM. ATM participates in the DSBs-repair response via phosphorylating and stabilizing the Nibrin/MRN complex on the DNA lesion (127). Our surprising findings from the neutral Comet assays (Figure 9C) suggest that TNF induces dsDNA breaks and ATM activation over a time consistent with

activation of the NF-κB signaling pathway. The mechanism for how TNF induces

dsDNA breaks is not currently clear. However, compared the level of DSBs

induced by VP-16, we can conclude that TNF induced DSBs is very gentle but

enough to activate ATM. An earlier study suggested that increased mitochondrial

formation of ROS is responsible for inducing DNA damage after TNF exposure

based on the finding that cell pretreatment with a reducing agent (dithiothreitol) or

a ferric ion chelator (desferoxamine) prevented TNF-induced DNA damage (198).

Another possibility is that DSB are produced by the process of base excision

repair of oxidized DNA bases, generated by TNFα-induced oxidative stress.

Recently, we have demonstrated that TNF-induces accumulation of 8-oxoG in

DNA and the subsequent recruitment of 8-oxoguanine glycosylase 1 (OGG1), an

8-oxoG repair enzyme on the NF-κB dependent gene promoter is essential for

their mRNA expression (144). This intriguing finding provides a mechanism to

explain how oxidative DNA damage potentially regulates transcriptional

expression of NF-κB dependent genes in TNF pathway. This suggests the post-

DNA lesion events could be an epigenetic mechanism to modulate gene

expression. It will be of interest to examine the effects of OGG1 deficiency on

TNF-induced DSBs.

Earlier work using robust exogenous ROS exposure (e.g., hydrogen peroxide at

supraphysiological 250 μM concentrations) has concluded that oxidative stresses

activate ATM. Here, nuclear oxidation leads to Cys-2991 oxidation of ATM and

formation of disulfide dimers. Subsequently, ATM undergoes inter-molecular autophosphorylation to produce the characteristic Ser 1981 phosphorylation, a signature of activated ATM (137). Our finding that ATM undergoes serine autophosphorylation by physiological receptor-coupled pathways is novel to our knowledge. Mitochondrial- as well as NADPH-oxidase-derived ROS has been implicated in the TNF-induced cytotoxicity and apoptosis (110,198-202). Alternatively, TNF also induces ROS resulting in guanine, DCFDA oxidation and formation of carbonylated proteins (112). It is surprising that ATM autophosphorylation is antioxidant-resistant, and instead, ROS is required for nuclear export of the activated ATM by disrupting complex formation with IKKγ. These observations suggest that a separate nuclear signal stimulates ATM phosphorylation; this mechanism will require further exploration. Although, the ATM activation after genotoxic stress usually progress with slower kinetic as compared to a rapid activation after TNF exposure. The broad difference in the kinetic of ATM pathway activation by these two exposures suggests that ATM could be warranted to perform unique cellular function in DSB repair and activation of the innate immunity pathway.

In studies of the prototypical genotoxic stress induced ATM-NF-κB activation pathway, Ser 1981 autophosphorylated ATM is required for phosphorylation of IKKγ, triggering a sumoylation-for-ubiquitination exchange on IKKγ. The ubiquitinated IKKγ-ATM complex is then exported from the nucleus (141). In a

manner similar to that produced by genotoxic stimuli, our findings for the absence of detectable cytoplasmic ATM in IKKγ$^{-/-}$ cells clearly suggests the vital role of IKKγ in TNF-induced ATM nuclear export (Figure 9F). Together with our co-immunoprecipitation results, these data suggest that TNF-induced ATM nuclear export also requires binding to nuclear IKKγ (Figure 9G). Interestingly, IKKγ-ubiquitin association is ROS dependent, where TNF induces the IKKγ interaction with ubiquitin, but this is blocked by free radical scavenger treatment (Figure 9H).

The ubiquitination of IKKγ is a critical regulatory step in controlling IKK activation. Here, IKKγ is well established to be ubiquitinated both by Lys (K) 63-linked chemistry and linear ubiquitination by TRAF6 and the LUBAC E3 ligases, respectively (203). K63-linked modification of cytoplasmic IKKγ promotes oligomerization of the IKK-α and –β kinases, resulting in IKK autoactivation (204). Recent work has also shown that IKKγ binds to free polyubiquitin chains, triggering activation of the innate immune response. Our study extends the understanding of the effects of ROS on controlling IKKγ association or ubiquitination. One limitation of the trypsin-based SID-SRM assay is that it is unable to differentiate between free polyubiquitin chains, or covalent K63 linked chemistries. Our confirmatory experiments suggest that IKKγ may be binding to unconjugated polyubiquitin chains. However, we cannot exclude the possibility that the abundance of covalently linked Ub-IKKγ is below the limit of our assay detection. Further investigation is required on this issue. The nuclear IKKγ

ubiquitin ligase(s) and ROS-dependent pathways controlling them will require further investigation.

In ATM$^{-/-}$ MEFs as well as shRNA-mediated ATM knockdown cells, we observed cytoplasmic accumulation of phosphorylated IκBα and a delay in TNF-induced IκBα degradation (Figures. 10B and 10D). IKK-mediated Ser phosphorylation of IκBα at NH2 terminal Ser-32 and Ser-36 is coupled with ubiquitination of Lys-20 and Lys-21 by the recruitment of SKP1-CUL-1-F-box protein (SCF) ubiquitin ligase in association with F-box protein β-TrCP. The SCF$^{\beta\text{-}TrCP}$ E3-ubiquitin ligase is essential for IκBα degradation and subsequent p50•RelA release into the nucleus because ablation of β-TrCP results in accumulation of IκBs and complete inhibition of NF-κB activation (205-207). Our co-immunoprecipitation experiments showing: 1. that cytoplasmic ATM binds to β-TrCP in a TNF inducible manner; 2. pIκBα is stabilized in ATM deficient cells; and 3. Decreased β-TrCP recruitment occurs on pIκBα in ATM-deficient cells together suggest that ATM may serve as a scaffold for the formation of a viable E3-ligase- pIκBα complex in the TNF pathway (Figure 10H). This data also explains observations of reduced RelA nuclear translocation after TNF stimulus (Figure 10J).

Earlier, ATM was shown to regulate SCF$^{\beta\text{-}TrCP}$ mediated-ubiquitination and degradation of mdm2 after DNA damage. Here, activated ATM directly

phosphorylates casein kinase Iδ (CKIδ) resulting nuclear translocation of phospho-CKIδ wherein it phosphorylates mdm2 thereby subjecting to subsequent ubiquitination by SCF$^{\beta\text{-TrCP}}$ (208). Similar to ATM-mediated activation of CKIδ and mdm2 degradation, genotoxic stress induced ATM activates IKK leading to IκBα phosphorylation subjecting to ubiquitination and degradation (209). However, in the TNF response pathway, ATM seems to directly work at the level of E3 ubiquitin ligase recruitment to facilitate IκBα degradation.

The delayed clearance of IκBα in ATM deficient cells may be the result of other ancillary pathways responsible for IκBα degradation in the absence of ATM. In this context, we have reported a calpain-dependent degradation of IκBα after TNF exposure (210). Alternatively, a recent report suggests an IKK activation-independent pathway of IκBα degradation following ultraviolet irradiation, a potent ATM inducer. In this pathway, stimulus dependent nuclear accumulate IKKβ serves as an adaptor protein that constitutively interacts with β-TrCP through heterogeneous ribonucleoprotein-U (hnRNP-U) leading to IκBα ubiquitination and degradation (211). Studies to elucidate these pathways of IκBα degradation in absence of ATM is under investigation in our laboratory.

Several reports have suggested that release of RelA from cytoplasmic inhibitors is necessary, but not sufficient to induce gene expression after TNF treatment

(212-214). The post-translational modifications of RelA, especially phosphorylation at Ser 276 and Ser 536 are reported to have a significant effect on its ability to interact with transcriptional co-activators to initiate transcriptional initiation. Ablation of ATM specifically affects RelA Ser 276 phosphorylation further suggest a vital role of ROS in ATM mediated signaling events in TNF-induced NF-κB pathway (Figures 11A, 11B, 11C and 11D). Ser 276 phosphorylation is controlled in a stimulus-dependent manner by the ribosomal S6 kinases, PKAc and MSK1 (111,112). PKAc is the major kinase activated by the TNF pathway (112). Our data for the first time shows that ATM is required for TNF induced activation of PKAc, via its interaction with ATM in the cytoplasm (Figures 11G and 11H). Whether ATM directly phosphorylates and activates PKAc, or whether it functions in a scaffolding complex to promote its association with RelA will require further investigation.

Earlier, we have reported that phospho-Ser 276 RelA binds to the transcriptional elongation complex containing CDK-9 and cyclin T1. The immediate early genes requiring binding of phospho-Ser 276 RelA are activated by chromatin targeting of the CDK9/CCNT1 complex through transcriptional elongation (45). Consistent with these findings, we observed knockdown of ATM specifically effects CDK9 and phospho-Ser 2 CTD Pol II recruitment and expression of IL-8 and Gro-β (Figures 12A and 12B). Interestingly, IκBα is RelA 276-independent and resistant to ATM deficiency (Figure 12C). Earlier studies have shown that IκBα gene

expression is independent of phospho-Ser 276 RelA and CDK9 (46). Interestingly, another group has identified that in the VP-16 induced NF-κB activation, ATM binds to RelA directly and phosphorylates RelA on Ser 547, a post-translational modification that represses a subset of NF-κB dependent genes (215). It is presently unknown to us whether TNF induced NF-κB activation involves RelA phosphorylation on Ser 547. This question and the relationship between Ser 276 and Ser 547 phosphorylation will require further investigation.

Our findings for these multiple roles of ATM in regulating the innate pathway have implications for ataxia-telengiectasia (A-T), a rare autosomal recessive disorder. A-T affected patients lack a functional ATM protein and exhibit wide array of systemic defects including immunodeficiency, cerebral degeneration, progressive ataxia, premature aging, increased incidence of lymphoid tumorigenesis and type-2 diabetes (138). This phenotype suggests a vital role for ATM in the regulation of multiple cellular functions. More than half of A-T patients show humoral and cellular immunodeficiency that significantly contributes to morbidity and mortality in these subjects (118,216,217). One mechanism proposed to explain immunodeficiency has been immunoglobulin deficiency (both IgA and IgG2) but the role of ATM in innate immunity has not been investigated. Our studies suggest that ATM deficiency in A-T may be associated with primary defects in the innate pathway, affecting both the magnitude and kinetics of the

NF-κB response. Defects in innate signaling in A-T could be a unifying explanation for global defects in adaptive immunity.

In conclusion, our current study provides a novel role of nuclear kinase ATM in TNF-induced NF-κB activation pathway. A rapidly activated ATM after TNF exposure regulates expression of a subset of genes by controlling two key steps in the pathway: 1. facilitating optimal IκBα degradation by forming a viable IκBα-β-TrCP-ubiquitin ligase complex, and 2. RelA Ser 276 phosphorylation.
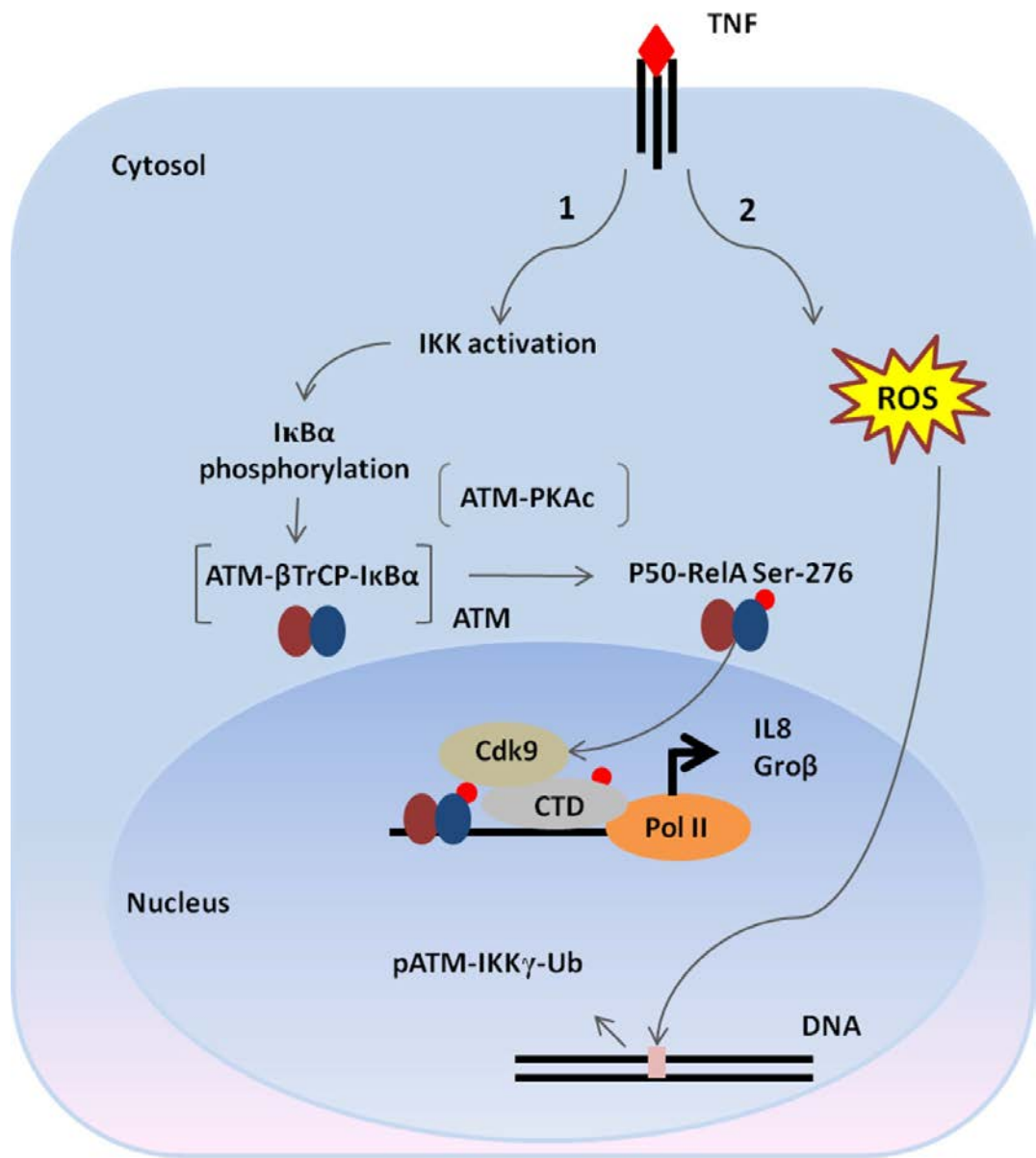
Figure 23. The model for the role of ATM in TNF pathway. Binding of TNF to the TNF receptor on the plasma membrane activates two parallel pathways: 1) IKK complex activation resulting in IκBα phosphorylation and 2) ROS generation leading to DNA double-strand breaks. The latter produces ATM activation and IKKγ-dependent nuclear export. Once in the cytosol, ATM facilitate two important steps of NF-κB activation pathway: rapid IκBα degradation by forming a complex with β-TrCP and RelA Ser 276 phosphorylation by interacting with PKAc.

6.3 ATM regulates the antiviral IFN pathway

In this study, we investigated the role of ATM in regulating antiviral immune response pathway. Our data suggests that infection of RSV activates ATM and the activated ATM is essential for RSV-induced RelA Ser 276 phosphorylation. Furthermore, IRF7 gene expression is phospho-Ser 276 RelA-dependent, and IRF7 is a primary regulator of RIG-I gene expression. The gene expression of RIG-I is required for the downstream IFN and ISG expression and therefore affect antiviral immune response. Our study demonstrated the role of ATM in the antiviral INF pathway through coupling RSV-phospho-Ser 276 RelA-IRF7-RIG-I-IFN/ISG pathway.

Double-stranded DNA breaks are well-established to be the prototypical activating stimulus for ATM (127). Our previous data demonstrated that TNF can activate ATM through gentle DSBs. Here we observed that RSV stimulation also activate ATM. Earlier, several groups reported that some DNA virus, like Simian virus, can activate DNA damage response and ATM kinase (179,180). Also, other groups have reported that RSV can affect lung epithelial cell cycle through a p53-dependent pathway (181,182). These findings further indicate the possibility that ATM is activated by RSV induced DSBs. However, how RSV activate ATM is still required further investigation. Our previous work has demonstrated that RSV can induce ROS (111), which may be another potential

mechanism to activate ATM. The differences of mechanism among prototypical induced ATM activation, TNF induced ATM activation, and RSV induced ATM activation are worthwhile to explore.

Our earlier work has demonstrated RSV-induced RelA Ser 276 phosphorylation is PKAc-independent but MSK1-dependent (81,111). MSK1, which is phosphorylated on Ser 376 and activated by RSV-induced ROS, serves as an upstream kinase to phosphorylate RelA on Ser 276. Here we observed that ATM is required for RSV induced RelA Ser 276 phosphorylation. We propose that ATM is involved in the activation of MSK1 by directly or indirectly phosphorylating MSK1 on Ser 376. Further study is required to elucidate the details of mechanism of the requirement of ATM on MSK1 activation and RelA Ser 276 phosphorylation.

The gene expression of IRF7 is NF-κB-dependent but IRF3 independent (183,218). However, how NF-κB regulates IRF7 gene expression was unknown. Here, we observed that knockdown of ATM significantly blocked RSV and poly(I•C) induced IRF7 gene expression (Figure 19), similar result was also shown in RelA Ser276A cells (Figure 20A). These results indicate that IRF7 gene expression is phospho-Ser 276 RelA dependent. Furthermore, our ChIP assay data that knockdown of ATM specifically affects CDK9 and phospho-Ser 2 CTD

Pol II recruitment indicates the mechanism of how phospho-Ser 276 RelA affect IRF gene expression.

RIG-I, of which gene expression is IRF7-dependent but IRF3 independent (184), functions as a PRR and is a sensor for viruses. Together with MDA5, RIG-I is involved in activating MAVS and antiviral response (166). Our experiment demonstrated that depletion of ATM or the mutation of pRelA Ser 276 significantly blocked RIG-I gene expression. Furthermore, our ChIP assay data demonstrated that both IRF7 and RelA bind to RIG-I gene promoter and induce RIG-I gene expression. The depletion of ATM significantly blocks IRF7, RelA and pPolII's binding to RIG-I gene promoter. These findings demonstrated a RSV-induced ATM-NF-κB-IRF7-RIG-I pathway.

We also observed that depletion of ATM significantly blocks type I, type III and ISG gene expressions without affecting IRF3 gene expression. This surprising finding raised a question why antiviral immune response is blocked even with an induced IRF3 gene expression upon RSV infection. Earlier, we have found that, in the early stage of poly(I•C) stimulation, the RIG-I proteins decrease, indicating a continuous degradation of RIG-I (184). Previous report has shown that, upon dsRNA stimulation, RIG-I undergoes inducible K63-mediated ubiquitination, a modification that help its association with MAVS (219). After that, K48-linked ubiquitination of RIG-I is mediated by RNF125 family, which promote RIG-I

degradation through proteasome (220). Since knockdown of ATM significantly blocks RIG-I gene expression, the total level of RIG-I will be maintained at a relatively low level in the cells and disrupt the antiviral response even with a high level of IRF3. This result further demonstrated that resynthesized RIG-I plays a key role in antiviral response as a PRR.

Overall, our current findings reveal a RSV-phospho-Ser 276 RelA-IRF7-RIG-I antiviral response pathway which is mediated by ATM. Our findings further demonstrated the significance of resynthesized RIG-I in antiviral response (Figure 24).
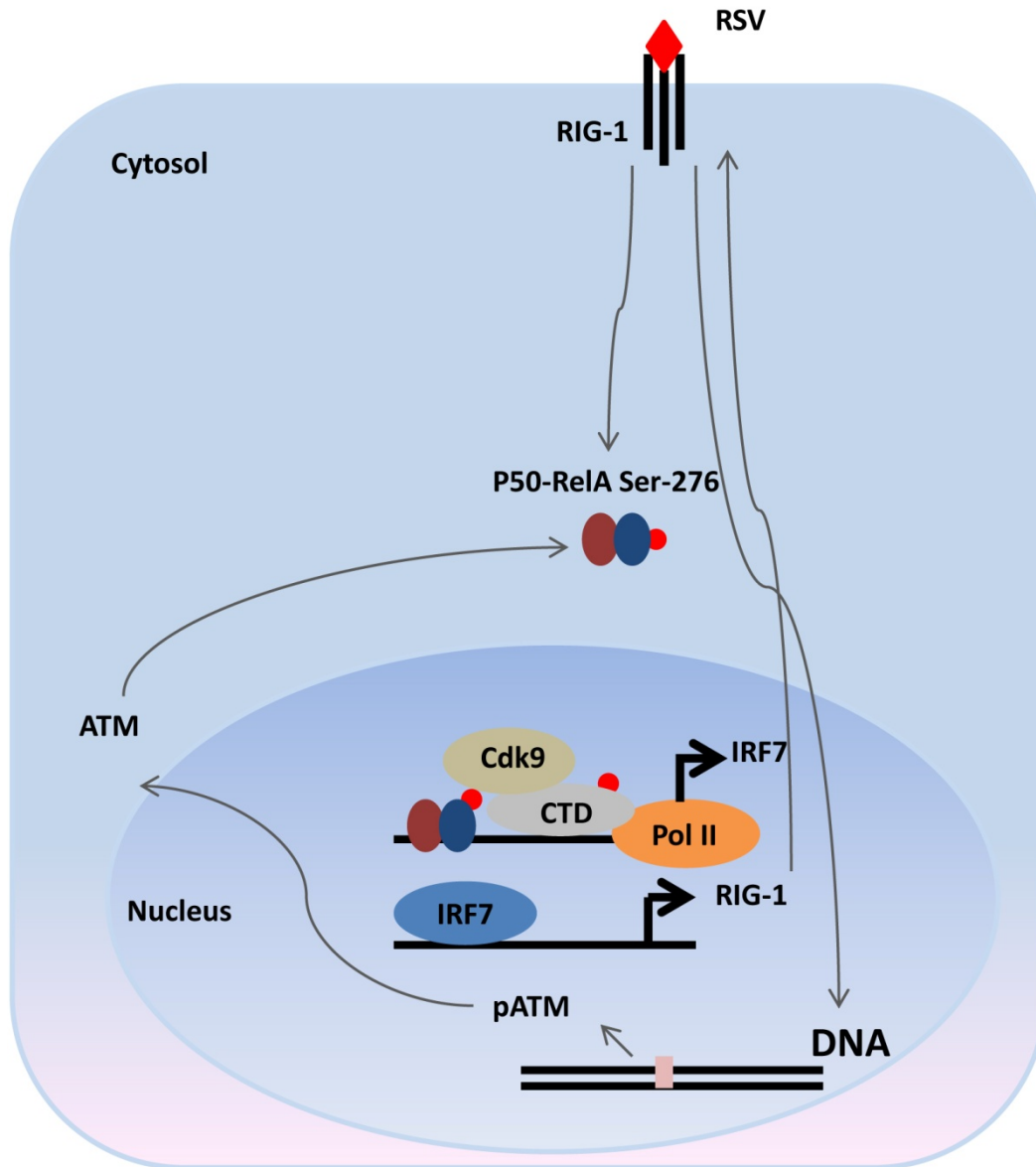
Figure 24. The model for the role of ATM in RSV-induced NF-κB pathway for antiviral response. RSV-induced RelA Ser 276 phosphorylation is required for IRF7 gene expression. The RIG-1 gene expression is mediated by IRF7 and resynthesized RIG-I plays essential role in antiviral response. ATM in required in this pathway by mediating Ser 276 phosphorylation.

6.4 Future directions

Despite our intensively investigations on the role of ATM in TNF- and RSV-induced NF-κB activation, there are still some unknown fields including but not limited to: 1. Whether the ATM kinase activity plays an essential role in the cytosol. For this, a cell staining using pATM and β-TrCP/PKAc antibodies could be a useful tool to investigate whether the bindings of ATM to β-TrCP and PKAc require ATM kinase activity; 2. The role of ATM in the negative feedback of IκBα degradation and RelA phosphorylation. For this, we can measure the level of ATM in the CE and pATM in the NE given the extended stimulation time of TNF and RSV. We can also compare the phospho-Ser 276 RelA cytoplasmic IκBα level in ATM WT and ATM knockdown cells upon longer TNF and RSV stimulation. Furthermore, the immunoprecipitation can be done to investigate the binding between A20 and/or cylindromatosis (CYLD) deubiquitinating enzyme and ATM to reveal the role of ATM in the negative feedback of NF-κB pathway; 3. Whether nuclear ATM and/or pATM is involved in the binding RelA and coactivators to DNA. For this, the immunoprecipitation assay between RelA and ATM/pATM using the NE upon TNF and RSV stimulation can reveal the interaction of RelA in ATM/pATM in the nucleus. Furthermore, the ChIP assay can be conduct to detect whether ATM is involved in the binding of RelA to DNA and whether ATM can bind to the DNA directly to repair the DSBs in the promoter. More work should be done to answer these questions and get a deeper understanding in the NF-κB pathway.

REFERENCES

1.   Alberts, B., Johnson, A., Lewis, J., Raff, M., Roberts, K. and Walter, P. (2008) Molecular biology of the cell. *New York: Garland Science*, **1**.

2.   Beck, G. and Habicht, G.S. (1996) Immunity and the invertebrates. *Scientific American*, **275**, 60-63, 66.

3.   Medzhitov, R. (2001) Toll-like receptors and innate immunity. *Nature reviews. Immunology*, **1**, 135-145.

4.   Janeway, C.A., Travers, P., Walport, M. and Shlomchik, M.J. (2001) Innate immunity.

5.   Akira, S., Uematsu, S. and Takeuchi, O. (2006) Pathogen recognition and innate immunity. *Cell*, **124**, 783-801.

6.   Mayer, G. (2010) Immunology-Chapter One Innate (Non-specific) Immunity.

7.   Barza, M. (1993) Anatomical barriers for antimicrobial agents. *European journal of clinical microbiology & infectious diseases : official publication of the European Society of Clinical Microbiology*, **12 Suppl 1**, S31-35.

8.   Akira, S., Takeda, K. and Kaisho, T. (2001) Toll-like receptors: critical proteins linking innate and acquired immunity. *Nature immunology*, **2**, 675-680.

9.   Janeway, C.A., Jr. and Medzhitov, R. (2002) Innate immune recognition. *Annual review of immunology*, **20**, 197-216.

10. Thompson, M.R., Kaminski, J.J., Kurt-Jones, E.A. and Fitzgerald, K.A. (2011) Pattern recognition receptors and the innate immune response to viral infection. *Viruses*, **3**, 920-940.

11. Kumar, H., Kawai, T. and Akira, S. (2009) Pathogen recognition in the innate immune response. *The Biochemical journal*, **420**, 1-16.

12. Collins, T. (1999) Acute and chronic inflammation. *Pathologic basis of disease*, 50-88.

13. Chandrasoma, P. and Taylor, C.R. (2005) Part A. General Pathology, Section II. The Host Response to Injury, Chapter 3. The Acute Inflammatory Response, sub-section Cardinal Clinical Signs, Concise Pathology. *Concise Pathology*.

14. Thomas, P.G., Dash, P., Aldridge, J.R., Jr., Ellebedy, A.H., Reynolds, C., Funk, A.J., Martin, W.J., Lamkanfi, M., Webby, R.J., Boyd, K.L. *et al.* (2009) The intracellular sensor NLRP3 mediates key innate and healing responses to influenza A virus via the regulation of caspase-1. *Immunity*, **30**, 566-575.

15. Allen, I.C., Scull, M.A., Moore, C.B., Holl, E.K., McElvania-TeKippe, E., Taxman, D.J., Guthrie, E.H., Pickles, R.J. and Ting, J.P. (2009) The NLRP3 inflammasome mediates in vivo innate immunity to influenza A virus through recognition of viral RNA. *Immunity*, **30**, 556-565.

16. Hoebe, K., Janssen, E. and Beutler, B. (2004) The interface between innate and adaptive immunity. *Nature immunology*, **5**, 971-974.

17. Litman, G.W., Rast, J.P. and Fugmann, S.D. (2010) The origins of vertebrate adaptive immunity. *Nature reviews. Immunology*, **10**, 543-553.

18. Abbas, A.K., Lichtman, A.H. and Pillai, S. (1994) *Cellular and molecular immunology*. Elsevier Health Sciences.

19. Janeway, C.A., Travers, P., Walport, M. and Capra, J.D. (2001) *Immunobiology: the immune system in health and disease*. Churchill Livingstone.

20. Sen R, B.D. (1986) Multiple nuclear factors interact with the immunoglobulin enhancer sequences. *Cell*, **46**, 705–716.

21. Hayden, M.S. and Ghosh, S. (2004) Signaling to NF-kappaB. *Genes Dev*, **18**, 2195-2224.

22. Ghosh, S., May, M.J. and Kopp, E.B. (1998) NF-kappa B and Rel proteins: evolutionarily conserved mediators of immune responses. *Annual review of immunology*, **16**, 225-260.

23. Fitzgerald, D.C., Meade, K.G., McEvoy, A.N., Lillis, L., Murphy, E.P., MacHugh, D.E. and Baird, A.W. (2007) Tumour necrosis factor-alpha (TNF-alpha) increases nuclear factor kappaB (NFkappaB) activity in and interleukin-8 (IL-8) release from bovine mammary epithelial cells. *Veterinary immunology and immunopathology*, **116**, 59-68.

24. Basu, S., Rosenzweig, K.R., Youmell, M. and Price, B.D. (1998) The DNA-dependent protein kinase participates in the activation of NF kappa B following DNA damage. *Biochemical and biophysical research communications*, **247**, 79-83.

25. Chandel, N.S., Trzyna, W.C., McClintock, D.S. and Schumacker, P.T. (2000) Role of oxidants in NF-kappa B activation and TNF-alpha gene transcription induced by hypoxia and endotoxin. *Journal of immunology (Baltimore, Md. : 1950)*, **165**, 1013-1021.

26. Vallabhapurapu, S. and Karin, M. (2009) Regulation and function of NF-kappaB transcription factors in the immune system. *Annual review of immunology*, **27**, 693-733.

27. Skaug, B., Jiang, X. and Chen, Z.J. (2009) The role of ubiquitin in NF-kappaB regulatory pathways. *Annual review of biochemistry*, **78**, 769-796.

28. Wullaert, A., Bonnet, M.C. and Pasparakis, M. (2011) NF-kappaB in the regulation of epithelial homeostasis and inflammation. *Cell research*, **21**, 146-158.

29. Beg, A.A., Sha, W.C., Bronson, R.T. and Baltimore, D. (1995) Constitutive NF-kappa B activation, enhanced granulopoiesis, and neonatal lethality in I kappa B alpha-deficient mice. *Genes & Development*, **9**, 2736-2746.

30. Jiang, D., Liang, J., Fan, J., Yu, S., Chen, S., Luo, Y., Prestwich, G.D., Mascarenhas, M.M., Garg, H.G., Quinn, D.A. *et al.* (2005) Regulation of lung injury and repair by Toll-like receptors and hyaluronan. *Nature medicine*, **11**, 1173-1179.

31. Egan, L.J., de Lecea, A., Lehrman, E.D., Myhre, G.M., Eckmann, L. and Kagnoff, M.F. (2003) Nuclear factor-kappa B activation promotes restitution of wounded intestinal epithelial monolayers. *American journal of physiology. Cell physiology*, **285**, C1028-1035.

32. McDonald, P.P. (2004) Transcriptional regulation in neutrophils: teaching old cells new tricks. *Advances in immunology*, **82**, 1-48.

33. Francois, S., El Benna, J., Dang, P.M.C., Pedruzzi, E., Gougerot-Pocidalo, M.A. and Elbim, C. (2005) Inhibition of Neutrophil Apoptosis by TLR Agonists in Whole Blood: Involvement of the Phosphoinositide 3-Kinase/Akt and NF- B Signaling Pathways, Leading to Increased Levels of Mcl-1, A1, and Phosphorylated Bad. *The Journal of Immunology*, **174**, 3633-3642.

34. Siebenlist, U., Franzoso, G. and Brown, K. (1994) Structure, regulation and function of NF-kappa B. *Annual review of cell biology*, **10**, 405-455.

35. Ghosh, S. and Karin, M. (2002) Missing pieces in the NF-kappaB puzzle. *Cell*, **109 Suppl**, S81-96.

36. Senftleben, U., Cao, Y., Xiao, G., Greten, F.R., Krahn, G., Bonizzi, G., Chen, Y., Hu, Y., Fong, A., Sun, S.C. *et al.* (2001) Activation by IKKalpha of a second, evolutionary conserved, NF-kappa B signaling pathway. *Science*, **293**, 1495-1499.

37. Jacobs, M.D. and Harrison, S.C. (1998) Structure of an IkappaBalpha/NF-kappaB complex. *Cell*, **95**, 749-758.

38. Kanarek, N. and Ben-Neriah, Y. (2012) Regulation of NF-κB by ubiquitination and degradation of the IκBs. *Immunological reviews*, **246**, 77-94.

39. Karin, M. (1999) The Beginning of the End: I B Kinase (IKK) and NF- B Activation. *Journal of Biological Chemistry*, **274**, 27339-27342.

40. Beg, A.A. and Baldwin, A.S. (1993) The I kappa B proteins: multifunctional regulators of Rel/NF-kappa B transcription factors. *Genes & Development*, **7**, 2064-2070.

41. Deshaies, R.J. (1999) SCF and Cullin/Ring H2-based ubiquitin ligases. *Annual review of cell and developmental biology*, **15**, 435-467.

42. Kanarek, N., Grivennikov, S.I., Leshets, M., Lasry, A., Alkalay, I., Horwitz, E., Shaul, Y.D., Stachler, M., Voronov, E., Apte, R.N. *et al.* (2014) Critical role for IL-1beta in DNA damage-induced mucositis. *Proceedings of the National Academy of Sciences of the United States of America*, **111**, E702-711.

43. Brasier, A.R. (2006) The NF-kappaB regulatory network. *Cardiovascular toxicology*, **6**, 111-130.

44. Karin, M. and Ben-Neriah, Y. (2000) Phosphorylation meets ubiquitination: the control of NF-[kappa]B activity. *Annual review of immunology*, **18**, 621-663.

45. Nowak, D.E., Tian, B., Jamaluddin, M., Boldogh, I., Vergara, L.A., Choudhary, S. and Brasier, A.R. (2008) RelA Ser276 phosphorylation is required for activation of a subset of NF-kappaB-dependent genes by recruiting cyclin-dependent kinase 9/cyclin T1 complexes. *Molecular and cellular biology*, **28**, 3623-3638.

46. Tian, B., Zhao, Y., Kalita, M., Edeh, C.B., Paessler, S., Casola, A., Teng, M.N., Garofalo, R.P. and Brasier, A.R. (2013) CDK9-dependent transcriptional elongation in the innate interferon-stimulated gene

response to respiratory syncytial virus infection in airway epithelial cells. *Journal of virology*, **87**, 7075-7092.

47. Bonizzi, G. and Karin, M. (2004) The two NF-kappaB activation pathways and their role in innate and adaptive immunity. *Trends in immunology*, **25**, 280-288.

48. Sun, S.-C. (2011) Non-canonical NF-κB signaling pathway. *Cell research*, **21**, 71-85.

49. Sun, S.C. (2012) The noncanonical NF-κB pathway. *Immunological reviews*, **246**, 125-140.

50. Vallabhapurapu, S., Matsuzawa, A., Zhang, W., Tseng, P.H., Keats, J.J., Wang, H., Vignali, D.A., Bergsagel, P.L. and Karin, M. (2008) Nonredundant and complementary functions of TRAF2 and TRAF3 in a ubiquitination cascade that activates NIK-dependent alternative NF-kappaB signaling. *Nature immunology*, **9**, 1364-1370.

51. Zarnegar, B.J., Wang, Y., Mahoney, D.J., Dempsey, P.W., Cheung, H.H., He, J., Shiba, T., Yang, X., Yeh, W.C., Mak, T.W. *et al.* (2008) Noncanonical NF-kappaB activation requires coordinated assembly of a regulatory complex of the adaptors cIAP1, cIAP2, TRAF2 and TRAF3 and the kinase NIK. *Nature immunology*, **9**, 1371-1378.

52. Morrison, M.D., Reiley, W., Zhang, M. and Sun, S.C. (2005) An atypical tumor necrosis factor (TNF) receptor-associated factor-binding motif of B cell-activating factor belonging to the TNF family (BAFF) receptor

mediates induction of the noncanonical NF-kappaB signaling pathway. *The Journal of biological chemistry*, **280**, 10018-10024.

53. Sun, S.C., Ganchi, P.A., Ballard, D.W. and Greene, W.C. (1993) NF-kappa B controls expression of inhibitor I kappa B alpha: evidence for an inducible autoregulatory pathway. *Science*, **259**, 1912-1915.

54. Lin, X., Mu, Y., Cunningham, E.T., Jr., Marcu, K.B., Geleziunas, R. and Greene, W.C. (1998) Molecular determinants of NF-kappaB-inducing kinase action. *Molecular and cellular biology*, **18**, 5899-5907.

55. Ling, L., Cao, Z. and Goeddel, D.V. (1998) NF-kappaB-inducing kinase activates IKK-alpha by phosphorylation of Ser-176. *Proceedings of the National Academy of Sciences of the United States of America*, **95**, 3792-3797.

56. Lipniacki, T., Paszek, P., Brasier, A.R., Luxon, B. and Kimmel, M. (2004) Mathematical model of NF-kappaB regulatory module. *Journal of theoretical biology*, **228**, 195-215.

57. Basak, S., Kim, H., Kearns, J.D., Tergaonkar, V., O'Dea, E., Werner, S.L., Benedict, C.A., Ware, C.F., Ghosh, G., Verma, I.M. *et al.* (2007) A fourth IkappaB protein within the NF-kappaB signaling module. *Cell*, **128**, 369-381.

58. Qing, G. and Xiao, G. (2005) Essential role of IkappaB kinase alpha in the constitutive processing of NF-kappaB2 p100. *The Journal of biological chemistry*, **280**, 9765-9768.

59.   Dejardin, E., Droin, N.M., Delhase, M., Haas, E., Cao, Y., Makris, C., Li, Z.W., Karin, M., Ware, C.F. and Green, D.R. (2002) The lymphotoxin-beta receptor induces different patterns of gene expression via two NF-kappaB pathways. *Immunity*, **17**, 525-535.

60.   Choudhary, S., Kalita, M., Fang, L., Patel, K.V., Tian, B., Zhao, Y., Edeh, C.B. and Brasier, A.R. (2013) Inducible tumor necrosis factor (TNF) receptor-associated factor-1 expression couples the canonical to the non-canonical NF-kappaB pathway in TNF stimulation. *The Journal of biological chemistry*, **288**, 14612-14623.

61.   Knight, D.A. and Holgate, S.T. (2003) The airway epithelium: structural and functional properties in health and disease. *Respirology (Carlton, Vic.)*, **8**, 432-446.

62.   Hehlgans, T. and Pfeffer, K. (2005) The intriguing biology of the tumour necrosis factor/tumour necrosis factor receptor superfamily: players, rules and the games. *Immunology*, **115**, 1-20.

63.   MacEwan, D.J. (2002) TNF receptor subtype signalling: differences and cellular consequences. *Cellular signalling*, **14**, 477-492.

64.   Silke, J. (2011) The regulation of TNF signalling: what a tangled web we weave. *Current opinion in immunology*, **23**, 620-626.

65.   Chan, F.K. (2007) Three is better than one: pre-ligand receptor assembly in the regulation of TNF receptor signaling. *Cytokine*, **37**, 101-107.

66.   Wajant, H., Pfizenmaier, K. and Scheurich, P. (2003) Tumor necrosis factor signaling. *Cell death and differentiation*, **10**, 45-65.

67. Zheng, C., Kabaleeswaran, V., Wang, Y., Cheng, G. and Wu, H. (2010) Crystal structures of the TRAF2: cIAP2 and the TRAF1: TRAF2: cIAP2 complexes: affinity, specificity, and regulation. *Molecular cell*, **38**, 101-113.

68. Chen, Z.J. and Sun, L.J. (2009) Nonproteolytic functions of ubiquitin in cell signaling. *Molecular cell*, **33**, 275-286.

69. Mahoney, D.J., Cheung, H.H., Mrad, R.L., Plenchette, S., Simard, C., Enwere, E., Arora, V., Mak, T.W., Lacasse, E.C., Waring, J. *et al.* (2008) Both cIAP1 and cIAP2 regulate TNFalpha-mediated NF-kappaB activation. *Proceedings of the National Academy of Sciences of the United States of America*, **105**, 11778-11783.

70. Varfolomeev, E., Goncharov, T., Fedorova, A.V., Dynek, J.N., Zobel, K., Deshayes, K., Fairbrother, W.J. and Vucic, D. (2008) c-IAP1 and c-IAP2 are critical mediators of tumor necrosis factor alpha (TNFalpha)-induced NF-kappaB activation. *The Journal of biological chemistry*, **283**, 24295-24299.

71. Glezen, W.P., Taber, L.H., Frank, A.L. and Kasel, J.A. (1986) Risk of primary infection and reinfection with respiratory syncytial virus. *American journal of diseases of children (1960)*, **140**, 543-546.

72. Hall, C.B., Weinberg, G.A., Iwane, M.K., Blumkin, A.K., Edwards, K.M., Staat, M.A., Auinger, P., Griffin, M.R., Poehling, K.A., Erdman, D. *et al.* (2009) The burden of respiratory syncytial virus infection in young children. *The New England journal of medicine*, **360**, 588-598.

73.   Nair, H., Nokes, D.J., Gessner, B.D., Dherani, M., Madhi, S.A., Singleton, R.J., O'Brien, K.L., Roca, A., Wright, P.F., Bruce, N. *et al.* (2010) Global burden of acute lower respiratory infections due to respiratory syncytial virus in young children: a systematic review and meta-analysis. *Lancet*, **375**, 1545-1555.

74.   Welliver, R.C. (2004) Respiratory syncytial virus infection: therapy and prevention. *Paediatric respiratory reviews*, **5 Suppl A**, S127-133.

75.   Zorc, J.J. and Hall, C.B. (2010) Bronchiolitis: recent evidence on diagnosis and management. *Pediatrics*, **125**, 342-349.

76.   Hall, C.B., Douglas, R.G., Jr., Schnabel, K.C. and Geiman, J.M. (1981) Infectivity of respiratory syncytial virus by various routes of inoculation. *Infection and immunity*, **33**, 779-783.

77.   Zhang, L., Peeples, M.E., Boucher, R.C., Collins, P.L. and Pickles, R.J. (2002) Respiratory Syncytial Virus Infection of Human Airway Epithelial Cells Is Polarized, Specific to Ciliated Cells, and without Obvious Cytopathology. *Journal of virology*, **76**, 5654-5666.

78.   Aherne, W., Bird, T., Court, S.D., Gardner, P.S. and McQuillin, J. (1970) Pathological changes in virus infections of the lower respiratory tract in children. *Journal of clinical pathology*, **23**, 7-18.

79.   Welliver, T.P., Garofalo, R.P., Hosakote, Y., Hintz, K.H., Avendano, L., Sanchez, K., Velozo, L., Jafri, H., Chavez-Bueno, S., Ogra, P.L. *et al.* (2007) Severe human lower respiratory tract illness caused by respiratory syncytial virus and influenza virus is characterized by the absence of

pulmonary cytotoxic lymphocyte responses. *The Journal of infectious diseases*, **195**, 1126-1136.

80. Garofalo, R., Sabry, M., Jamaluddin, M., Yu, R.K., Casola, A., Ogra, P.L. and Brasier, A.R. (1996) Transcriptional activation of the interleukin-8 gene by respiratory syncytial virus infection in alveolar epithelial cells: nuclear translocation of the RelA transcription factor as a mechanism producing airway mucosal inflammation. *Journal of virology*, **70**, 8773-8781.

81. Brasier, A.R., Tian, B., Jamaluddin, M., Kalita, M.K., Garofalo, R.P. and Lu, M. (2011) RelA Ser276 phosphorylation-coupled Lys310 acetylation controls transcriptional elongation of inflammatory cytokines in respiratory syncytial virus infection. *Journal of virology*, **85**, 11752-11769.

82. Tian, B., Zhang, Y., Luxon, B.A., Garofalo, R.P., Casola, A., Sinha, M. and Brasier, A.R. (2002) Identification of NF- B-Dependent Gene Networks in Respiratory Syncytial Virus-Infected Cells. *Journal of virology*, **76**, 6800-6814.

83. Zhang, Y., Luxon, B.A., Casola, A., Garofalo, R.P., Jamaluddin, M. and Brasier, A.R. (2001) Expression of respiratory syncytial virus-induced chemokine gene networks in lower airway epithelial cells revealed by cDNA microarrays. *Journal of virology*, **75**, 9044-9058.

84. Ray, A., Cot, M., Puzo, G., Gilleron, M. and Nigou, J. (2013) Bacterial cell wall macroamphiphiles: pathogen-/microbe-associated molecular patterns detected by mammalian innate immune system. *Biochimie*, **95**, 33-42.

85.   Loo, Y.M. and Gale, M., Jr. (2011) Immune signaling by RIG-I-like receptors. *Immunity*, **34**, 680-692.

86.   Liu, P., Jamaluddin, M., Li, K., Garofalo, R.P., Casola, A. and Brasier, A.R. (2007) Retinoic acid-inducible gene I mediates early antiviral response and Toll-like receptor 3 expression in respiratory syncytial virus-infected airway epithelial cells. *Journal of virology*, **81**, 1401-1411.

87.   Bibeau-Poirier, A. and Servant, M.J. (2008) Roles of ubiquitination in pattern-recognition receptors and type I interferon receptor signaling. *Cytokine*, **43**, 359-367.

88.   Kato, H., Sato, S., Yoneyama, M., Yamamoto, M., Uematsu, S., Matsui, K., Tsujimura, T., Takeda, K., Fujita, T., Takeuchi, O. *et al.* (2005) Cell type-specific involvement of RIG-I in antiviral response. *Immunity*, **23**, 19-28.

89.   Kawai, T., Takahashi, K., Sato, S., Coban, C., Kumar, H., Kato, H., Ishii, K.J., Takeuchi, O. and Akira, S. (2005) IPS-1, an adaptor triggering RIG-I- and Mda5-mediated type I interferon induction. *Nature immunology*, **6**, 981-988.

90.   Geisbert, T., Huang, C., Kolokoltsova, O.A., Yun, N.E., Seregin, A.V., Poussard, A.L., Walker, A.G., Brasier, A.R., Zhao, Y., Tian, B. *et al.* (2012) Junín Virus Infection Activates the Type I Interferon Pathway in a RIG-I-Dependent Manner. *PLoS Neglected Tropical Diseases*, **6**, e1659.

91.   Yoneyama, M. and Fujita, T. (2008) Structural mechanism of RNA recognition by the RIG-I-like receptors. *Immunity*, **29**, 178-181.

92.   Yount, J.S., Gitlin, L., Moran, T.M. and Lopez, C.B. (2008) MDA5
       participates in the detection of paramyxovirus infection and is essential for
       the early activation of dendritic cells in response to Sendai Virus defective
       interfering particles. *Journal of immunology (Baltimore, Md. : 1950)*, **180**,
       4910-4918.

93.   Seth, R.B., Sun, L., Ea, C.K. and Chen, Z.J. (2005) Identification and
       characterization of MAVS, a mitochondrial antiviral signaling protein that
       activates NF-kappaB and IRF 3. *Cell*, **122**, 669-682.

94.   Doyle, S., Vaidya, S., O'Connell, R., Dadgostar, H., Dempsey, P., Wu, T.,
       Rao, G., Sun, R., Haberland, M., Modlin, R. *et al.* (2002) IRF3 mediates a
       TLR3/TLR4-specific antiviral gene program. *Immunity*, **17**, 251-263.

95.   Sha, Q., Truong-Tran, A.Q., Plitt, J.R., Beck, L.A. and Schleimer, R.P.
       (2004) Activation of airway epithelial cells by toll-like receptor agonists.
       American journal of respiratory cell and molecular biology, **31**, 358-364.

96.   Yamamoto, M., Sato, S., Hemmi, H., Hoshino, K., Kaisho, T., Sanjo, H.,
       Takeuchi, O., Sugiyama, M., Okabe, M., Takeda, K. *et al.* (2003) Role of
       adaptor TRIF in the MyD88-independent toll-like receptor signaling
       pathway. *Science*, **301**, 640-643.

97.   Schoggins, J.W. and Rice, C.M. (2011) Interferon-stimulated genes and
       their antiviral effector functions. *Current opinion in virology*, **1**, 519-525.

98.   Sadler, A.J. and Williams, B.R. (2008) Interferon-inducible antiviral
       effectors. *Nature reviews. Immunology*, **8**, 559-568.

99. Der, S.D., Zhou, A., Williams, B.R. and Silverman, R.H. (1998) Identification of genes differentially regulated by interferon alpha, beta, or gamma using oligonucleotide arrays. *Proceedings of the National Academy of Sciences of the United States of America*, **95**, 15623-15628.

100. Smith, P.L., Lombardi, G. and Foster, G.R. (2005) Type I interferons and the innate immune response--more than just antiviral cytokines. *Molecular immunology*, **42**, 869-877.

101. Thomas, E., Gonzalez, V.D., Li, Q., Modi, A.A., Chen, W., Noureddin, M., Rotman, Y. and Liang, T.J. (2012) HCV infection induces a unique hepatic innate immune response associated with robust production of type III interferons. *Gastroenterology*, **142**, 978-988.

102. Schneider, W.M., Chevillotte, M.D. and Rice, C.M. (2014) Interferon-stimulated genes: a complex web of host defenses. *Annual review of immunology*, **32**, 513-545.

103. Jamaluddin, M., Casola, A., Garofalo, R.P., Han, Y., Elliott, T., Ogra, P.L. and Brasier, A.R. (1998) The major component of IkappaBalpha proteolysis occurs independently of the proteasome pathway in respiratory syncytial virus-infected pulmonary epithelial cells. *Journal of virology*, **72**, 4849-4857.

104. Liu, T., Castro, S., Brasier, A.R., Jamaluddin, M., Garofalo, R.P. and Casola, A. (2004) Reactive oxygen species mediate virus-induced STAT activation: role of tyrosine phosphatases. *The Journal of biological chemistry*, **279**, 2461-2469.

105. Haeberle, H.A., Takizawa, R., Casola, A., Brasier, A.R., Dieterich, H.J., Van Rooijen, N., Gatalica, Z. and Garofalo, R.P. (2002) Respiratory syncytial virus-induced activation of nuclear factor-kappaB in the lung involves alveolar macrophages and toll-like receptor 4-dependent pathways. *The Journal of infectious diseases*, **186**, 1199-1206.

106. Liu, P., Li, K., Garofalo, R.P. and Brasier, A.R. (2008) Respiratory syncytial virus induces RelA release from cytoplasmic 100-kDa NF-kappa B2 complexes via a novel retinoic acid-inducible gene-I{middle dot}NF-kappa B-inducing kinase signaling pathway. *The Journal of biological chemistry*, **283**, 23169-23178.

107. Choudhary, S., Boldogh, S., Garofalo, R., Jamaluddin, M. and Brasier, A.R. (2005) Respiratory syncytial virus influences NF-kappaB-dependent gene expression through a novel pathway involving MAP3K14/NIK expression and nuclear complex formation with NF-kappaB2. *Journal of virology*, **79**, 8948-8959.

108. Casola, A., Burger, N., Liu, T., Jamaluddin, M., Brasier, A.R. and Garofalo, R.P. (2001) Oxidant tone regulates RANTES gene expression in airway epithelial cells infected with respiratory syncytial virus. Role in viral-induced interferon regulatory factor activation. *The Journal of biological chemistry*, **276**, 19715-19722.

109. Fink, K., Duval, A., Martel, A., Soucy-Faulkner, A. and Grandvaux, N. (2008) Dual role of NOX2 in respiratory syncytial virus- and sendai virus-

induced activation of NF-kappaB in airway epithelial cells. *Journal of immunology (Baltimore, Md. : 1950)*, **180**, 6911-6922.

110. Kim, J.J., Lee, S.B., Park, J.K. and Yoo, Y.D. (2010) TNF-alpha-induced ROS production triggering apoptosis is directly linked to Romo1 and Bcl-X(L). *Cell death and differentiation*, **17**, 1420-1434.

111. Jamaluddin, M., Tian, B., Boldogh, I., Garofalo, R.P. and Brasier, A.R. (2009) Respiratory syncytial virus infection induces a reactive oxygen species-MSK1-phospho-Ser-276 RelA pathway required for cytokine expression. *Journal of virology*, **83**, 10605-10615.

112. Jamaluddin, M., Wang, S., Boldogh, I., Tian, B. and Brasier, A.R. (2007) TNF-alpha-induced NF-kappaB/RelA Ser(276) phosphorylation and enhanceosome formation is mediated by an ROS-dependent PKAc pathway. *Cellular signalling*, **19**, 1419-1433.

113. Gatti, R.A., Berkel, I., Boder, E., Braedt, G., Charmley, P., Concannon, P., Ersoy, F., Foroud, T., Jaspers, N.G., Lange, K. *et al.* (1988) Localization of an ataxia-telangiectasia gene to chromosome 11q22-23. *Nature*, **336**, 577-580.

114. Savitsky, K., Bar-Shira, A., Gilad, S., Rotman, G., Ziv, Y., Vanagaite, L., Tagle, D.A., Smith, S., Uziel, T., Sfez, S. *et al.* (1995) A single ataxia telangiectasia gene with a product similar to PI-3 kinase. *Science*, **268**, 1749-1753.

115. Gatti, R.A., Becker-Catania, S., Chun, H.H., Sun, X., Mitui, M., Lai, C.H., Khanlou, N., Babaei, M., Cheng, R., Clark, C. *et al.* (2001) The

pathogenesis of ataxia-telangiectasia. Learning from a Rosetta Stone. *Clinical reviews in allergy & immunology*, **20**, 87-108.

116. McKinnon, P.J. (2004) ATM and ataxia telangiectasia. *EMBO reports*, **5**, 772-776.

117. Taylor, A.M. and Byrd, P.J. (2005) Molecular pathology of ataxia telangiectasia. *Journal of clinical pathology*, **58**, 1009-1015.

118. Nowak-Wegrzyn, A., Crawford, T.O., Winkelstein, J.A., Carson, K.A. and Lederman, H.M. (2004) Immunodeficiency and infections in ataxia-telangiectasia. *The Journal of pediatrics*, **144**, 505-511.

119. Reiman, A., Srinivasan, V., Barone, G., Last, J.I., Wootton, L.L., Davies, E.G., Verhagen, M.M., Willemsen, M.A., Weemaes, C.M., Byrd, P.J. *et al.* (2011) Lymphoid tumours and breast cancer in ataxia telangiectasia; substantial protective effect of residual ATM kinase activity against childhood tumours. *British journal of cancer*, **105**, 586-591.

120. McGrath-Morrow, S., Lefton-Greif, M., Rosquist, K., Crawford, T., Kelly, A., Zeitlin, P., Carson, K.A. and Lederman, H.M. (2008) Pulmonary function in adolescents with ataxia telangiectasia. *Pediatric pulmonology*, **43**, 59-66.

121. Schroeder, S.A., Swift, M., Sandoval, C. and Langston, C. (2005) Interstitial lung disease in patients with ataxia-telangiectasia. *Pediatric pulmonology*, **39**, 537-543.

122. Abraham, R.T. (2001) Cell cycle checkpoint signaling through the ATM and ATR kinases. *Genes Dev*, **15**, 2177-2196.

123. Bakkenist, C.J. and Kastan, M.B. (2003) DNA damage activates ATM through intermolecular autophosphorylation and dimer dissociation. *Nature*, **421**, 499-506.

124. Stracker, T.H. and Petrini, J.H. (2011) The MRE11 complex: starting from the ends. *Nature reviews. Molecular cell biology*, **12**, 90-103.

125. Williams, G.J., Lees-Miller, S.P. and Tainer, J.A. (2010) Mre11-Rad50-Nbs1 conformations and the control of sensing, signaling, and effector responses at DNA double-strand breaks. *DNA repair*, **9**, 1299-1306.

126. Difilippantonio, S., Celeste, A., Fernandez-Capetillo, O., Chen, H.T., Reina San Martin, B., Van Laethem, F., Yang, Y.P., Petukhova, G.V., Eckhaus, M., Feigenbaum, L. *et al.* (2005) Role of Nbs1 in the activation of the Atm kinase revealed in humanized mouse models. *Nature cell biology*, **7**, 675-685.

127. Lee, J.H. and Paull, T.T. (2007) Activation and regulation of ATM kinase activity in response to DNA double-strand breaks. *Oncogene*, **26**, 7741-7748.

128. Smith, J., Tho, L.M., Xu, N. and Gillespie, D.A. (2010) The ATM-Chk2 and ATR-Chk1 pathways in DNA damage signaling and cancer. *Advances in cancer research*, **108**, 73-112.

129. Kang, J., Ferguson, D., Song, H., Bassing, C., Eckersdorff, M., Alt, F.W. and Xu, Y. (2005) Functional interaction of H2AX, NBS1, and p53 in ATM-dependent DNA damage responses and tumor suppression. *Molecular and cellular biology*, **25**, 661-670.

130. Kim, S.T., Xu, B. and Kastan, M.B. (2002) Involvement of the cohesin protein, Smc1, in Atm-dependent and independent responses to DNA damage. *Genes Dev*, **16**, 560-570.

131. Kurz, E.U. and Lees-Miller, S.P. (2004) DNA damage-induced activation of ATM and ATM-dependent signaling pathways. *DNA repair*, **3**, 889-900.

132. Yazdi, P.T., Wang, Y., Zhao, S., Patel, N., Lee, E.Y. and Qin, J. (2002) SMC1 is a downstream effector in the ATM/NBS1 branch of the human S-phase checkpoint. *Genes Dev*, **16**, 571-582.

133. Ditch, S. and Paull, T.T. (2012) The ATM protein kinase and cellular redox signaling: beyond the DNA damage response. *Trends in biochemical sciences*, **37**, 15-22.

134. Ousset, M., Bouquet, F., Fallone, F., Biard, D., Dray, C., Valet, P., Salles, B. and Muller, C. (2010) Loss of ATM positively regulates the expression of hypoxia inducible factor 1 (HIF-1) through oxidative stress: Role in the physiopathology of the disease. *Cell cycle (Georgetown, Tex.)*, **9**, 2814-2822.

135. Kamsler, A., Daily, D., Hochman, A., Stern, N., Shiloh, Y., Rotman, G. and Barzilai, A. (2001) Increased oxidative stress in ataxia telangiectasia evidenced by alterations in redox state of brains from Atm-deficient mice. *Cancer research*, **61**, 1849-1854.

136. Okuno, Y., Nakamura-Ishizu, A., Otsu, K., Suda, T. and Kubota, Y. (2012) Pathological neoangiogenesis depends on oxidative stress regulation by ATM. *Nature medicine*, **18**, 1208-1216.

137. Guo, Z., Deshpande, R. and Paull, T.T. (2010) ATM activation in the presence of oxidative stress. *Cell cycle (Georgetown, Tex.)*, **9**, 4805-4811.

138. Shiloh, Y. (2003) ATM and related protein kinases: safeguarding genome integrity. *Nature reviews. Cancer*, **3**, 155-168.

139. Meylan, E., Tschopp, J. and Karin, M. (2006) Intracellular pattern recognition receptors in the host response. *Nature*, **442**, 39-44.

140. McCool, K.W. and Miyamoto, S. (2012) DNA damage-dependent NF-kappaB activation: NEMO turns nuclear signaling inside out. *Immunological reviews*, **246**, 311-326.

141. Wu, Z.H., Shi, Y., Tibbetts, R.S. and Miyamoto, S. (2006) Molecular linkage between the kinase ATM and NF-kappaB signaling in response to genotoxic stimuli. *Science,* **311**, 1141-1146.

142. Suematsu, N. (2003) Oxidative Stress Mediates Tumor Necrosis Factor-alpha-Induced Mitochondrial DNA Damage and Dysfunction in Cardiac Myocytes. *Circulation*, **107**, 1418-1423.

143. Wheelhouse, N.M., Chan, Y.S., Gillies, S.E., Caldwell, H., Ross, J.A., Harrison, D.J. and Prost, S. (2003) TNF-alpha induced DNA damage in primary murine hepatocytes. *International journal of molecular medicine*, **12**, 889-894.

144. Ba, X., Bacsi, A., Luo, J., Aguilera-Aguirre, L., Zeng, X., Radak, Z., Brasier, A.R. and Boldogh, I. (2014) 8-oxoguanine DNA glycosylase-1 augments proinflammatory gene expression by facilitating the recruitment

of site-specific transcription factors. *Journal of immunology (Baltimore, Md. : 1950)*, **192**, 2384-2394.

145. Zhang, J.H. (1999) A Simple Statistical Parameter for Use in Evaluation and Validation of High Throughput Screening Assays. *Journal of Biomolecular Screening*, **4**, 67-73.

146. Rieber, N., Knapp, B., Eils, R. and Kaderali, L. (2009) RNAither, an automated pipeline for the statistical analysis of high-throughput RNAi screens. *Bioinformatics*, **25**, 678-679.

147. Ueba, O. (1978) Respiratory syncytial virus. I. Concentration and purification of the infectious virus. *Acta medica Okayama*, **32**, 265-272.

148. Foy, E., Li, K., Wang, C., Sumpter, R., Jr., Ikeda, M., Lemon, S.M. and Gale, M., Jr. (2003) Regulation of interferon regulatory factor-3 by the hepatitis C virus serine protease. *Science*, **300**, 1145-1148.

149. Ray, S., Ju, X., Sun, H., Finnerty, C.C., Herndon, D.N. and Brasier, A.R. (2013) The IL-6 trans-signaling-STAT3 pathway mediates ECM and cellular proliferation in fibroblasts from hypertrophic scar. *The Journal of investigative dermatology*, **133**, 1212-1220.

150. Forbus, J., Spratt, H., Wiktorowicz, J., Wu, Z., Boldogh, I., Denner, L., Kurosky, A., Brasier, R.C., Luxon, B. and Brasier, A.R. (2006) Functional analysis of the nuclear proteome of human A549 alveolar epithelial cells by HPLC-high resolution 2-D gel electrophoresis. *Proteomics*, **6**, 2656-2672.

151. Nowak, D.E., Tian, B. and Brasier, A.R. (2005) Two-step cross-linking method for identification of NF-kappaB gene network by chromatin immunoprecipitation. *BioTechniques*, **39**, 715-725.

152. Zhao, Y. and Brasier, A.R. (2013) Applications of selected reaction monitoring (SRM)-mass spectrometry (MS) for quantitative measurement of signaling pathways. *Methods (San Diego, Calif.)*, **61**, 313-322.

153. Zhao, Y., Tian, B., Edeh, C.B. and Brasier, A.R. (2013) Quantitation of the dynamic profiles of the innate immune response using multiplex selected reaction monitoring-mass spectrometry. *Molecular & cellular proteomics : MCP*, **12**, 1513-1529.

154. Bacsi, A., Aguilera-Aguirre, L., Szczesny, B., Radak, Z., Hazra, T.K., Sur, S., Ba, X. and Boldogh, I. (2013) Down-regulation of 8-oxoguanine DNA glycosylase 1 expression in the airway epithelium ameliorates allergic lung inflammation. *DNA repair*, **12**, 18-26.

155. Malo, N., Hanley, J.A., Cerquozzi, S., Pelletier, J. and Nadon, R. (2006) Statistical practice in high-throughput screening data analysis. *Nature biotechnology*, **24**, 167-175.

156. Duran, A., Diaz-Meco, M.T. and Moscat, J. (2003) Essential role of RelA Ser311 phosphorylation by zetaPKC in NF-kappaB transcriptional activation. *The EMBO journal*, **22**, 3910-3918.

157. Sun, W., Ge, N., Yu, Y., Burlingame, S., Li, X., Zhang, M., Ye, S., Fu, S. and Yang, J. (2010) Phosphorylation of Thr-516 and Ser-520 in the kinase activation loop of MEKK3 is required for lysophosphatidic acid-mediated

optimal IkappaB kinase beta (IKKbeta)/nuclear factor-kappaB (NF-kappaB) activation. *The Journal of biological chemistry*, **285**, 7911-7918.

158. New, L., Jiang, Y. and Han, J. (2003) Regulation of PRAK subcellular location by p38 MAP kinases. *Molecular biology of the cell*, **14**, 2603-2616.

159. Folmer, F., Blasius, R., Morceau, F., Tabudravu, J., Dicato, M., Jaspars, M. and Diederich, M. (2006) Inhibition of TNFalpha-induced activation of nuclear factor kappaB by kava (Piper methysticum) derivatives. *Biochemical pharmacology*, **71**, 1206-1218.

160. Tian, B., Nowak, D.E. and Brasier, A.R. (2005) A TNF-induced gene expression program under oscillatory NF-kappaB control. *BMC genomics*, **6**, 137.

161. Lau, A., Swinbank, K.M., Ahmed, P.S., Taylor, D.L., Jackson, S.P., Smith, G.C. and O'Connor, M.J. (2005) Suppression of HIV-1 infection by a small molecule inhibitor of the ATM kinase. *Nature cell biology*, **7**, 493-500.

162. Olive, P.L., Wlodek, D. and Banath, J.P. (1991) DNA double-strand breaks measured in individual cells subjected to gel electrophoresis. *Cancer research*, **51**, 4671-4676.

163. Halasi, M., Wang, M., Chavan, T.S., Gaponenko, V., Hay, N. and Gartel, A.L. (2013) ROS inhibitor N-acetyl-L-cysteine antagonizes the activity of proteasome inhibitors. *The Biochemical journal*, **454**, 201-208.

164. Hinz, M., Stilmann, M., Arslan, S.C., Khanna, K.K., Dittmar, G. and Scheidereit, C. (2010) A cytoplasmic ATM-TRAF6-cIAP1 module links

nuclear DNA damage signaling to ubiquitin-mediated NF-kappaB activation. *Molecular cell*, **40**, 63-74.

165. Zeng, W., Sun, L., Jiang, X., Chen, X., Hou, F., Adhikari, A., Xu, M. and Chen, Z.J. (2010) Reconstitution of the RIG-I pathway reveals a signaling role of unanchored polyubiquitin chains in innate immunity. *Cell*, **141**, 315-330.

166. Hou, F., Sun, L., Zheng, H., Skaug, B., Jiang, Q.X. and Chen, Z.J. (2011) MAVS forms functional prion-like aggregates to activate and propagate antiviral innate immune response. *Cell*, **146**, 448-461.

167. Choudhary, S., Rosenblatt, K.P., Fang, L., Tian, B., Wu, Z.H. and Brasier, A.R. (2011) High throughput short interfering RNA (siRNA) screening of the human kinome identifies novel kinases controlling the canonical nuclear factor-kappaB (NF-kappaB) activation pathway. *The Journal of biological chemistry*, **286**, 37187-37195.

168. Winston, J.T., Strack, P., Beer-Romero, P., Chu, C.Y., Elledge, S.J. and Harper, J.W. (1999) The SCFbeta-TRCP-ubiquitin ligase complex associates specifically with phosphorylated destruction motifs in IkappaBalpha and beta-catenin and stimulates IkappaBalpha ubiquitination in vitro. *Genes Dev*, **13**, 270-283.

169. Latres, E., Chiaur, D.S. and Pagano, M. (1999) The human F box protein beta-Trcp associates with the Cul1/Skp1 complex and regulates the stability of beta-catenin. *Oncogene*, **18**, 849-854.

170. Liang, C., Zhang, M. and Sun, S.C. (2006) beta-TrCP binding and processing of NF-kappaB2/p100 involve its phosphorylation at serines 866 and 870. *Cellular signalling*, **18**, 1309-1317.

171. Jaamaa, S., Af Hallstrom, T.M., Sankila, A., Rantanen, V., Koistinen, H., Stenman, U.H., Zhang, Z., Yang, Z., De Marzo, A.M., Taari, K. *et al.* (2010) DNA damage recognition via activated ATM and p53 pathway in nonproliferating human prostate tissue. *Cancer research*, **70**, 8630-8641.

172. Zhong, H., Voll, R.E. and Ghosh, S. (1998) Phosphorylation of NF-kappa B p65 by PKA stimulates transcriptional activity by promoting a novel bivalent interaction with the coactivator CBP/p300. *Molecular cell*, **1**, 661-671.

173. Jiang, X., Takahashi, N., Matsui, N., Tetsuka, T. and Okamoto, T. (2003) The NF-kappa B activation in lymphotoxin beta receptor signaling depends on the phosphorylation of p65 at serine 536. *The Journal of biological chemistry*, **278**, 919-926.

174. Spooren, A., Kolmus, K., Vermeulen, L., Van Wesemael, K., Haegeman, G. and Gerlo, S. (2010) Hunting for serine 276-phosphorylated p65. *Journal of biomedicine & biotechnology*, **2010**, 275892.

175. Nakai, Y., Hamagaki, S., Takagi, R., Taniguchi, A. and Kurimoto, F. (1999) Plasma concentrations of tumor necrosis factor-alpha (TNF-alpha) and soluble TNF receptors in patients with anorexia nervosa. *The Journal of clinical endocrinology and metabolism*, **84**, 1226-1228.

176. Damas, P., Reuter, A., Gysen, P., Demonty, J., Lamy, M. and Franchimont, P. (1989) Tumor necrosis factor and interleukin-1 serum levels during severe sepsis in humans. *Critical care medicine*, **17**, 975-978.

177. Foster, K.A., Oster, C.G., Mayer, M.M., Avery, M.L. and Audus, K.L. (1998) Characterization of the A549 cell line as a type II pulmonary epithelial cell model for drug metabolism. *Experimental cell research*, **243**, 359-366.

178. Jamaluddin, M., Wang, S., Garofalo, R.P., Elliott, T., Casola, A., Baron, S. and Brasier, A.R. (2001) IFN-beta mediates coordinate expression of antigen-processing genes in RSV-infected pulmonary epithelial cells. *American journal of physiology. Lung cellular and molecular physiology*, **280**, L248-257.

179. Rohaly, G., Korf, K., Dehde, S. and Dornreiter, I. (2010) Simian virus 40 activates ATR-Delta p53 signaling to override cell cycle and DNA replication control. *Journal of virology*, **84**, 10727-10747.

180. Hein, J., Boichuk, S., Wu, J., Cheng, Y., Freire, R., Jat, P.S., Roberts, T.M. and Gjoerup, O.V. (2009) Simian virus 40 large T antigen disrupts genome integrity and activates a DNA damage response via Bub1 binding. *Journal of virology*, **83**, 117-127.

181. Bian, T., Gibbs, J.D., Orvell, C. and Imani, F. (2012) Respiratory syncytial virus matrix protein induces lung epithelial cell cycle arrest through a p53 dependent pathway. *PloS one*, **7**, e38052.

182. Wu, W., Tran, K.C., Teng, M.N., Heesom, K.J., Matthews, D.A., Barr, J.N. and Hiscox, J.A. (2012) The interactome of the human respiratory syncytial virus NS1 protein highlights multiple effects on host cell biology. *Journal of virology*, **86**, 7777-7789.

183. Lu, R., Moore, P.A. and Pitha, P.M. (2002) Stimulation of IRF-7 gene expression by tumor necrosis factor alpha: requirement for NFkappa B transcription factor and gene accessibility. *The Journal of biological chemistry*, **277**, 16592-16598.

184. Bertolusso, R., Tian, B., Zhao, Y., Vergara, L., Sabree, A., Iwanaszko, M., Lipniacki, T., Brasier, A.R. and Kimmel, M. (2014) Dynamic cross talk model of the epithelial innate immune response to double-stranded RNA stimulation: coordinated dynamics emerging from cell-level noise. *PloS one*, **9**, e93396.

185. Leitges, M., Sanz, L., Martin, P., Duran, A., Braun, U., Garcia, J.F., Camacho, F., Diaz-Meco, M.T., Rennert, P.D. and Moscat, J. (2001) Targeted disruption of the zetaPKC gene results in the impairment of the NF-kappaB pathway. *Molecular cell*, **8**, 771-780.

186. Kai, M., Yasuda, S., Imai, S., Toyota, M., Kanoh, H. and Sakane, F. (2009) Diacylglycerol kinase alpha enhances protein kinase Czeta-dependent phosphorylation at Ser311 of p65/RelA subunit of nuclear factor-kappaB. *FEBS letters*, **583**, 3265-3268.

187. Huang, X., Chen, L.Y., Doerner, A.M., Pan, W.W., Smith, L., Huang, S., Papadimos, T.J. and Pan, Z.K. (2009) An atypical protein kinase C (PKC

zeta) plays a critical role in lipopolysaccharide-activated NF-kappa B in human peripheral blood monocytes and macrophages. *Journal of immunology (Baltimore, Md. : 1950)*, **182**, 5810-5815.

188. Brasier, A.R. (2008) Expanding role of cyclin dependent kinases in cytokine inducible gene expression. *Cell cycle (Georgetown, Tex.)*, **7**, 2661-2666.

189. Loyer, P., Trembley, J.H., Katona, R., Kidd, V.J. and Lahti, J.M. (2005) Role of CDK/cyclin complexes in transcription and RNA splicing. *Cellular signalling*, **17**, 1033-1051.

190. Vanden Bush, T.J. and Bishop, G.A. (2011) CDK-mediated regulation of cell functions via c-Jun phosphorylation and AP-1 activation. *PloS one*, **6**, e19468.

191. Perkins, N.D. (1997) Regulation of NF-kappa B by Cyclin-Dependent Kinases Associated with the p300 Coactivator. *Science*, **275**, 523-527.

192. Sims, R.J., 3rd, Belotserkovskaya, R. and Reinberg, D. (2004) Elongation by RNA polymerase II: the short and long of it. *Genes Dev*, **18**, 2437-2468.

193. Jhou, R.S., Sun, K.H., Sun, G.H., Wang, H.H., Chang, C.I., Huang, H.C., Lu, S.Y. and Tang, S.J. (2009) Inhibition of cyclin-dependent kinases by olomoucine and roscovitine reduces lipopolysaccharide-induced inflammatory responses via down-regulation of nuclear factor kappaB. *Cell proliferation*, **42**, 141-149.

194. Harper, J.W. and Elledge, S.J. (1998) The role of Cdk7 in CAK function, a retro-retrospective. *Genes Dev*, **12**, 285-289.

195. Wu, Z.H., Wong, E.T., Shi, Y., Niu, J., Chen, Z., Miyamoto, S. and Tergaonkar, V. (2010) ATM- and NEMO-dependent ELKS ubiquitination coordinates TAK1-mediated IKK activation in response to genotoxic stress. *Molecular cell*, **40**, 75-86.

196. Rosato, R.R., Kolla, S.S., Hock, S.K., Almenara, J.A., Patel, A., Amin, S., Atadja, P., Fisher, P.B., Dent, P. and Grant, S. (2010) Histone deacetylase inhibitors activate NF-kappaB in human leukemia cells through an ATM/NEMO-related pathway. *The Journal of biological chemistry*, **285**, 10064-10077.

197. Tian, B., Nowak, D.E., Jamaluddin, M., Wang, S. and Brasier, A.R. (2005) Identification of direct genomic targets downstream of the nuclear factor-kappaB transcription factor mediating tumor necrosis factor signaling. *The Journal of biological chemistry*, **280**, 17435-17448.

198. Shoji, Y., Uedono, Y., Ishikura, H., Takeyama, N. and Tanaka, T. (1995) DNA damage induced by tumour necrosis factor-alpha in L929 cells is mediated by mitochondrial oxygen radical formation. *Immunology*, **84**, 543-548.

199. Corda, S., Laplace, C., Vicaut, E. and Duranteau, J. (2001) Rapid reactive oxygen species production by mitochondria in endothelial cells exposed to tumor necrosis factor-alpha is mediated by ceramide. *American journal of respiratory cell and molecular biology*, **24**, 762-768.

200. Meier, B., Radeke, H.H., Selle, S., Younes, M., Sies, H., Resch, K. and Habermehl, G.G. (1989) Human fibroblasts release reactive oxygen species in response to interleukin-1 or tumour necrosis factor-alpha. *The Biochemical journal*, **263**, 539-545.

201. Kim, Y.S., Morgan, M.J., Choksi, S. and Liu, Z.G. (2007) TNF-induced activation of the Nox1 NADPH oxidase and its role in the induction of necrotic cell death. *Molecular cell*, **26**, 675-687.

202. Li, Q., Spencer, N.Y., Oakley, F.D., Buettner, G.R. and Engelhardt, J.F. (2009) Endosomal Nox2 facilitates redox-dependent induction of NF-kappaB by TNF-alpha. *Antioxidants & redox signaling*, **11**, 1249-1263.

203. Chen, Z.J. (2012) Ubiquitination in signaling to and activation of IKK. *Immunological reviews*, **246**, 95-106.

204. Poyet, J.L., Srinivasula, S.M., Lin, J.H., Fernandes-Alnemri, T., Yamaoka, S., Tsichlis, P.N. and Alnemri, E.S. (2000) Activation of the Ikappa B kinases by RIP via IKKgamma /NEMO-mediated oligomerization. *The Journal of biological chemistry*, **275**, 37966-37977.

205. Kanarek, N. and Ben-Neriah, Y. (2012) Regulation of NF-kappaB by ubiquitination and degradation of the IkappaBs. *Immunological reviews*, **246**, 77-94.

206. Hayden, M.S. and Ghosh, S. (2008) Shared principles in NF-kappaB signaling. *Cell*, **132**, 344-362.

207. Nakayama, K., Hatakeyama, S., Maruyama, S., Kikuchi, A., Onoe, K., Good, R.A. and Nakayama, K.I. (2003) Impaired degradation of inhibitory

subunit of NF-kappa B (I kappa B) and beta-catenin as a result of targeted disruption of the beta-TrCP1 gene. *Proceedings of the National Academy of Sciences of the United States of America*, **100**, 8752-8757.

208. Wang, Z., Inuzuka, H., Zhong, J., Fukushima, H., Wan, L., Liu, P. and Wei, W. (2012) DNA damage-induced activation of ATM promotes beta-TRCP-mediated Mdm2 ubiquitination and destruction. *Oncotarget*, **3**, 1026-1035.

209. Wu, Z.H. and Miyamoto, S. (2007) Many faces of NF-kappaB signaling induced by genotoxic stress. *Journal of molecular medicine (Berlin, Germany)*, **85**, 1187-1202.

210. Han, Y., Weinman, S., Boldogh, I., Walker, R.K. and Brasier, A.R. (1999) Tumor necrosis factor-alpha-inducible IkappaBalpha proteolysis mediated by cytosolic m-calpain. A mechanism parallel to the ubiquitin-proteasome pathway for nuclear factor-kappab activation. *The Journal of biological chemistry*, **274**, 787-794.

211. Tsuchiya, Y., Asano, T., Nakayama, K., Kato, T., Jr., Karin, M. and Kamata, H. (2010) Nuclear IKKbeta is an adaptor protein for IkappaBalpha ubiquitination and degradation in UV-induced NF-kappaB activation. *Molecular cell*, **39**, 570-582.

212. Chen, L.F. and Greene, W.C. (2004) Shaping the nuclear action of NF-kappaB. *Nature reviews. Molecular cell biology*, **5**, 392-401.

213. Neumann, M. and Naumann, M. (2007) Beyond IkappaBs: alternative regulation of NF-kappaB activity. *FASEB journal : official publication of the*

Federation of American Societies for Experimental Biology, **21**, 2642-2654.

214. Perkins, N.D. (2006) Post-translational modifications regulating the activity and function of the nuclear factor kappa B pathway. *Oncogene*, **25**, 6717-6730.

215. Sabatel, H., Di Valentin, E., Gloire, G., Dequiedt, F., Piette, J. and Habraken, Y. (2012) Phosphorylation of p65(RelA) on Ser(547) by ATM represses NF-kappaB-dependent transcription of specific genes after genotoxic stress. *PloS one*, **7**, e38246.

216. Staples, E.R., McDermott, E.M., Reiman, A., Byrd, P.J., Ritchie, S., Taylor, A.M. and Davies, E.G. (2008) Immunodeficiency in ataxia telangiectasia is correlated strongly with the presence of two null mutations in the ataxia telangiectasia mutated gene. *Clinical and experimental immunology*, **153**, 214-220.

217. Oxelius, V.A., Berkel, A.I. and Hanson, L.A. (1982) IgG2 deficiency in ataxia-telangiectasia. *The New England journal of medicine*, **306**, 515-517.

218. Ning, S., Huye, L.E. and Pagano, J.S. (2005) Regulation of the transcriptional activity of the IRF7 promoter by a pathway independent of interferon signaling. *The Journal of biological chemistry*, **280**, 12262-12270.

219. Gack, M.U., Shin, Y.C., Joo, C.H., Urano, T., Liang, C., Sun, L., Takeuchi, O., Akira, S., Chen, Z., Inoue, S. *et al.* (2007) TRIM25 RING-finger E3

ubiquitin ligase is essential for RIG-I-mediated antiviral activity. *Nature*, **446**, 916-920.

220. Arimoto, K., Takahashi, H., Hishiki, T., Konishi, H., Fujita, T. and Shimotohno, K. (2007) Negative regulation of the RIG-I signaling by the ubiquitin ligase RNF125. *Proceedings of the National Academy of Sciences of the United States of America*, **104**, 7500-7505.

Vita

Ling Fang was born in Fuyang, Anhui Province in P.R.China on May 1st, 1987. In 2008, he graduated from Life Science School in Sun Yat-sen University (Guangzhou, P.R. China). In the same year, after gaining B.S degree, he was admitted by The Ph.D. program of GSBS (Graduate School of Biomedical Science) in UTMB (The University of Texas Medical Branch). After several rotations, he joined the Ph.D. program in BMB (The Department of Biochemistry and Molecular Biology) in 2009.

EDUCATION

B.S. in Biochemistry   Sep 2004 to Jun 2008
Sun Yat-sen University, Guangzhou, China

PUBLICATION

- **Fang L**, Choudhary S, Zhao Y, Edeh CB, Yang, C, Boldogh, I, Brasier AR. ATM regulates NF-κB-dependent immediate-early genes via RelA Ser-276 phosphorylation coupled to CDK9 promoter recruitment. *Nucleic Acids Research* 2014   (In press) doi: 10.1093/nar/gku529.

- Choudhary S, Kalita M, **Fang L**, Patel KV, Tian B, Zhao Y, Edeh CB, Brasier AR. Inducible tumor necrosis factor (TNF) receptor-associated factor-1 expression couples the canonical to the non-canonical NF-κB pathway in TNF stimulation. *J Biol Chem*, 288(20), 14612-23, 2013

- Choudhary S, Rosenblatt KP, **Fang L**, Tian B, Wu ZH, Brasier AR. High throughput short interfering RNA (siRNA) screening of the human kinome identifies novel kinases controlling the canonical nuclear factor-κB (NF-κB) activation pathway. *J Biol Chem*, 286(43), 37187-95, 2011

CONFERENCE PRESENTAION & POSTER

- **Fang L**, Choudhary S, Brasier A. ATM regulates NF-κB-dependent genes via RelA Ser 276 phosphorylation. Oral Presentation at 55th National Student Research Forum, Apr 24, 2014

- **Fang L**, Patel K, Choudhary S, Brasier A. The Role of ATM in TNF-α Induced NF-κB Activation. Oral Presentation at 53rd Annual National Student Research Forum, Apr 26, 2012

- Kalita M, Choudhary S, **Fang L**, Patel KV, Tian B, Zhao Y, Edeh CB, Brasier AR. An integrated computational-experimental approach to identify the coupling mechanism between the canonical and non-canonical NF-κB pathway in inflammation. First Annual Poster Session, Institute of Translational Sciences (ITS), UTMB, Galveston, TX, Feb. 20, 2013

- Patel KV, Choudhary S, Kalita M, **Fang L**, Tian B, Zhao Y, Edeh CB, Brasier AR. Inducible TNF receptor associated factor 1 stabilizes NF-κB inducing kinase. 10th Annual AMA Research Symposium, Honolulu, Hawaii, Nov. 9-10, 2012

- Kalita M, **Fang L**, Choudhary S, Brasier AR. Understanding interactions of canonical and non-canonical NF-κB pathways in cancer. Third Annual Innovations in Cancer Prevention and Research Conference, Austin, TX, Oct. 24-26, 2012

HONORS AND AWARDS

- Best Oral Presentation in Translational Science at 55th National Student Research Forum   Apr 2014

- Best Oral Presentation in Microbiology and Immunology at 53rd Annual National Student Research Forum   Apr 2012

This dissertation was typed by Ling Fang